ELUCIDATING THE ROLE OF EUKARYOTIC INITIATION FACTOR 5B (EIF5B) IN NON-CANONICAL TRANSLATION INITIATION

KAMIKO RHIANNA BRESSLER
Bachelor of Science, University of Lethbridge, 2018

A thesis submitted
in partial fulfilment of the requirements for the degree of

MASTER OF SCIENCE

in

BIOCHEMISTRY

Department of Chemistry and Biochemistry
University of Lethbridge
LETHBRIDGE, ALBERTA, CANADA

ELUCIDATING THE ROLE OF EUKARYOTIC INITIATION FACTOR 5B (EIF5B)
IN NON-CANONICAL TRANSLATION INITIATION

KAMIKO BRESSLER

Date of Defense: June 7, 2019

Dr. Nehal Thakor Thesis Supervisor	Assistant Professor	Ph.D.
Dr. Marc Roussel Thesis Examination Committee Member	Professor	Ph.D.
Dr. Igor Kovalchuk Thesis Examination Committee Member	Professor	Ph.D.
Dr. Mark Bayfield External Examiner York University Toronto, Ontario	Associate Professor	Ph.D.
Dr. Michael Gerken Chair, Thesis Examination Committee	Professor	Ph.D.

ABSTRACT

Cap-dependent translation drives the global synthesis of proteins. Under stress conditions global protein production is attenuated, yet the translation of ATF4 is upregulated through uORF- mediated translation initiation. eIF5B has been shown to deliver initiator-tRNA during non-canonical translation initiation. As such, we defined the role of eIF5B in the non-canonical translation of ATF4, and p27. Through polysome profiling and luciferase reporter assays, we confirmed that eIF5B facilitates uORF2-mediated repression of ATF4 translation. We determined that eIF5B has transcriptome-wide effects on signaling pathways, verifying activation of the JNK arm of the MAPK pathway and upregulation of dyskerin. I investigated the role eIF5B has in regulation of p27, and suggest that the mechanism is IRES-dependent. This study furthers the understanding into mechanisms of alternative translation initiation, which is critical to gene expression regulation.

PREFACE

Contributions of Authors

A version of Chapter 1 has been adapted and published. [Sharma, D. K., Bressler, K., Patel, H., Balasingam, N. & Thakor, N. Role of Eukaryotic Initiation Factors during Cellular Stress and Cancer Progression. *Journal of nucleic acids* **2016**, 8235121-8235119, doi:10.1155/2016/8235121 (2016)]. I contributed to writing the manuscript, and designed the figures included in Chapter 1 (Figure 1.1, Figure 1.2, Figure 1.3). I received assistance from Divya Khandige Sharma, Harshil Patel, Nirujah Balasingam, and Dr. Nehal Thakor in writing the manuscript.

Chapter 2 has been published. [Ross, J. A., Bressler, K. R. & Thakor, N. Eukaryotic Initiation Factor 5B (eIF5B) Cooperates with eIF1A and eIF5 to Facilitate uORF2-Mediated Repression of ATF4 Translation. *Int J Mol Sci* **19**, doi:10.3390/ijms19124032 (2018)]. I contributed to writing the manuscript, and performing the experiments. I received assistance from Dr. Joseph Ross in writing the manuscript, and in experimental work shown in Figure 2.3 and Figure 2.6. The experiment shown in Figure 2.4 was performed by Dr. Nehal Thakor.

Figure 3.6 (modified in thesis to excluded TRAIL treatment) of Chapter 3 has been published. [Ross, J. A. et al. Eukaryotic initiation factor 5B (eIF5B) provides a critical cell survival switch to glioblastoma cells via regulation of apoptosis. Cell Death Dis 10, 57, doi:10.1038/s41419-018-1283-5 (2019)]. I performed the experimental work shown

in Figure 3.6. Writing of the manuscript, and experimental work (both not included in this thesis) were performed by Dr. Joseph Ross, Keiran Vanden Dungen, Mikayla Fredriksen, Divya Khandige Sharma, Nirujah Balasingam, and Dr. Nehal Thakor. Experimental work shown in Figure 3.1 was performed in collaboration with Dr. Igor Kovalchuk's laboratory, with assistance received from Dr. Slava Ilnystkyy. I received assistance from Dr. Joseph Ross in experimental work shown in Figure 3.2.

Check the first pages of these chapters to see similar information. Permission of all co-authors and publishers was received for publication in this thesis.

ACKNOWLEDGEMENTS

I would first like to thank my supervisor, Dr. Nehal Thakor for his continual guidance, support, and mentorship. I have learned countless valuable lessons from my years in the Thakor laboratory.

I would like to thank my committee members, Dr. Marc Roussel and Dr. Igor Kovalchuk for their helpful conversations and suggestions. Thank you in addition to my external examiner Dr. Mark Bayfield, for reading and critiquing my work, and my thesis chair Dr. Michael Gerken.

I would also like to thank my past and current lab mates, including but not limited to, Justin, Divya, Nirujah, Keiran, Keith, Rachana, Deesha, Kush, and Joe, for their dedicated assistance and support.

Lastly, I would like to thank my parents and friends for their motivation, patience, and unconditional support.

TABLE OF CONTENTS

LIST OF TABLES:

LIST OF FIGURES:

LIST OF ABBREVIATIONS:

AD	Alzheimer's disease
Apaf-1	apoptotic protease-activating factor 1
ATF3	activating transcription factor 3
ATF4	activating transcription factor 4
BACE1	β-site APP-cleaving enzyme 1
Bcl2	B cell lymphoma 2
Bcl-xL	B cell lymphoma extra-large
CAK	CDK activating kinase
CARE	C-EBP-ATF response elements
CDK	cyclin dependent kinase
Cdc2	cell division control 2
CDS	coding sequence
CHOP	C/EBP-homologous protein
cIAP1	cellular inhibitor of apoptosis protein 1
CKI	cyclin dependent kinase inhibitor
CLOCK	circadian locomotor output cycles kaput
CSFV	classical swine fever virus
CrPV	cricket paralysis virus
Caspase	cysteine aspartic protease
DEG	differentially expressed gene
DKC1	dyskerin pseudouridine synthase
DMEM	Dulbecco's high modified Eagle's medium
DPC4	deleted in pancreatic cancer 4
ECM	extracellular matrix
EGF	epidermal growth factors
eIF	eukaryotic initiation factor
eIF5MP	eukaryotic initiation factor 5 mimic protein
Elk-1	ETS-1 like protein
ER	endoplasmic reticulum
ERK	extracellular signal-regulated kinase
FACS	fluorescence activated cell sorting
FBS	fetal bovine serum
GADD34	growth and DNA damage-inducible protein 34
GAGE	generally applicable gene set enrichment
GCN2	general control non-derepressible
GO	gene ontology
HCV	hepatitis C virus
HIF-1α	hypoxia inducible factor 1
HRI	heme-regulated eIF2α kinase
IF2	initiation factor 2
ITAF	IRES trans-acting factor
IRES	internal ribosome entry site
ISR	integrated stress response
JNK	jun N-terminal kinase

KEGG	Kyoto encyclopedia of genes and genomes
KIP	kinase inhibitory protein
MAPK	mitogen activated protein kinase
MENIN	multiple endocrine neoplasia type 1
MKK	MAPK kinase
MKKK	MAPK kinase kinase
mRNA	messenger ribonucleic acid
MYC	myelocytomatosis
m^7G	methylated guanosine cap
NFAT4	nuclear factor of activated T cells
Nrf2	nuclear factor erythroid-derived 2- like 2
ORF	open reading frame
P-site	peptidyl site
PBS	phosphate-buffered saline
PC-3	human prostate cancer cell line
PERK	PKR-like ER kinase
PI	propidium iodide
PIC	pre-initiation complex
PIM	proto-oncogene serine/threonine protein kinase
PKR	double-stranded RNA-dependent protein kinase
PP1	protein phosphatase 1
Ppp1r15a	protein phosphatase 1 regulatory subunit 15A
RNP	ribonucleoprotein
ROS	reactive oxygen species
rRNA	ribosomal ribonucleic acid
RT-qPCR	real time quantitative polymerase chain reaction
SAPK	stress-activated protein kinase
siRNA	small interfering ribonucleic acid
snoRNA	small nucleolar ribonucleic acid
SDS PAGE	sodium dodecyl sulfate- polyacrylamide gel electrophoresis
TC	ternary complex
TRAIL	TNF-related apoptosis-inducing ligand
Trib3	tribbles homologue 3
tRNA	transfer ribonucleic acid
TUN	tunicamycin
uORF	upstream open reading frame
UPR	unfolded protein response
UTR	untranslated region
UV	ultraviolet radiation
VEGF	vascular endothelial growth factor
Wars	tryptophanyl-TRNA synthetase
X-DC	X-linked dyskeratosis congenita
XIAP	X-linked inhibitor of apoptosis protein

CHAPTER 1

General Introduction

Parts of this chapter have been adapted and published in the *Journal of Nucleic Acids* (2016), Article ID 8235121

Role of eukaryotic initiation factors during cellular stress and cancer progression

Divya Khandige Sharma*, **Kamiko Bressler***, Harshil Patel*, Nirujah Balasingam, and Nehal Thakor

* Contributed equally as co-first authors

General Introduction

This thesis investigates the role of eIF5B in the non-canonical translation of *ATF4* and *p27*. These proteins have roles in the ISR and the cell cycle, respectively, and both are known to be regulated through non-canonical translation. The transcript of *ATF4* contains two uORF elements, and the transcript of *p27* contains both a uORF and an IRES element. Upon depletion of eIF5B, I observed enhanced expression of both ATF4 and p27 at the protein level and determined that eIF5B regulates the translation of *ATF4* and *p27* mRNAs. Specifically, eIF5B utilizes a uORF-dependent mechanism for the regulation of *ATF4,* and likely an IRES-dependent mechanism for the regulation of *p27.* This thesis adds knowledge to the mechanisms of protein synthesis by furthering the understanding of non-canonical translation initiation.

1.1 Importance of regulation of translation in protein synthesis

Regulation of protein translation is a critical step of the gene expression process, which allows cellular adaptation during stress conditions by rapidly reprograming the proteome output without the requirement for changes in RNA synthesis. Translation consists of three phases: initiation, elongation, and termination, with initiation being rate-limiting and thus an important regulatory target.[1] In conditions such as heat shock, hypoxia, endoplasmic reticulum (ER) stress, and apoptosis, an immediate change in protein levels is required, highlighting the importance of translational regulation, responsible for efficient adaptation to physiological conditions.[2]

Transcriptome analysis is a widely accepted method for analyzing gene expression during stress conditions. However, there is emerging evidence that shows a limited

correlation between the transcriptome and the corresponding proteome. This suggests that not all transcripts are translated at equal levels.[3] Epidermal growth factor (EGF) treatment of serum-starved HeLa cells resulted in only 4.8% differentially expressed genes (DEGs), where a DEG represents a significant change in both the transcriptome and translatome in the same direction (homodirectionally).[4] Rather, the 95.2% of uncoupled DEGs represent a significant change in either the transcriptome or translatome or an inverse relationship between the transcriptome and translatome (or no change at all).[4] Using parallel genome-scale measurements of mRNA and corresponding protein levels and half-lives, mRNAs were found to explain 40% of the variability in protein levels, with translation efficiency being the best predictor of protein levels in mouse fibroblasts.[5] Accordingly, translational control is considered to play a central role in eukaryotic gene expression.

In a wide range of cell types, inappropriate translation is responsible for the dysregulated production of oncogenes, tumor suppressors, and eukaryotic translation factors.[6-8] In particular, during cellular stress, global levels of protein synthesis are reduced, however, there is a selective translation of a specific subset of mRNAs. These transcripts typically encode critical pro-survival proteins that are translated by alternative (non-canonical) mechanisms.[2,9,10] Significantly, many important mRNAs utilize non-canonical mechanisms of translational regulation, which is now realized to be critical to our understanding of cellular biology.

1.2 Canonical translation initiation in protein synthesis

Eukaryotic cap-dependent translation initiation includes the recognition and recruitment of mRNA onto the small ribosomal (the 40S) subunit, followed by ribosomal

scanning in a 5′ to 3′ direction. Subsequently, the 60S large ribosomal subunit is recruited, forming the 80S initiation complex. At this stage, an initiator methionyl-tRNAi (initiator-tRNA) is in the ribosomal peptidyl (P) site at the mRNA start codon.[1,11] Canonical initiation is a complex process utilizing more than 25 proteins, including a minimum of twelve eukaryotic initiation factors (eIFs).[12] The rate of initiation varies between different mRNAs and is influenced by accessibility to the methylated guanosine cap structure (m^7G cap) at the 5′ terminus of the mRNA, the length and secondary structure of the 5′ untranslated region (UTR), the sequence and secondary structure surrounding the start codon, and the poly(A) tail.[13,14]

Initiation begins with the assembly of an eIF4F complex comprising of eIF4E, eIF4G, and eIF4A onto the 5′ m^7G cap. eIF4E binds to the m^7G cap, which then interacts with the multi-domain scaffold protein eIF4G and the ATP-dependent RNA helicase eIF4A (unwinds RNA structure).[1] eIF4G has two isoforms which can be translated non-canonically and are cleavage targets of caspase 3 during apoptosis.[15] The ternary complex (eIF2-GTP-met-tRNAi) associated with a 40S ribosomal subunit is then recruited to the 5′ end of the mRNA *via* a critical link between eIF4G and eIF3. This interaction forms the 43S preinitiation complex (PIC). eIF1 and eIF1A assist in stimulating recruitment of the ternary complex, as well as acting synergistically to promote continuous ribosomal scanning for AUG start codons.[16] The 43S PIC then scans the 5′ UTR of the mRNA, with the help of eIF4A, until an initiation codon in the optimal context is recognized.[17] eIF5 and eIF5B then mediate subsequent hydrolysis of GTP to release the bound initiation factors from the 48S complex, leaving the start codon in the ribosomal P-site with the initiator-

tRNA and allowing 60S ribosomal subunit to bind.[18] The now competent 80S initiation complex then proceeds to translation elongation (Figure 1.1).
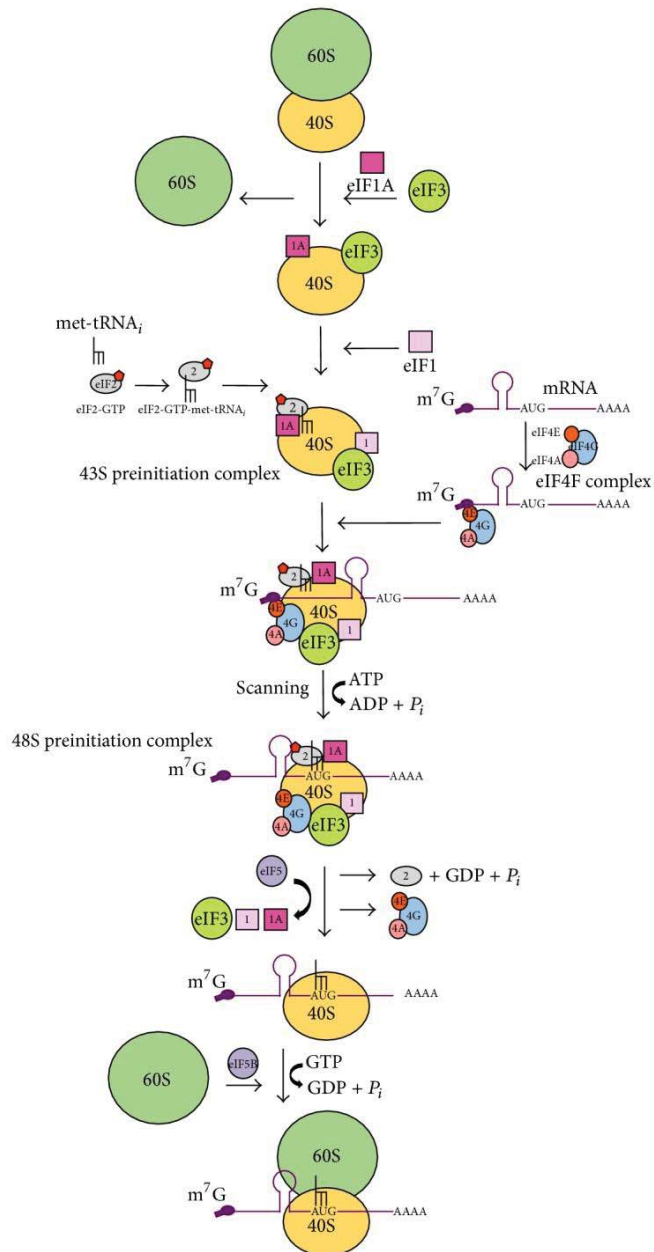
Figure 1.1 An overview of eukaryotic translation initiation. Most eukaryotic mRNAs contain a 5′ m^{7}G cap which is bound by eukaryotic initiation factor 4F complex (eIF4E, eIF4G, and eIF4A). The 43S preinitiation ribosome complex which contains ternary complex (eIF2-GTP-initiator-tRNA) is recruited to the 5′ end of mRNAs *via* eIF3-eIF4G interaction. With the help of eIF4A (RNA helicase), the preinitiation complex is thought to scan mRNA until the start codon (AUG) is found. Subsequently, the 48S initiation complex is formed and the ternary complex delivers initiator-tRNA into the P-site of the ribosome. Then, eIF5 binds to the 48S initiation complex and induces GTPase activity of

eIF2α. Upon GTP hydrolysis, all protein factors are released from the 40S ribosome subunit. Subsequently, eIF2α is recharged with GTP by "GDP to GTP" exchange factor eIF2B. Finally, eIF5B unites the 60S and 40S ribosome subunits to form the 80S initiation complex and translation elongation commences.

1.3 Effects of the ISR on translation initiation

The ISR is a highly complex signalling pathway which is activated by a wide range of physiological conditions including extrinsic factors such as hypoxia, amino acid or nutrient deprivation and viral infection, as well as intrinsic factors including endoplasmic reticulum (ER) stress and the unfolded protein response (UPR).[19,20]

Specific stressors result in initial phosphorylation of eIF2's alpha (α) subunit at serine 51 by members of a family of four kinases: PKR-like ER kinase (PERK) (ER stress), double-stranded RNA-dependent protein kinase (PKR) (viral infection), heme-regulated eIF2α kinase (HRI) (heme deprivation), and general control non-derepressible 2 (GCN2) (amino acid deprivation).[19] When phosphorylated, eIF2α is locked in an inactive GDP-bound state, as eIF2B cannot exchange eIF2's GDP for GTP.[21] Consequently, the ternary complex cannot be formed, which is necessary for delivering initiator-tRNA in cap-dependent translation initiation. This results in a reduction of global protein synthesis. However, translation of specific transcripts such as *ATF4* is favored, promoting cell survival and adaptation.[20] One of ATF4's downstream targets, growth, and DNA damage-inducible protein 34 (GADD34), is the protein responsible for regulating the protein phosphatase 1 (PP1) complex that acts to dephosphorylate eIF2α as a negative feedback loop.[20] However, long periods of intense stress can result in the activation of cell death through dimer formation with CHOP, and subsequently, apoptosis.[22]

1.4 Non-canonical translation initiation

During stress conditions that result in activation of the ISR, as previously described, alternative mechanisms that are mediated by *cis*-acting sequences in specific mRNA subsets, such as uORFs and IRESs, drive the translation of stress response mRNAs.[6,9,23] These mechanisms differ from canonical translation initiation, as they do not always require ribosomal complexes binding to the mRNA 5' cap, ribosome scanning, or a multitude of initiation factors.[24] Interestingly, mRNAs including *Reaper, Notch2, B cell lymphoma 2 (Bcl-2),* and *(hypoxia-inducible factor 1) HIF-1α, XIAP, and cIAP1* are translated *via* non-canonical mechanisms and are key factors contributing to processes of viral infection, and cancer progression.[24-29]

1.4.1 IRES-mediated translation

Translation initiation mediated by IRESs is a mechanism that operates during stress conditions. IRESs are RNA sequence elements that were initially discovered in the 5' leader sequences of poliovirus' and encephalomyocarditis virus' genomic RNA that lack the 5' cap structure but are efficiently translated in the host cell.[17,30] Thus, cap-dependent recognition/scanning is bypassed, and the 40S ribosome is directly recruited to the mRNA.

The viral IRES elements comprise secondary and tertiary structures that play a role in direct interactions with the translation initiation machinery.[23] Mutations in viral IRESs such as hepatitis C virus (HCV), classical swine fever virus (CSFV), and cricket paralysis virus (CrPV) affect their secondary and tertiary RNA structures and render these IRESs inactive.[31] These viral IRESs are classified based on structural and sequence similarities, as well as their requirement for eIFs and other protein factors for translation initiation.[18,23]

Picornavirus IRES elements are examples of types I and II IRESs, which require eIF4G, eIF4A, and eIF3 to assemble 48S initiation complexes.[30] Type III viral IRESs require eIF4G, with the HCV IRES being an exception; the HCV IRES interacts with eIF3 for recruitment of the 40S ribosomal subunit in close proximity to the start codon, circumventing the requirement for the 5′ cap structure.[2,18] Although IRES-mediated translation operates independently of many canonical initiation factors, it often requires RNA-binding proteins known as IRES *trans*-acting factors (ITAFs).

Many cellular mRNAs are known to harbour IRES elements, but unlike viral IRESs, they do not share structural or sequence similarities.[23,32] However, viral and cellular IRES can participate in multiple interactions with canonical initiation factors and ITAFs to recruit the ribosome.[23] In fact, despite sequence and structural dissimilarities, cellular IRESs are reported to share critical ITAFs.[23] IRES elements have been identified in mRNAs encoding stress response proteins (pro- and anti-apoptotic), such as X-linked inhibitor of apoptosis protein (XIAP), cellular inhibitor of apoptosis 1 (cIAP1), B cell lymphoma extra-large (Bcl-xL), Bcl-2, Bag-1, apoptotic protease-activating factor 1 (Apaf-1), hypoxia-induced factor 1α (HIF-1α), p53, L-myc, N-myc, and c-myc.[2,9,27,28,33,34] The IRES-dependent translation of *HIF-1α* specifically is critical to the hypoxic tumor environment, as it is a transcription factor. In prostate cancer (PC-3 cell line), *HIF-1α* transcript has been shown to be associated with polysomes at significantly high levels, despite attenuation of global cap-dependent translation.[25,35] The presence of IRES elements in the *HIF-1α* transcript, suggests the importance of non-canonical translation in cell-fate determining decisions.

1.4.2 uORF-mediated translation

A recent study has revealed that approximately 49% of human transcripts contain uORFs.[36] uORFs are mRNA elements that contain one or more start codon(s) in the 5' UTR of a transcript (Figure 1.2). Recent ribosome profiling data reveals that uORFs can exist out-of-frame relative to the main coding sequence.[37] However, an overlap can also occur between uORFs and the coding sequence, in which alternative translation of an upstream, in-frame start codon of a gene can possibly produce an extended protein product.[38] uORFs typically act as negative regulators of cap-dependent translation initiation, as scanning ribosomes encounter uORFs before the downstream start codon. In these situations, ribosomes will either translate the uORF and miss the coding sequence entirely, or dissociate from the uORF and potentially re-initiate at the correct start codon. However, for uORF-containing transcripts under stress conditions, translation of the main coding ORF is less commonly repressed, and can even be preferentially translated.
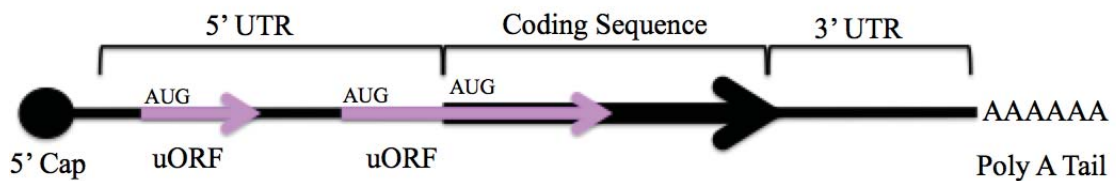
Figure 1.2: Schematic diagram of the *ATF4* mRNA. Two uORFs are shown in the 5' UTR, including the second, which is overlapping the main coding sequence of ATF4. This mRNA is preferentially translated during the ISR when eIF2α is phosphorylated. During these conditions, the less ternary complex is formed, and as such more ribosomes pass over *ATF4*'s second uORF, and thus initiate translation downstream at the main coding sequence.

The mechanism of uORF-mediated translation enhancing protein expression functions primarily during eIF2α phosphorylation conditions and is known to affect

proteins involved in cell cycle regulation and apoptosis.[39] Typical examples of uORF-mediated translation regulation include GCN4 (the yeast transcriptional activator) [40], and ATF4 in mammals.[41] Under normal cellular conditions, translation initiation occurs from the start codons located in the 5′ UTR of mRNA, which leads to the translation of small uORFs. Re-initiation of terminated ribosomes at the correct start codon occurs with lower probability, as the ribosomal complex is likely to scan over the correct start codon while waiting for initiator-tRNA; thus, the translation of the main coding sequence is inhibited in these conditions.[42] However, during stress conditions, eIF2α phosphorylation attenuates translation of uORF sequences and allows the translation of main coding sequence (Figure 1.3). This occurs because there is a lower concentration of ternary complex available, and as such, ribosomal complexes possibly have a higher probability of scanning past the uORFs in the 5'UTR of a transcript without initiating (due to lack of ternary complex). In this situation, more ribosomal complexes will reach the correct start codon before encountering ternary complex and will subsequently initiate translation of the coding sequence.
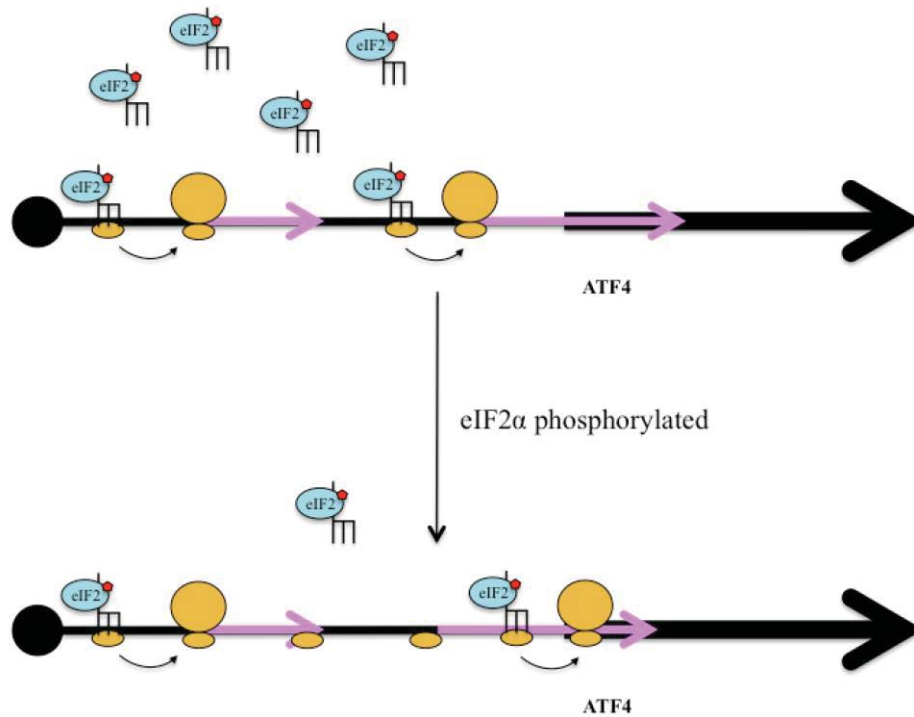
Figure 1.3: Diagram showing physiological cell conditions (top), during which an abundance of the ternary complex is available to form initiation complexes, and as such *ATF4*'s two uORFs (purple) are highly translated, resulting in lower translation of downstream *ATF4*'s main coding sequence (black). During cell stress (bottom), eIF2α is phosphorylated, resulting in a low concentration of ternary complex, which allows ribosomal complexes to reach *ATF4*'s main coding sequence to be translated.

The complexity of RNA structure in the 5′ UTR also plays a crucial role in uORF-mediated translation. For example, translation of *β*-site APP-cleaving enzyme 1 (BACE1), which is implicated in Alzheimer's disease (AD) progression, is regulated through uORFs.[43] However, high GC content and complexity of the RNA secondary structure are also crucial decisive factors for uORF-mediated translation of BACE1.[43] Additionally, recent genome-level studies indicate that RNA secondary structure is negatively correlated with uORF translational efficiency as upstream structures can restrict or even arrest ribosomal complexes.[44]

1.4.3 Role of eIF5B in non-canonical translation

As previously mentioned, eIF5B has a role in the canonical initiation of translation, promoting 60S ribosome subunit joining, and pre-40S subunit proofreading. However, eIF5B has been shown to have critical non-canonical roles as well. eIF5B is the homologue of bacterial initiation factor 2 (IF2), which delivers initiator-tRNA to the ribosome. eIF5B has been confirmed to directly interact with initiator-tRNA, with elevated eIF5B levels resulting in increased eIF5B complexes with initiator-tRNA in THP1 cells.[45] Further, eIF5B can parallel eIF2's role in the IRES-dependent translation of the viral mRNAs of CSFV, and HCV, as well as the cellular mRNA of XIAP.[9,31,46] eIF5B was recently shown to deliver initiator-tRNA under hypoxic stress conditions, suggesting that eIF5B had been evolutionarily retained for dependence on pathways involving the stress response and carbon metabolism.[47] Additionally, we have recently shown that eIF5B regulates the translation of a group of IRES-containing mRNAs encoding anti-apoptotic and pro-survival proteins in U343 cells.[48] These findings implicate eIF5B to have roles in non-canonical translation possibly through its ability to interact with and deliver initiator-tRNA.

1.5 Non-canonical translation of ATF4 and its role in the ISR

ATF4 is known to be regulated under stress conditions at the translational level.[41] *ATF4* contains two uORFs: an upstream uORF encoding three amino acids, and a longer overlapping uORF that overlaps through the main coding sequence.[41] It has been reported that upon eIF2α phosphorylation, re-initiation of translation at the coding sequence results in approximately five-fold higher *ATF4* expression.[41] ATF4 is additionally known to be transcriptionally regulated by transcription factors including nuclear factor erythroid-

derived 2- like 2 (Nrf2) in oxidative stress, and circadian locomotor output cycles kaput (CLOCK) in response to the chemotherapeutic drug cisplatin.[49] IRES-dependent translation initiation has been shown for an alternatively spliced variant of human ATF4.[50]

ATF4 is a leucine zipper transcription factor and is perhaps the best-characterized effector of the ISR. ATF4 itself is a transcription factor that functions in the regulation of obesity, glucose homeostasis, energy, and neural plasticity through its roles in the regulation of metabolic and redox processes.[51] During stress, ATF4 binds C-EBP-ATF response elements (CARE) sequences to transcriptionally activate its targets. It forms homo and heterodimers with other transcription factors, including C/EBP-homologous protein (CHOP), as well as activating transcription factor 3 (ATF3), protein phosphatase 1 regulatory subunit 15A (Ppp1r15a), tribbles homologue 3 (Trib3), and tryptophanyl-tRNA synthetase (Wars), which all serve to adapt to and endure stress.[51] However, during persistent and chronic cellular stress, ATF4 promotes apoptosis and cell death through activation of Bcl-2 family proteins including Bim, and Noxa.[52,53]

1.6 Non-canonical translation of p27 and its role in the regulation of the cell cycle

p27 is regulated transcriptionally, translationally, and post-translationally.[54] Transcriptionally, *p27* is regulated by transcription factor multiple endocrine neoplasia type 1 (MENIN), and oncogenic transcription factors myelocytomatosis (MYC) and proto-oncogene serine/threonine protein kinase (PIM).[55] Post-translationally, p27 is regulated by modifications to alter its cellular localization and mediate its degradation through E3 ubiquitin ligases.[55] Most commonly, p27 is phosphorylated at various amino acids, to both target them for degradation and localize p27 to the cytoplasm, where it is degraded.[55]

p27 is known to have an IRES element and a uORF in its 5' UTR. The IRES was found to allow efficient *p27* translation under conditions where cap-dependent translation was reduced.[56] Additionally, the uORF has been shown to highly conserved in both sequence and position in humans, chickens, and mice.[57] Gopfert *et al*. (2003) identified a novel 114 nucleotide element of a G/C- rich hairpin domain predicted to form stem loops that overlap and appear to contribute to *p27* translational regulation.[57] Despite the elements in the transcript of *p27* that have been identified, much of the mechanism of how these various elements function in translation initiation is unknown.

p27 is a protein mainly characterized by its ability to bind with cyclins and cyclin-dependent kinases (CDKs), influencing regulation of the cell cycle. The interactions between CDKs and partnering cyclins allow cell cycle progression, while cyclin-dependent kinase inhibitors prevent these interactions and halt the cell cycle.[58] As such, p27 is a CKI that can prevent activation of cyclin-CDK2 or cyclin D-CDK4 complexes, thus halting the cell cycle at G1, causing cell cycle arrest.[55] Consequently, the loss of a single *p27* allele significantly increases tumor incidence *via* CDK-mediated cell cycle entry and is implicated in disease progression and cancer.[55] As both *ATF4* and *p27* contain elements which would allow for non-canonical translation initiation, I hypothesized that eIF5B might have a role in their regulation.

1.7 Research aims and objectives

As eIF5B is known to interact with and deliver initiator-tRNA during translation initiation of specific IRES-containing mRNAs, and the mechanism of uORF-mediated translation initiation depends on the availability of ternary complex to deliver initiator-tRNA to the translating ribosome, I wanted to investigate the potential role of eIF5B in

uORF-mediated translation. As such, I hypothesized that eIF5B regulates *ATF4* at the translational level through a uORF-dependent mechanism, and consequently, eIF5B has a critical role in the ISR. My first objective was to define the role of eIF5B in the uORF-mediated translation initiation of *ATF4*. Specifically, I aimed to confirm that eIF5B represses the translation of *ATF4* through its uORF elements, and determine whether the eIF5B-dependent mechanism operates in parallel with the known eIF2-dependent mechanism.

My second objective was to examine transcriptome changes in control and eIF5B depleted cells and characterize the signaling pathways affected by the levels of eIF5B. As I showed through my first objective that eIF5B facilitates repression of master transcription factor ATF4, I hypothesized that eIF5B regulates other signaling pathways. I hypothesized that eIF5B regulates other transcription factors at the translational level, which affects various signaling pathways. Upon completion of this experiment in collaboration with Dr. Igor Kovalchuk, I specifically aimed to validate activation of the JNK-arm of the MAPK pathway and upregulation of dyskerin in eIF5B depleted cells. Further, I hypothesized that eIF5B regulates *p27* at the translational level, through an IRES-dependent mechanism, *via* regulating the levels of *DKC1* and consequently has a critical role in cell cycle regulation. I aimed to confirm that eIF5B represses the translation of *p27* through its IRES element, and determine whether eIF5B has a role in the regulation of the cell cycle.

References

1   Sharma, D. K., Bressler, K., Patel, H., Balasingam, N. & Thakor, N. Role of Eukaryotic Initiation Factors during Cellular Stress and Cancer Progression. *Journal of nucleic acids* **2016**, 8235121-8235119, doi:10.1155/2016/8235121 (2016).

2   Holcik, M. & Sonenberg, N. Translational control in stress and apoptosis. *Nat Rev Mol Cell Biol* **6**, 318-327, doi:10.1038/nrm1618 (2005).

3   Wang, T. *et al.* Translating mRNAs strongly correlate to proteins in a multivariate manner and their translation ratios are phenotype specific. *Nucleic Acids Res* **41**, 4743-4754, doi:10.1093/nar/gkt178 (2013).

4   Tebaldi, T. *et al.* Widespread uncoupling between transcriptome and translatome variations after a stimulus in mammalian cells. *BMC Genomics* **13**, 220, doi:10.1186/1471-2164-13-220 (2012).

5   Schwanhausser, B. *et al.* Global quantification of mammalian gene expression control. *Nature* **473**, 337-342, doi:10.1038/nature10098 (2011).

6   Ruggero, D. Translational control in cancer etiology. *Cold Spring Harb Perspect Biol* **5**, doi:10.1101/cshperspect.a012336 (2013).

7   Kong, J. & Lasko, P. Translational control in cellular and developmental processes. *Nat Rev Genet* **13**, 383-394, doi:10.1038/nrg3184 (2012).

8   Bhat, M. *et al.* Targeting the translation machinery in cancer. *Nat Rev Drug Discov* **14**, 261-278, doi:10.1038/nrd4505 (2015).

9   Thakor, N. & Holcik, M. IRES-mediated translation of cellular messenger RNA operates in eIF2α- independent manner during stress. *Nucleic Acids Research* **40**, 541-552, doi:10.1093/nar/gkr701 (2012).

10   Silvera, D., Formenti, S. C. & Schneider, R. J. Translational control in cancer. *Nat Rev Cancer* **10**, 254-266, doi:10.1038/nrc2824 (2010).

11   Preiss, T. & M, W. H. Starting the protein synthesis machine: eukaryotic translation initiation. *Bioessays* **25**, 1201-1211, doi:10.1002/bies.10362 (2003).

12   Gebauer, F. & Hentze, M. W. Molecular mechanisms of translational control. *Nat Rev Mol Cell Biol* **5**, 827-835, doi:10.1038/nrm1488 (2004).

13   Gingold, H. & Pilpel, Y. Determinants of translation efficiency and accuracy. *Mol Syst Biol* **7**, 481, doi:10.1038/msb.2011.14 (2011).

14   Pestova, T. V. & Kolupaeva, V. G. The roles of individual eukaryotic translation initiation factors in ribosomal scanning and initiation codon selection. *Genes Dev* **16**, 2906-2922, doi:10.1101/gad.1020902 (2002).

15   Byrd, M. P., Zamora, M. & Lloyd, R. E. Generation of multiple isoforms of eukaryotic translation initiation factor 4GI by use of alternate translation initiation codons. *Mol Cell Biol* **22**, 4499-4511, doi:10.1128/mcb.22.13.4499-4511.2002 (2002).

16   Maduzia, L. L., Moreau, A., Poullet, N., Chaffre, S. & Zhang, Y. The role of eIF1 in translation initiation codon selection in Caenorhabditis elegans. *Genetics* **186**, 1187-1196, doi:10.1534/genetics.110.121541 (2010).

17   Graber, T. E. & Holcik, M. Cap-independent regulation of gene expression in apoptosis. *Mol Biosyst* **3**, 825-834, doi:10.1039/b708867a (2007).

18   Jackson, R. J., Hellen, C. U. & Pestova, T. V. The mechanism of eukaryotic translation initiation and principles of its regulation. *Nat Rev Mol Cell Biol* **11**, 113-127, doi:10.1038/nrm2838 (2010).

19   Dever, T. E. *et al.* Phosphorylation of initiation factor 2 alpha by protein kinase GCN2 mediates gene-specific translational control of GCN4 in yeast. *Cell* **68**, 585-596 (1992).

20   Harding, H. P. *et al.* An integrated stress response regulates amino acid metabolism and resistance to oxidative stress. *Mol Cell* **11**, 619-633 (2003).

21   Sudhakar, A. *et al.* Phosphorylation of serine 51 in initiation factor 2 alpha (eIF2 alpha) promotes complex formation between eIF2 alpha(P) and eIF2B and causes inhibition in the guanine nucleotide exchange activity of eIF2B. *Biochemistry* **39**, 12929-12938 (2000).

22   Su, N. & Kilberg, M. S. C/EBP homology protein (CHOP) interacts with activating transcription factor 4 (ATF4) and negatively regulates the stress-dependent induction of the asparagine synthetase gene. *J Biol Chem* **283**, 35106-35117, doi:10.1074/jbc.M806874200 (2008).

23   Komar, A. A. & Hatzoglou, M. Cellular IRES-mediated translation: the war of ITAFs in pathophysiological states. *Cell Cycle* **10**, 229-240, doi:10.4161/cc.10.2.14472 (2011).

24   Pestova, T. V. *et al.* Molecular mechanisms of translation initiation in eukaryotes. *Proc Natl Acad Sci U S A* **98**, 7029-7036, doi:10.1073/pnas.111145798 (2001).

25   Fitzgerald, K. D. & Semler, B. L. Bridging IRES elements in mRNAs to the eukaryotic translation apparatus. *Biochim Biophys Acta* **1789**, 518-528, doi:10.1016/j.bbagrm.2009.07.004 (2009).

26   Lang, K. J., Kappel, A. & Goodall, G. J. Hypoxia-inducible factor-1alpha mRNA contains an internal ribosome entry site that allows efficient translation during normoxia and hypoxia. *Mol Biol Cell* **13**, 1792-1801, doi:10.1091/mbc.02-02-0017 (2002).

27   Shaltouki, A., Harford, T. J., Komar, A. A. & Weyman, C. M. IRES-mediated translation of the pro-apoptotic Bcl2 family member PUMA. *Translation (Austin)* **1**, e24391, doi:10.4161/trla.24391 (2013).

28   Graber, T. E., Baird, S. D., Kao, P. N., Mathews, M. B. & Holcik, M. NF45 functions as an IRES trans-acting factor that is required for translation of cIAP1 during the unfolded protein response. *Cell Death Differ* **17**, 719-729, doi:10.1038/cdd.2009.164 (2010).

29   Holcik, M. & Korneluk, R. G. Functional characterization of the X-linked inhibitor of apoptosis (XIAP) internal ribosome entry site element: role of La autoantigen in XIAP translation. *Mol Cell Biol* **20**, 4648-4657 (2000).

30   Sweeney, T. R., Abaeva, I. S., Pestova, T. V. & Hellen, C. U. The mechanism of translation initiation on Type 1 picornavirus IRESs. *EMBO J* **33**, 76-92, doi:10.1002/embj.201386124 (2014).

31   Pestova, T. V., de Breyne, S., Pisarev, A. V., Abaeva, I. S. & Hellen, C. U. eIF2-dependent and eIF2-independent modes of initiation on the CSFV IRES: a common role of domain II. *EMBO J* **27**, 1060-1072, doi:10.1038/emboj.2008.49 (2008).

32   Balvay, L., Soto Rifo, R., Ricci, E. P., Decimo, D. & Ohlmann, T. Structural and functional diversity of viral IRESes. *Biochim Biophys Acta* **1789**, 542-557, doi:10.1016/j.bbagrm.2009.07.005 (2009).

33   Halaby, M. J., Harris, B. R., Miskimins, W. K., Cleary, M. P. & Yang, D. Q. Deregulation of Internal Ribosome Entry Site-Mediated p53 Translation in Cancer Cells with Defective p53 Response to DNA Damage. *Mol Cell Biol* **35**, 4006-4017, doi:10.1128/MCB.00365-15 (2015).

34   Ungureanu, N. H. *et al.* Internal ribosome entry site-mediated translation of Apaf-1, but not XIAP, is regulated during UV-induced cell death. *J Biol Chem* **281**, 15155-15163, doi:10.1074/jbc.M511319200 (2006).

35   Thomas, J. D. & Johannes, G. J. Identification of mRNAs that continue to associate with polysomes during hypoxia. *RNA* **13**, 1116-1131, doi:10.1261/rna.534807 (2007).

36   Barbosa, C., Peixeiro, I. & Romao, L. Gene Expression Regulation by Upstream Open Reading Frames and Human Disease. *PLOS GENETICS* **9**, e1003529, doi:10.1371/journal.pgen.1003529 (2013).

37   Calvo, S. E., Pagliarini, D. J. & Mootha, V. K. Upstream open reading frames cause widespread reduction of protein expression and are polymorphic among humans. *Proceedings of the National Academy of Sciences* **106**, 7507-7512, doi:10.1073/pnas.0810916106 (2009).

38   Ingolia, N. T. *et al.* Ribosome profiling reveals pervasive translation outside of annotated protein-coding genes. *Cell Rep* **8**, 1365-1379, doi:10.1016/j.celrep.2014.07.045 (2014).

39   Holcik, M. Could the eIF2α-Independent Translation Be the Achilles Heel of Cancer? *Frontiers in oncology* **5**, 264, doi:10.3389/fonc.2015.00264 (2015).

40   Gunisova, S. & Valasek, L. S. Fail-safe mechanism of GCN4 translational control--uORF2 promotes reinitiation by analogous mechanism to uORF1 and thus secures its key role in GCN4 expression. *Nucleic Acids Res* **42**, 5880-5893, doi:10.1093/nar/gku204 (2014).

41   Vattem, K. M. & Wek, R. C. Reinitiation involving upstream ORFs regulates ATF4 mRNA translation in mammalian cells. *Proceedings of the National*

Academy of Sciences of the United States of America **101**, 11269-11274, doi:10.1073/pnas.0400541101 (2004).

42   Poyry, T. A., Kaminski, A., Connell, E. J., Fraser, C. S. & Jackson, R. J. The mechanism of an exceptional case of reinitiation after translation of a long ORF reveals why such events do not generally occur in mammalian mRNA translation. *Genes Dev* **21**, 3149-3162, doi:10.1101/gad.439507 (2007).

43   Koh, D. C., Edelman, G. M. & Mauro, V. P. Physical evidence supporting a ribosomal shunting mechanism of translation initiation for BACE1 mRNA. *Translation (Austin)* **1**, e24400, doi:10.4161/trla.24400 (2013).

44   Chew, G. L., Pauli, A. & Schier, A. F. Conservation of uORF repressiveness and sequence features in mouse, human and zebrafish. *Nat Commun* **7**, 11663, doi:10.1038/ncomms11663 (2016).

45   Lee, S. *et al.* Upregulation of eIF5B controls cell-cycle arrest and specific developmental stages. *Proc Natl Acad Sci U S A* **111**, E4315-4322, doi:10.1073/pnas.1320477111 (2014).

46   Terenin, I. M., Dmitriev, S. E., Andreev, D. E. & Shatsky, I. N. Eukaryotic translation initiation machinery can operate in a bacterial-like mode without eIF2. *Nat Struct Mol Biol* **15**, 836-841, doi:10.1038/nsmb.1445 (2008).

47   Ho, J. J. D. *et al.* Oxygen-Sensitive Remodeling of Central Carbon Metabolism by Archaic eIF5B. *Cell Reports* **22**, 17-26, doi:10.1016/j.celrep.2017.12.031 (2018).

48   Ross, J. A. *et al.* Eukaryotic initiation factor 5B (eIF5B) provides a critical cell survival switch to glioblastoma cells via regulation of apoptosis. *Cell Death Dis* **10**, 57, doi:10.1038/s41419-018-1283-5 (2019).

49   Dey, S. *et al.* Both transcriptional regulation and translational control of ATF4 are central to the integrated stress response. *J Biol Chem* **285**, 33165-33174, doi:10.1074/jbc.M110.167213 (2010).

50   Chan, C. P., Kok, K. H., Tang, H. M., Wong, C. M. & Jin, D. Y. Internal ribosome entry site-mediated translational regulation of ATF4 splice variant in mammalian unfolded protein response. *Biochim Biophys Acta* **1833**, 2165-2175, doi:10.1016/j.bbamcr.2013.05.002 (2013).

51   Pakos-Zebrucka, K. *et al.* The integrated stress response. *EMBO Rep* **17**, 1374-1395, doi:10.15252/embr.201642195 (2016).

52   Chen, D. *et al.* ATF4 promotes angiogenesis and neuronal cell death and confers ferroptosis in a xCT-dependent manner. *Oncogene* **36**, 5593-5608, doi:10.1038/onc.2017.146 (2017).

53   Iurlaro, R. & Munoz-Pinedo, C. Cell death induced by endoplasmic reticulum stress. *FEBS J* **283**, 2640-2652, doi:10.1111/febs.13598 (2016).

54   Yoon, H. *et al.* p27 transcriptionally coregulates cJun to drive programs of tumor progression. *Proc Natl Acad Sci U S A* **116**, 7005-7014, doi:10.1073/pnas.1817415116 (2019).

55   Hnit, S. S. *et al.* p27(Kip1) signaling: Transcriptional and post-translational regulation. *Int J Biochem Cell Biol* **68**, 9-14, doi:10.1016/j.biocel.2015.08.005 (2015).

56   Kullmann, M., Gopfert, U., Siewe, B. & Hengst, L. ELAV/Hu proteins inhibit p27 translation via an IRES element in the p27 5'UTR. *Genes Dev* **16**, 3087-3099, doi:10.1101/gad.248902 (2002).

57   Gopfert, U., Kullmann, M. & Hengst, L. Cell cycle-dependent translation of p27 involves a responsive element in its 5 '-UTR that overlaps with a uORF. *HUMAN MOLECULAR GENETICS* **12**, 1767-1779, doi:10.1093/hmg/ddg177 (2003).

58   Lim, S. & Kaldis, P. Cdks, cyclins and CKIs: roles beyond cell cycle regulation. *Development* **140**, 3079-3093, doi:10.1242/dev.091744 (2013).

CHAPTER 2

Eukaryotic Initiation Factor 5B (eIF5B) cooperates with eIF1A and eIF5 to facilitate uORF2-mediated repression of ATF4 translation

Joseph Ross,* **Kamiko Bressler,*** and Nehal Thakor

* Contributed equally as co-first authors

2.1 Abstract

A variety of cellular stresses lead to global translation attenuation due to phosphorylation of the alpha (α) subunit of eIF2, which decreases the availability of the eIF2-GTP-Met-tRNA ternary complex. However, a subset of mRNAs continues to be translated by non-canonical mechanisms under these conditions. In fact, although translation initiation of ATF4 is normally repressed by a uORF, decreased the availability of ternary complex leads to increased translation of the main ATF4-coding ORF. We show here that siRNA-mediated depletion of eIF5B—which can substitute for eIF2 in delivering initiator-tRNA—leads to increased levels of ATF4 protein in mammalian cells. This de-repression is not due to phosphorylation of eIF2α under conditions of eIF5B depletion. Although eIF5B depletion leads to a modest increase in the steady-state levels of ATF4 mRNA, we show by polysome profiling that the depletion of eIF5B enhances ATF4 expression primarily at the level of translation. Moreover, eIF5B silencing increases the expression of an ATF4-luciferase translational reporter by a mechanism requiring the repressive uORF2. Further experiments suggest that eIF5B cooperates with eIF1A and eIF5, but not eIF2A, to facilitate the uORF-mediated repression of ATF4 translation.

2.2 Introduction

Translation of mRNA is critical, yet highly energy-intensive, necessitating its stringent regulation.[1] Moreover, dysregulation of translation causes pathophysiological disorders, such as cancer.[2] Eukaryotic translation is regulated primarily at the initiation

23

stage, involving more than a twelve eIFs.[3] Physiological stress conditions lead to modifications of key eIFs, attenuating global mRNA translation. For example, phosphorylation of eIF2α is a well-characterized mechanism for preventing the translation of most mRNAs. However, non-canonical translation initiation mechanisms allow for the selective translation of a subset of mRNAs under such conditions.[1,3,4]

eIF2 is required to form the 'ternary complex', which delivers the initiator-tRNA to the 40S ribosomal subunit and is essential for translation initiation.[3] eIF2 exists in either a GDP- or GTP-bound state. Hydrolysis of eIF2-bound GTP is required for the transfer of initiator-tRNA to the 40S ribosomal subunit, releasing GDP. The exchange of GDP for GTP is catalyzed by the guanine exchange factor, eIF2B, and is necessary for the regeneration of the active ternary complex.[3] In response to a wide variety of stresses, such as viral infection, osmotic shock, or hypoxia, the alpha (α) subunit of eIF2 is phosphorylated at serine 51, increasing its binding affinity for eIF2B and sequestering both proteins in an inactive complex (reviewed in Ref. 5). The cellular concentration of eIF2B is limiting, such that even a low proportion of eIF2α phosphorylation results in inhibition of ternary complex re-formation.[5] Consequently, translation initiation is attenuated for most mRNAs. There are four kinases that act to phosphorylate eIF2α in response to stress: HRI, PKR, GCN2, PERK; collectively, the down-regulation of global translation mediated by these proteins and eIF2 is known as the ISR (reviewed in Ref. 7).

Although the global translation is inhibited during stress conditions, the translation of many mRNAs is unaffected by phosphorylation of eIF2α. In fact, the translation of some mRNAs is increased under conditions of eIF2α phosphorylation, such as ATF4. The *ATF4* mRNA encodes two short uORFs in its 5' UTR. uORFs are mRNA elements in the 5' UTR

of a protein-coding gene with a start codon that upstream, and often out of frame with the main coding sequence.[6] As ribosomes load onto the 5' cap of mRNA transcripts and scan for the first start codon, uORFs typically disrupt the translation of the downstream coding sequence. In the case of the ATF4 transcript, the 5'-most uORF (uORF1) encodes just 3 codons, while uORF2 encodes 59 codons and overlaps the start codon of the main ATF4 ORF.[7] Under normal conditions—when the ternary complex is relatively abundant—these uORFs engage the ribosome and initiation at uORF2 prevents initiation at the main coding sequence [8], resulting in low levels of ATF4 translation initiation (reviewed in Ref. 5). However, during stress conditions, the availability of the ternary complex becomes limited, which increases the probability that ribosomes will skip uORF2 without initiating. Therefore, when the ternary complex concentration is low, more ribosomes will bypass uORF2 and initiate translation of the main coding sequence.[8]

ATF4 regulates the transcription of many stress-response genes and is a master regulator of cellular adaptation to stress.[9] ATF4 binds to C/EBP-ATF response element (CARE) sequences of its target genes, including C/EBP homologous protein (CHOP), which is also a transcription factor that increases expression of a set of stress-response genes.[9,10] Another downstream target of ATF4 is GADD34, which acts as a point of negative feedback in the ISR: when activated, GADD34 binds and activates protein phosphatase 1 (PP1), thus reversing the phosphorylation of eIF2α and inactivating the ISR.[10,11]

A recent body of evidence suggests that another initiation factor, eIF5B, is able to substitute for eIF2 functionality in at least some contexts. For instance, under standard growth conditions, XIAP is produced *via* canonical eIF2-dependent translation initiation.

However, under conditions of cellular stress and eIF2α phosphorylation, IRES-dependent translation of *XIAP* mRNA relies on eIF5B.[12] eIF5B is homologous to bacterial and archaeal IF2, which delivers Met-tRNA-fMet to bacterial/archaeal ribosomes.[13,14] Under standard conditions, eIF5B is responsible for assisting in the joining of the 40S and 60S ribosomal subunits, as well as playing a role in stabilizing initiator-tRNA binding.[15] eIF5B was also shown to deliver initiator-tRNA into the P-site of the ribosome in an eIF2-independent translation initiation mechanism utilized by the CSFV and HCV IRESs.[16-18] Thus, eIF5B appears to be capable of substituting for eIF2 in initiator-tRNA-delivery to the ribosome. Additionally, eIF5B was shown to act as an essential translation factor during hypoxia by facilitating initiator-tRNA delivery to ribosomes for efficient cap-dependent translation of hypoxia-response proteins in glioblastoma cells.[19] We have recently demonstrated a role for eIF5B in the non-canonical translation of several anti-apoptotic and pro-survival proteins involved in glioblastoma survival and resistance to TRAIL.[20] In yeast cells, eIF5B has been shown to regulate translation of upstream open reading frame (uORF)-containing mRNAs involved in amino acid biosynthesis.[21] In mammalian cells, eIF5B has been shown to regulate cell cycle progression *via* regulating uORF-containing mRNAs such as *p27* and *p21*.[22]

These findings suggest a role for eIF5B in non-canonical mechanisms of translation initiation under cellular stress conditions. As eIF5B can apparently substitute for eIF2α in delivering initiator-tRNA during translation [16-19], we hypothesized that eIF5B might play a role in the uORF-mediated regulation of *ATF4* translation. We show here that depletion of eIF5B by RNAi leads to increased levels of ATF4 protein in two cell lines (HEK293T and U20S), which is not due to general phosphorylation of eIF2α under conditions of eIF5B

depletion. Depletion of eIF5B also leads to increased mRNA and protein levels of a downstream member of the ATF4 regulon, GADD34. Although eIF5B depletion leads to a modest increase in the steady-state levels of *ATF4* mRNA, a robust increase in *ATF4* translation is observed by polysome profiling analysis, suggesting that eIF5B represses ATF4 expression primarily at the level of translation. Moreover, eIF5B depletion leads to increased expression of an ATF4-luciferase translational reporter, and this de-repression requires intact uORF2. Finally, depletion of eIF1A and eIF5 each cause increased expression of ATF4, which is not synergistic with that caused by eIF5B depletion, suggesting that eIF5B cooperates with each of these factors in order to repress *ATF4* translation. Together, our data suggest that eIF5B facilitates the uORF-mediated repression of *ATF4* translation.

2.3 Materials and Methods

2.3.1 Cell Culture and Reagents

All cell lines were propagated in Dulbecco's high modified Eagle's medium (DMEM; HyClone) with 4 mM L-glutamine, 4500 mg/L glucose, and 1 mM sodium pyruvate, supplemented with 10% fetal bovine serum (FBS; Gibco) and 1% penicillin-streptomycin (Gibco). Cells were incubated at 37 ºC in a humidified 5% CO_2 incubator. Cell lines were routinely tested for mycoplasma contamination with a PCR mycoplasma detection kit (ABM). Reverse transfections were carried out using Lipofectamine RNAiMAX (Invitrogen) according to the manufacturer's instructions. Non-specific control siRNA (siC) was obtained from Qiagen. Stealth RNAiTM siRNAs targeting eIF5B (HSS114469/70/71) were obtained from Invitrogen. siRNA smart pools targeting eIF1A

(M-011262-02-0005), eIF2A (M-014766-01-0005), and eIF5 (M-021336-00-0005) were obtained from Dharmacon. Tunicamycin was obtained from Sigma-Aldrich.

2.3.2 Western Blotting

HEK293T cells were seeded at 200,000 cells/well (U20S cells were seeded at 300,000 cells/well) and reverse-transfected in 6-well plates. After 96 hours of incubation, cells were harvested in RIPA lysis buffer supplemented with protease and phosphatase inhibitors. Equal amounts of soluble protein (typically 25 μg per well) were resolved by SDS-PAGE and transferred onto nitrocellulose membranes (GE healthcare). Primary antibodies were detected with anti-rabbit-HRP conjugate (Abcam) in an AI600 imager (GE) and densitometry performed using the AI600 analysis software.

2.3.3 Polysome Profiling

HEK293T cells were seeded at 1 million cells per plate and reverse transfected in two 10-cm Petri plates per condition. After 96 hours, the control or eIF5B depleted cells were pooled, lysed in RNA lysis buffer, and subjected to polysome profiling as previously described [12,23]. Gradients were fractionated using a BR-188 density gradient fractionation system (BRANDEL). In the experiment presented in Figure 2.3, the levels of ATF4 mRNA are normalized to β-actin mRNA. In the experiment shown in Figure 2.4, the fractions were spiked with 100 ng of an *in vitro* transcribed chloramphenicol acetyltransferase (CAT) RNA, to ensure technical consistency in RNA isolation [12]. RNA was isolated essentially as described [23] except that proteinase K treatment was replaced by incubation with 1% SDS

at 65ºC for 1 min, and hot acid phenol:chloroform (5:1; Ambion) was used to extract the RNA for RT-qPCR analysis.

2.3.4 Luciferase Reporter Assays

HEK293T cells were seeded at 8000 cells per well in a 96-well plate and reverse transfected with control or eIF5B-specific siRNAs. After 48 hours, the cells were forward transfected with plasmids encoding the following ATF4-luc reporters: WT (p759), Mut1 (p760), Mut2 (p761), and Mut1+2 (p762). The ATF4-luciferase reporters were a kind gift from Dr. Ronald Wek [24]. After a further 48 hours, the cells were lysed and luciferase activity was measured using a firefly luciferase assay kit (E1500; Promega) and a Cytation 5 plate reader (BioTek). Immediately following the readings, RNA (for RT-qPCR analysis) was extracted from the lysates as described above.

2.3.5 RT-qPCR

After ethanol precipitating the RNA, cDNA was generated from equal volumes of RNA using the qScript cDNA synthesis kit (Quanta Biosciences). Quantitative PCR was performed in a CFX-96 real-time thermocycler (Bio-Rad) with PerfeCTa SYBR Green SuperMix (Quanta Biosciences) according to the manufacturer's instructions. Negative controls without template DNA were run in triplicate. Each reaction was run in triplicate with the following cycle conditions: 1 cycle at 95°C for 3 min followed by 45 cycles of 95°C for 15 s, the annealing temperature of 55°C for 35 s, and 72°C for 1 min. A melting curve step was added to check the purity of the PCR product. This step consisted of a ramp of the temperature from 65 to 95°C at an increment of 0.5°C and a hold for 5 seconds at

each step. Expression levels of ATF4 and GADD34 mRNAs (relative to β-actin mRNA) were determined using the ΔCt method. All other expression levels were determined by the standard curve method.

2.3.6 Statistical Analyses

Unless otherwise specified, all quantitative data represent the mean ± standard error on the mean (SEM) for at least 3 independent biological replicates. Statistical significance was determined by an unpaired, two-tailed t-test without assuming equal variance. The significance level was set at a p-value of 0.05. Data were analyzed using GraphPad Prism, version 7.

2.4 Results

2.4.1. eIF5B represses ATF4 independently of eIF2α.

Depletion of eIF5B led to a significant increase in ATF4 protein levels in HEK293T cells (~3.7-fold; Figure 2.1), suggesting a repressive role for eIF5B in ATF4 expression. A similar increase in ATF4 levels was observed in U20S cells upon eIF5B depletion (~5-fold; Figure 2.2), suggesting that this repressive role is not limited to the HEK293T cell line. As ATF4 levels are known to be upregulated by eIF2α-phosphorylation, we determined whether eIF5B depletion might be indirectly enhancing ATF4 levels through general stress-mediated phosphorylation of eIF2α. Levels of total and phospho-eIF2α were unchanged upon eIF5B depletion in HEK293T (Figure 2.1). In U2OS, eIF5B depletion led to a small increase in total eIF2α, while P-eIF2α remained unchanged (Figure 2.2). These

results indicate that depletion of eIF5B does not lead to increased phosphorylation of eIF2α and suggest that eIF5B might directly affect the expression of ATF4.

To confirm whether eIF5B plays a functional role in ATF4 regulation, we assessed the impact of eIF5B depletion on a downstream member of the ATF4 regulon, GADD34. Depletion of eIF5B led to roughly a 3.5- and a 3-fold increase in GADD34 protein levels in HEK293T and U2OS, respectively (Figure 2.1 and Figure 2.2). The RT-qPCR analysis revealed an increase in steady-state levels of the ATF4-encoding mRNA of ~2.2- and 5-fold in HEK293T and U2OS, respectively (Figure 2.1 and Figure 2.2), suggesting that eIF5B might repress transcription and/or promote turnover of the ATF4 mRNA. Similarly, the mRNA encoding GADD34 increased upon eIF5B depletion by ~3- and 30-fold in HEK293T and U2OS, respectively (Figure 2.1 and Figure 2.2). The increase in steady-state levels of GADD34 mRNA upon silencing eIF5B was expected, as GADD34 is activated by ATF4 at the level of transcription. Taken together, the data indicate that eIF5B represses ATF4 expression and, consequently, the ATF4-mediated transcriptional regulon.

Figure 2.1 Depletion of eIF5B leads to increased levels of the ATF4 protein. HEK293T cells were reverse-transfected with a non-specific control siRNA (siC) or an eIF5B-specific siRNA pool (si5B), incubated 96 hours, harvested in RIPA lysis buffer, and 20 µg of total protein resolved by SDS-PAGE before performing immunoblotting. (A) Representative images of immunoblots probing for eIF5B, ATF4, eIF2α, P-eIF2α, GADD34, or β-actin (internal control). (B-H) Quantitation of eIF5B (B), ATF4 (C), eIF2α (D), P-eIF2α (E), or GADD34 (F), normalized to β-actin, from HEK293T cells. (G, H) Total RNA was isolated from control or eIF5B depleted HEK263T cells and subjected to RT-qPCR analysis of steady-state mRNA levels for ATF4 (G) or GADD34 (H), normalized to β-actin mRNA. Data are expressed as mean ± SEM for at least 3 (B-F) and up to 4 (G, H) independent biological replicates. *, $p < 0.05$; **, $p < 0.01$; ***, $p < 0.001$; ****, $p < 0.0001$.
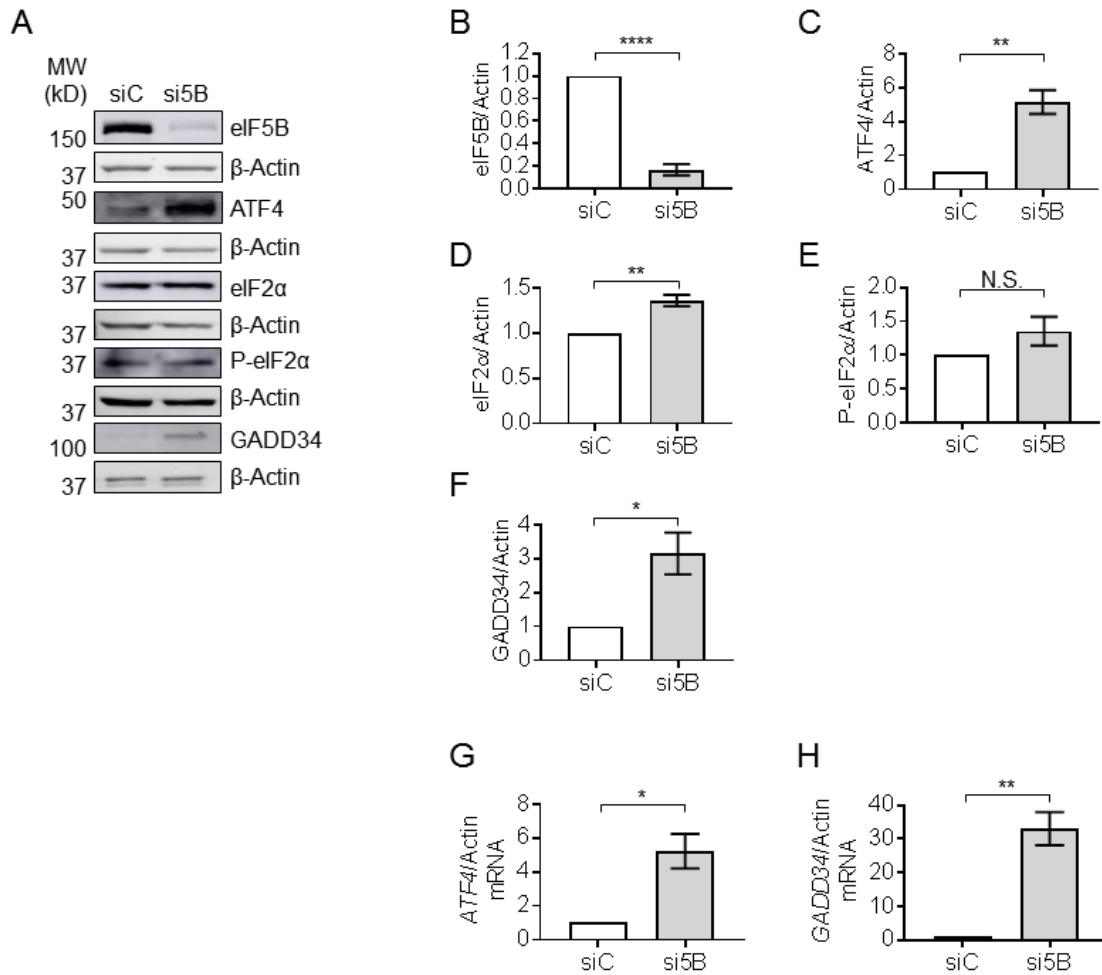
Figure 2.2 Depletion of eIF5B leads to increased levels of the ATF4 protein in U2OS cells. U2OS were reverse-transfected with a non-specific control siRNA (siC) or an eIF5B-specific siRNA pool (si5B), incubated 96 hours, harvested in RIPA lysis buffer, and 20 µg of total protein resolved by SDS-PAGE before performing immunoblotting. (A) Representative images of immunoblots probing for eIF5B, ATF4, eIF2α, P-eIF2α, GADD34, or β-actin (internal control). (B-F) Quantitation of eIF5B (B), ATF4 (C), eIF2α (D), P-eIF2α (E), or GADD34 (F), normalized to β-actin, from U2OS cells. (G, H) Total RNA was isolated from control or eIF5B-depleted U2OS cells and subjected to RT-qPCR analysis of steady-state mRNA levels for ATF4 (G) or GADD34 (H), normalized to β-actin mRNA. Data are expressed as mean ± SEM for at least 3 (B-E, G, H) and up to 4 (F) independent biological replicates. *, $p < 0.05$; **, $p < 0.01$; ***, $P < 0.001$; ****, $p < 0.0001$.

2.4.2 eIF5B represses translation of ATF4.

Steady-state levels of the *ATF4*-encoding mRNA increased ~2.3-fold upon eIF5B depletion in HEK293T cells (Figure 2.1), lower than the magnitude of the effect on ATF4 protein levels (~3.7-fold; Figure 2.1). This suggests that eIF5B might influence ATF4 levels post-transcriptionally. To investigate whether eIF5B represses the translation of *ATF4* mRNA, we conducted polysome profiling to determine the association of *ATF4* mRNA with translating polyribosomes versus monoribosomes. In this assay, cell lysates were fractionated by ultracentrifugation on a sucrose density gradient to separate monosomes from polysomes. Total RNA was isolated from each fraction and RT-qPCR was performed to quantify the association of an mRNA of interest with each fraction. The ratio of mRNA associated with polysomes versus monosomes gives a measure of translation efficiency, independent of steady-state mRNA levels.[12,23] The overall polysome profile of HEK293T cells was not drastically altered by silencing eIF5B (Figure 2.3 and Figure 2.4), indicating a minimal effect of eIF5B depletion on global translation. However, the proportion of *ATF4* mRNA associated with polysomes versus monosomes increased ~5-fold in response to eIF5B depletion (Figure 2.3), indicating an increased translation of *ATF4*. This was corroborated by an independent experiment (Figure 2.4). The observed effect of eIF5B on steady-state levels of the *ATF4* mRNA (Figure 2.1) might reflect an indirect effect of eIF5B on transcription or be a consequence of mRNA stabilization due to increased poly-ribosomal transit. Together, the results indicate that eIF5B downregulates *ATF4* at the translational level in HEK293T cells.
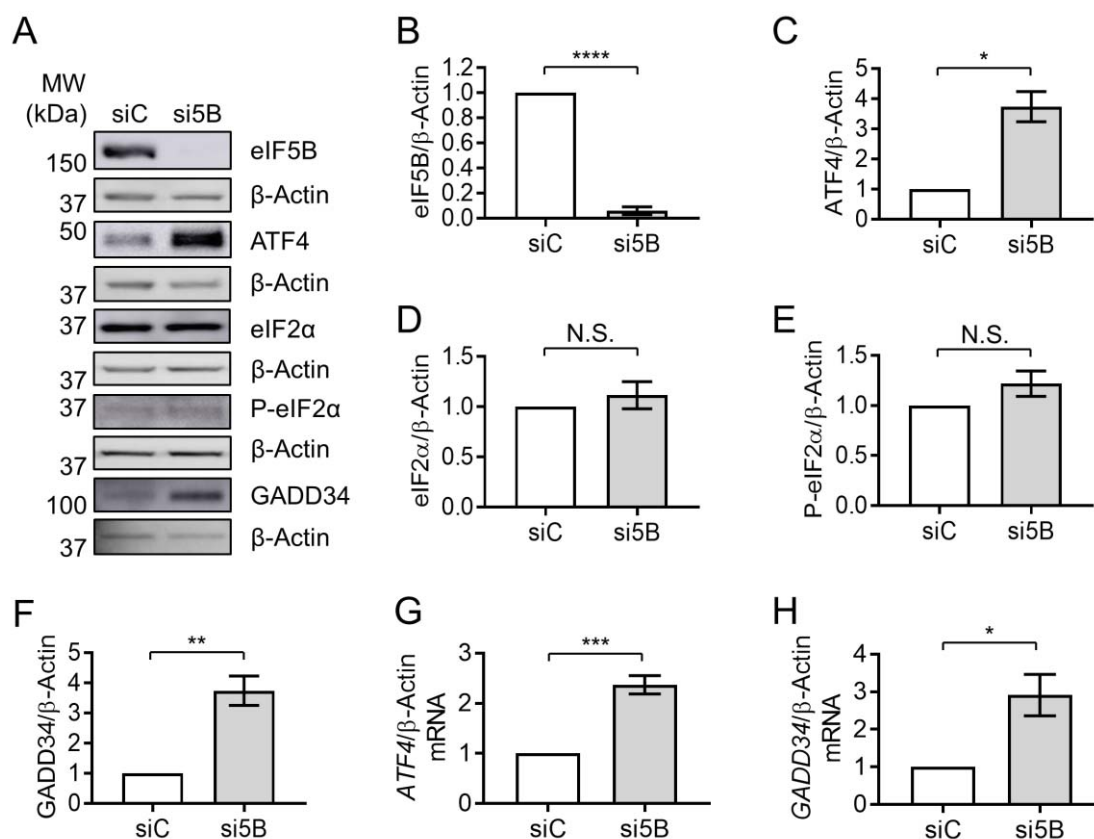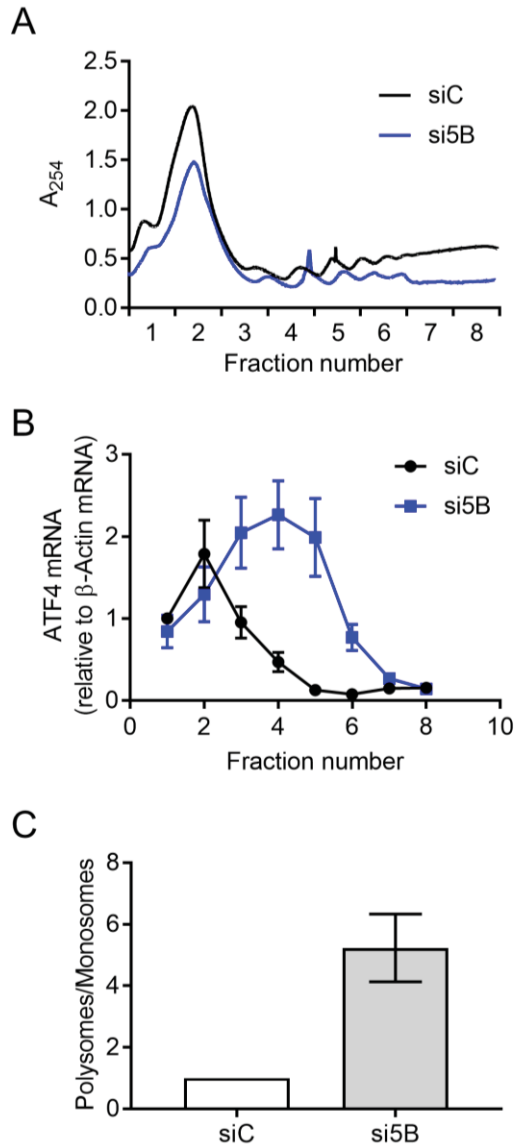
Figure 2.3 Depletion of eIF5B leads to increased translation of *ATF4*. HEK293T cells were reverse-transfected with a non-specific control siRNA (siC) or an eIF5B-specific siRNA pool (si5B), incubated 96 hours, harvested in RNA lysis buffer, and subjected to polysome profiling analysis. (A) A representative polysome profile from control versus eIF5B depleted HEK293T cells. (B) The proportion of *ATF4* mRNA (relative to *β-actin* mRNA) for each fraction from the panel (A). (C) Fractions 1-2 (representing monosomes) were pooled, as were fractions 3-8 (representing polysomes). The ratio of polysomes/monosomes is shown for a representative experiment. Data in panels B and C are expressed as the mean ± SD for technical triplicates. Assistance was received in this experiment from Dr. Joe Ross. An independent experiment is shown in Figure 2.4.
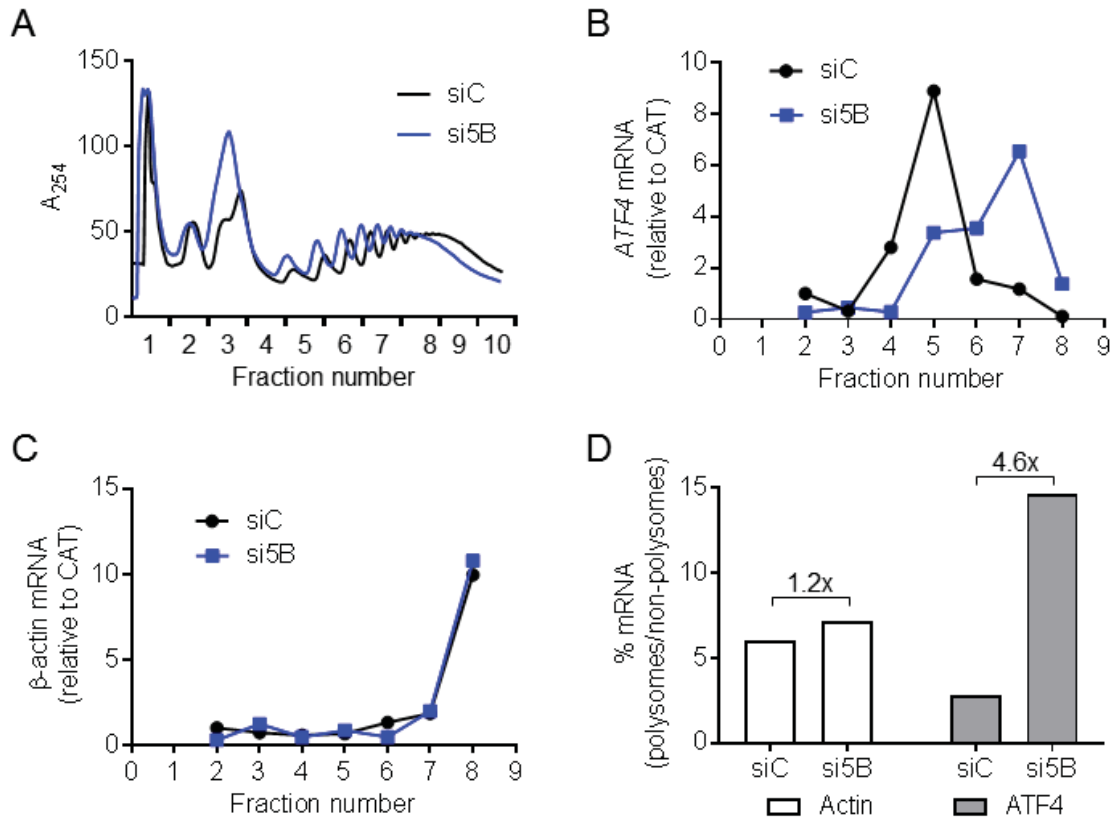
Figure 2.4 Depletion of eIF5B increases translation of *ATF4* in HEK293T cells. Control and eIF5B depleted HEK293T cells were subjected to polysome profiling analysis as described in materials and methods. (A) Polysome profile from control versus eIF5B depleted cells. (B) The proportion of *ATF4* mRNA for each fraction from panel (A) was normalized to an external control RNA (chloramphenicol acetyltransferase, *CAT*). (C) The proportion of *β-actin* mRNA for each fraction from panel (A) was normalized to *CAT*. (D) Fractions 1-3 (representing monosomes) were pooled, as were fractions 4-10 (representing polysomes). The ratio of polysomes/monosomes is shown. This experiment was performed by Dr. Nehal Thakor.

2.4.3. eIF5B facilitates uORF-mediated repression of ATF4 translation.

The initiation of *ATF4* translation is controlled by two upstream open reading frames (uORFs) (Figure 2.5).[24] A start codon mutation that inactivates the first (uORF1) was shown to decrease expression of luciferase from an ATF4-firefly luciferase fusion mRNA—consistent with a model wherein uORF1 recruits ribosomes onto the mRNA while uORF2, which overlaps the *ATF4* ORF, prevents translation initiation of *ATF4*.[24] As

eIF5B represses the translation of *ATF4*, we tested whether eIF5B represses expression of the ATF4-luc reporter and whether this repression depends on either uORF. Note that these ATF4-luc constructs are transcribed from a heterologous promoter [24] and that we normalized the luciferase activity to steady-state levels of ATF4-luc mRNA in order to ensure that the results reflected the translation of the construct rather than effects on transcription or mRNA turnover. Indeed, depletion of eIF5B led to a ~5-fold increase in translation of wild-type ATF4-luc (Figure 2.5). Mutation of uORF1 led to an overall decrease in ATF4-luc translation, as expected, but depletion of eIF5B still led to a ~5-fold increase (Figure 2.5), suggesting that eIF5B is able to repress *ATF4* translation when uORF1 is inactive. However, eIF5B depletion had no effect on the expression of ATF4-luc possessing either mutated uORF2 or the combined uORF1+2 mutations (Figure 2.5), suggesting that eIF5B represses *ATF4* translation by a mechanism involving the repressive uORF2.
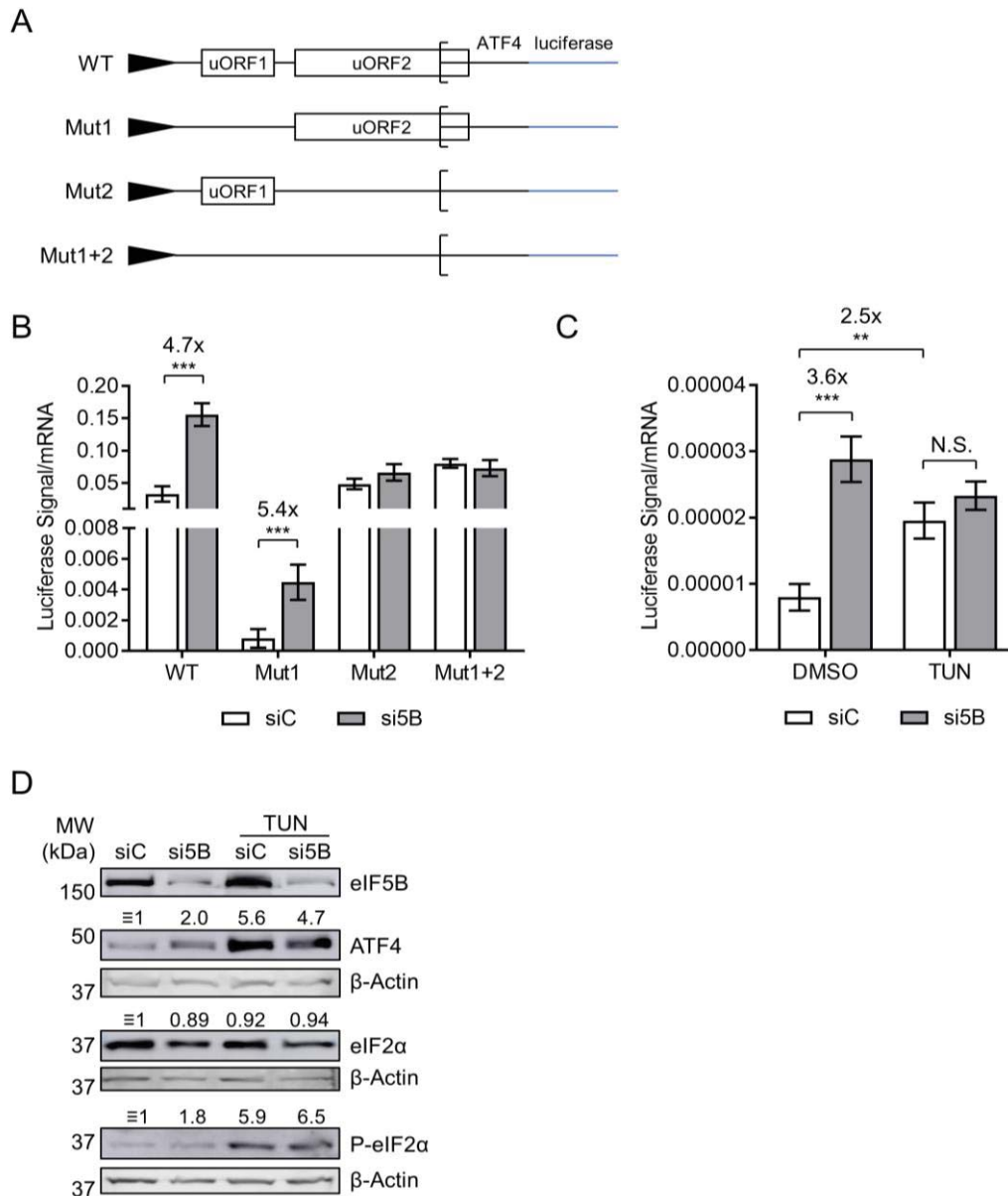
Figure 2.5 eIF5B represses *ATF4* translation by a uORF-dependent mechanism. (A) Schematic representation of the ATF4-firefly luciferase reporter fusions used in this study, all transcribed from a minimal TK promoter. Note that Mut1 and Mut2 possess a start codon mutation (ATG to AGG) that inactivates the regulatory functions of uORF1 and uORF2, respectively. Mut1+2 possesses both mutations. (B) Control or eIF5B depleted HEK293T cells were transfected with the above-mentioned plasmids (48 hours post siRNA transfection). After another 48 hours, the luminescence from firefly luciferase was measured and normalized to the steady-state levels of firefly luciferase mRNA (measured by RT-qPCR). (C) Luciferase levels were measured as in panel (B), except that the cells were treated with 5 µg/mL tunicamycin (TUN) for the last 6 hours of the incubation prior to harvesting. Data are expressed as mean ± SEM for 3 independent replicates. *, $p < 0.05$; **, $p < 0.01$; ***, $P < 0.001$. (D) Immunoblots probing for eIF5B, ATF4, eIF2α, P-eIF2α, or β-actin (internal control). Numbers above the blots represent their quantitation relative to β-actin.

38

2.4.4. eIF5B depletion and eIF2α phosphorylation do not cause a synergistic induction of ATF4.

The decreased availability of ternary complex under conditions of eIF2α phosphorylation leads to decreased translation initiation of uORF2 and increased initiation at the main *ATF4*-coding ORF.[24] As expected, treatment with tunicamycin—which blocks N-glycosylation of proteins, resulting in the accumulation of unfolded proteins and thus eIF2α phosphorylation [25]—increased expression of WT ATF4-luc (~2.5-fold; Figure 2.5). This effect was similar to that of eIF5B depletion (~3.6-fold; Figure 2.5). However, eIF5B depletion caused no further increase in ATF4-luc translation in tunicamycin-treated cells (Figure 2.5). Similar results were obtained when we measured steady-state levels of ATF4 protein (Figure 2.5). As expected, tunicamycin treatment lead to an increase in phosphorylation of eIF2α (Figure 2.5). The lack of synergy between eIF5B depletion and tunicamycin treatment suggests that they converge on a single point of regulation, such as the delivery of initiator-tRNA to the 40S ribosomal subunit or the availability of ternary complex.

2.4.5. eIF5B cooperates with eIF1A and eIF5 to repress ATF4 translation.

eIF1A and eIF5 have recently been shown to compete for binding to eIF5B, suggesting coordination of their activities during translation initiation.[26] Moreover, eIF2A (an initiator tRNA carrier) has been suggested to function synergistically with eIF5B in the eIF2-independent translation of an IRES-containing mRNA.[27] We therefore tested whether any of these eIFs play a role in ATF4 repression. Indeed, depletion of eIF1A and eIF5 led to a ~5- and a 6-fold increase in ATF4 protein levels, respectively, while depletion of

eIF2A had no effect (Figure 2.6). This pattern was matched exactly for expression of the ATF4-luc reporter construct (Figure 2.6), confirming that eIF1A and eIF5 repress ATF4 post-transcriptionally. In order to test whether eIF5B represses ATF4 expression in coordination with eIF1A, eIF2A, or eIF5, we depleted eIF5B either alone or in combination with each of these factors (Figure 2.6). Depletion of eIF5B alone or in combination with the non-specific control siRNA led to a ~3-fold and 2-fold increase in ATF4 levels, respectively, while depletion of eIF5B plus eIF2A led to a similar increase (~3-fold), consistent with the lack of eIF2A-mediated regulation (Figure 2.6). However, depletion of eIF5B in combination with eIF1A or eIF5 led to a ~4-fold and 6-fold increase in ATF4 levels, respectively (Figure 2.6). These increases were no larger than those seen upon depletion of eIF1A or eIF5 alone (Figure 2.6), suggesting that eIF5B depletion does not synergize with depletion of either eIF1A or eIF5. No increase in total or phospho-eIF2α was apparent upon depletion of any factor, confirming that the observed effects on ATF4 are not due to general stress-induced phosphorylation of eIF2α. Together, the data suggest that eIF1A and eIF5 cooperate with eIF5B in order to repress *ATF4* translation.
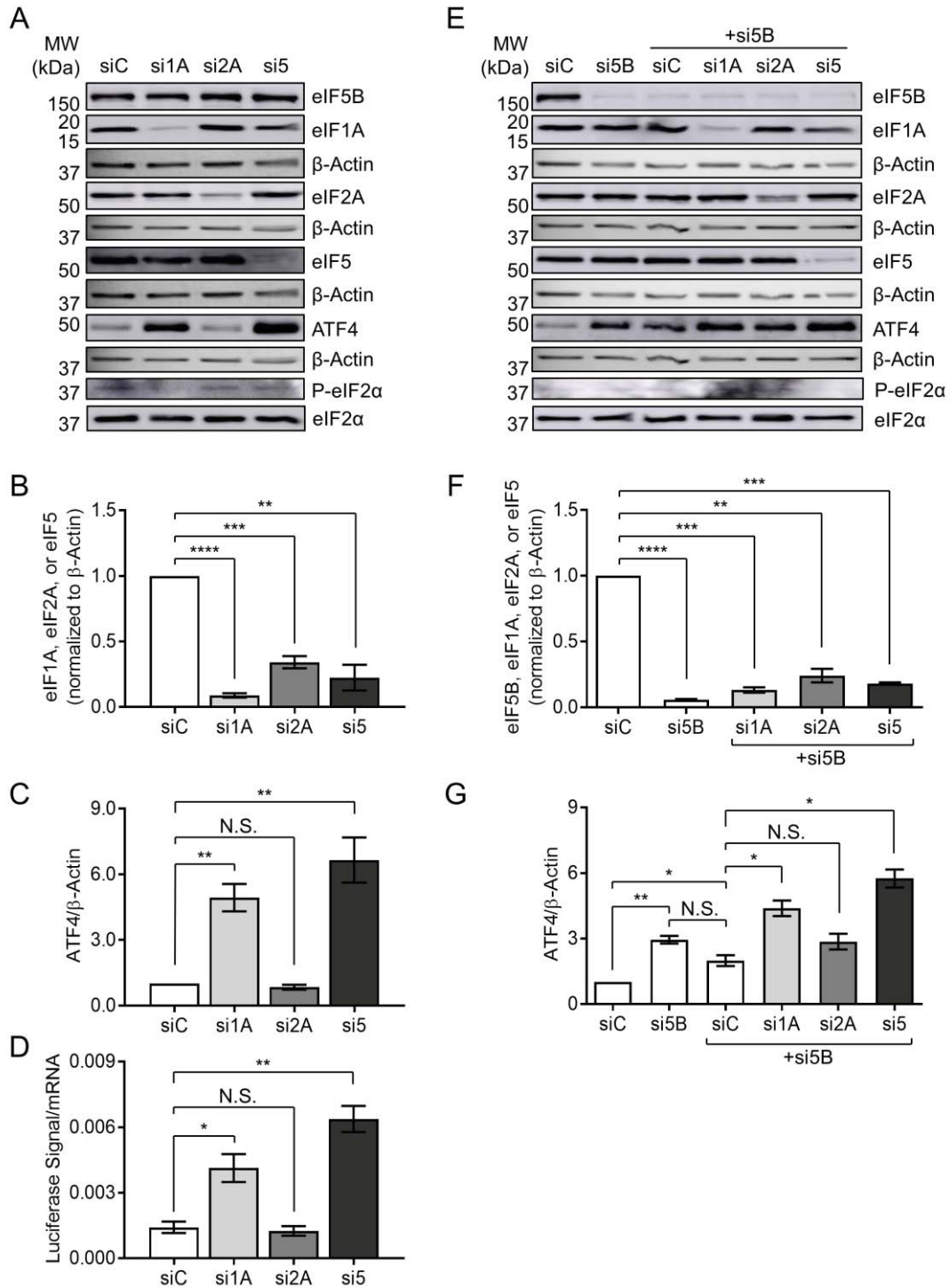
Figure 2.6 eIF5B cooperates with eIF1A and eIF5, but not eIF2A, to repress *ATF4* translation. (A) HEK293T cells were transfected with a control siRNA (siC) or siRNAs targeting eIF1A (si1A), eIF2A (si2A), or eIF5 (si5) and subjected to immunoblotting as described for Figure 2.1. Representative images are shown of immunoblots probing for eIF1A, eIF2A, eIF5, ATF4, eIF2α, P-eIF2α, or β-actin (internal control). (B) Quantitation of eIF1A, eIF2A, or eIF5, each normalized to β-actin. (C) Quantitation of ATF4,

normalized to β-actin. (D) HEK293T cells were depleted of eIF1A, eIF2A, or eIF5, as above, before measuring expression of the WT ATF4-luc reporter construct as in Figure 2.3B. (E) HEK293T cells were transfected with a control siRNA (siC), an siRNA targeting eIF5B (si5B), or si5B in combination with siC, si1A, si2A, or si5. Representative immunoblots probing for eIF5B, eIF1A, eIF2A, eIF5, ATF4, eIF2α, P-eIF2α, or β-actin (internal control), are shown. (F) Quantitation of eIF5B, eIF1A, eIF2A, or eIF5, each normalized to β-actin. (G) Quantitation of ATF4, normalized to β-actin. Data are expressed as mean ± SEM for 3 (panels B-D) or 2 (panels F, G) independent biological replicates. *, $p < 0.05$; **, $p < 0.01$; ***, $P < 0.001$; ****, $p < 0.0001$. Assistance was received in this experiment by Dr. Joe Ross.

2.5 Discussion

In this work, we identify a role for eIF5B in uORF-mediated repression of *ATF4* translation initiation. Depletion of eIF5B leads to increased translation of the *ATF4* transcript, and eIF5B-imposed repression of an ATF4-luciferase translational reporter requires the repressive uORF2 to be intact (Figures 2.1-2.5). Although we observed a modest increase in steady-state levels of the *ATF4* mRNA (Figure 2.1), polysome profiling analysis (Figure 2.3 and Figure 2.4) and translational reporter assays (Figure 2.5) demonstrate that eIF5B represses *ATF4* expression mainly at the level of translation. Although stress, such as ER stress, leads to transcriptional activation of *ATF4* [28], we observed no increase in eIF2α phosphorylation upon eIF5B depletion (Figure 2.1), suggesting that eIF5B depletion leads to increased levels of *ATF4* mRNA by an alternative mechanism. For instance, the effect of eIF5B on steady-state levels of the *ATF4* mRNA might reflect an indirect effect of eIF5B on transcription (e.g. *via* regulation of a transcription factor) or be a consequence of mRNA stabilization due to increased ribosomal transit.

Thus far, uORFs have been found in approximately half of human and mouse transcripts, with varied effects on protein expression—typically, uORFs reduce expression

42

by 30-80%.[29] Interestingly, uORFs are common to certain classes of mRNAs. For instance, they are present in two-thirds of oncogenes and in many genes encoding proteins involved in cell differentiation, cell cycle regulation, and the integrated stress response.[29] Reports have shown that ribosomes encountering uORFs either 1) translate the uORF and stall, causing mRNA decay, 2) translate the uORF and, with some probability, reinitiate at the coding sequence, or 3) scan over the uORF.[6,8] uORFs are known to show varying levels of translational regulation based on the nucleotide sequence surrounding the uORF, the distance of the uORF from the coding sequence (CDS), and the number of the uORFs present.[8] Importantly, as uORFs can cause a high reduction of protein expression (30-80%), they often affect phenotype. Calvo *et al*. (2009) identified uORFs created or deleted by a polymorphism in 509 genes correlating to at least 24 human diseases, including Alzheimer's disease, and several tumor types.[30] To date, three rare uORF-altering mutations have been reported to alter levels of essential proteins and cause human diseases: a hereditary form of thrombocythaemia caused by a mutation which eliminates a uORF, a familial predisposition to melanoma caused by the introduction of a uORF, and a hereditary hypotrichosis caused by disruption of a uORF.[30-32] Notably, 8-12% of melanoma is linked to mutations in CDKN2A of the chromosome 9 p21 locus, in which an alternative start codon is formed which leads to decreased levels of the functional protein.[33] Thus, understanding the mechanisms by which uORFs regulate gene expression has the potential to affect human phenotype and disease.[30]

We show in this work that repression of *ATF4* translation by eIF5B is unaffected by mutation of uORF1, but requires uORF2 to be intact (Figure 2.5). The existing literature indicates that uORF1 promotes *ATF4* translation, as disruption of uORF1 causes decreased

expression of ATF4-luc.[24] Moreover, translation of this uORF1 mutant still increases in the presence of thapsigargin, indicating that upregulation of *ATF4* translation under conditions of eIF2α phosphorylation does not depend on this uORF.[24] Conversely, disruption of uORF2 causes increased expression of ATF4-luc, which becomes insensitive to thapsigargin, indicating that uORF2 is responsible for inhibiting *ATF4* translation initiation when the ternary complex is abundant.[24] Thus, eIF5B appears to play a role in facilitating translation initiation at uORF2 instead of the main ATF4-coding ORF, similar to the situation when the ternary complex is abundant. We also observed increased expression of the WT ATF4-luc construct upon treating the cells with tunicamycin (Figure 2.5). Similar to thapsigargin, tunicamycin leads to phosphorylation of eIF2α [25] and thus limits ternary complex re-formation. Strikingly, the effects of tunicamycin treatment and eIF5B depletion were not additive (Figure 2.5), suggesting that both eIF5B and eIF2 converge on a single point of regulation, such as the delivery of initiator-tRNA during translation initiation. If eIF5B is capable of delivering initiator-tRNA to uORF2, then depletion of eIF5B might decrease the probability of translation initiation at uORF2 and increase the probability of initiation at the *ATF4* main coding ORF, similar to the situation when eIF2α is phosphorylated (Figure 2.7). This could explain why no additive increase in *ATF4* translation was observed when eIF5B depletion was combined with tunicamycin treatment.

Notably, an alternatively spliced variant of the human *ATF4* mRNA can be translated from an IRES.[34] However, this does not represent the majority of human *ATF4* transcripts. Moreover, the ATF4-luc reporter used in this work does not represent the IRES-encoding splice variant.[24] While it is possible that eIF5B regulates the IRES element

present in the *ATF4* splice variant, we observe an increase in *ATF4* translation upon eIF5B depletion (Figure 2.3 and Figure 2.4), which is in direct opposition to the established role of eIF5B in positively regulating IRES-dependent translation.[12,16-18] Moreover, no change (in either direction) was observed upon eIF5B depletion when uORF2 was mutated (Figure 2.5), confirming that eIF5B-mediated repression of *ATF4* involves this uORF. Together, these observations suggest that eIF5B represses translation of human *ATF4* by a uORF- rather than IRES-mediated mechanism, although we cannot rule out the possibility that eIF5B plays an additional role in IRES-mediated translation in the case of the splice variant.

Recent work has shown that eIF2A might function in a complex with eIF5B for the eIF2-independent translation of an IRES-encoding mRNA.[27] In this model, eIF2A functions as the initiator-tRNA carrier while eIF5B provides GTP-, mRNA- and ribosome-binding functions.[27] However, depletion of eIF2A had no effect on ATF4 levels (Figure 2.6). Moreover, the combined depletion of eIF2A and eIF5B had no effect on ATF4 levels above the effect of eIF5B depletion alone (Figure 2.6). These data suggest that eIF2A plays no role in the repression of ATF4 by eIF5B.

In contrast, depletion of eIF1A leads to a robust increase in *ATF4* translation, as did eIF5-depletion (Figure 2.6). Moreover, depletion of eIF1A in combination with eIF5B led to no further increase than depletion of eIF1A alone, and depletion of eIF5 plus eIF5B led to no further increase than depletion of eIF5 alone (Figure 2.6), suggesting that eIF5B cooperates with these factors to repress *ATF4* translation. An interaction between eIF1A and eIF5B is known to promote translation.[35] In fact, eIF5B overexpression has been shown to suppress the effects of a mutation in eIF1A [36], suggesting a certain amount of functional

redundancy. Recent work shows that eIF1A and eIF5 compete for binding to eIF5B in the context of a PIC in canonical translation initiation.[26] eIF5 is the GTPase-activating protein that promotes GTP hydrolysis by eIF2 upon delivery of initiator-tRNA to the start codon, at which point eIF2 is displaced from initiator-tRNA by eIF5B-GTP and is released as an eIF2:eIF5 complex.[37-40] Upon ribosomal subunit joining, eIF5B hydrolyzes GTP and is released along with eIF1A.[41-44] Lin *et al.* (2018) suggest a mechanism for coordination between the steps of start codon selection and ribosomal subunit joining: displacement of eIF2 from initiator-tRNA by eIF5B upon subunit joining may be coupled to the eIF1A-mediated displacement of eIF5 from eIF5B, enabling the eIF2-GDP:eIF5 complex to leave the ribosome.[26]

In *Saccharomyces cerevisiae*, overexpression of eIF5 mimics the effect of eIF2α phosphorylation, promoting translation of the yeast equivalent of the ATF4 protein, GCN4.[37] Specifically, overexpression of eIF5 in yeast increases the levels of an eIF2-eIF5 complex, which prevents eIF2B interaction and thus ternary complex re-formation.[37] Similarly, in human cells, overexpression of eIF5 or its mimic (eIF5MP) perturbs the function of eIF2 and induces *ATF4* translation by delaying re-initiation at uORF2.[45] As eIF5B interacts with eIF5 [26], it is possible that depletion of eIF5B leads to an increase in available eIF5, which would bind eIF2 and prevent ternary complex formation, leading to increased translation of *ATF4* (Figure 2.7). Similarly, eIF5 depletion would prevent GTP hydrolysis by eIF2, slowing its release from the PIC and subsequent reformation of the ternary complex (Figure 2.7). eIF1A depletion would prevent the displacement of eIF5 from eIF5B, slowing the release of eIF5:eIF2-GDP and subsequent reformation of the ternary complex (Figure 2.7). Finally, depletion of eIF5B itself could slow ternary complex

re-formation by preventing the displacement of eIF2-GDP from PIC-bound initiator-tRNA (Figure 2.7). Altogether, we suggest that any perturbation of the stoichiometry of eIF1A, eIF5, and/or eIF5B might lead to decreased translation of uORF2 and, thus, de-repression of ATF4 translation.

Overall, this work demonstrates a role for eIF5B in the uORF2-mediated repression of ATF4 translation—a role which also involves eIF1A and eIF5. Given the prevalence of uORFs in human transcripts, we suggest that eukaryotic initiation factors like eIF5B, eIF1A, and eIF5 might influence the translation of a previously unappreciated number of non-canonically translated mRNAs.
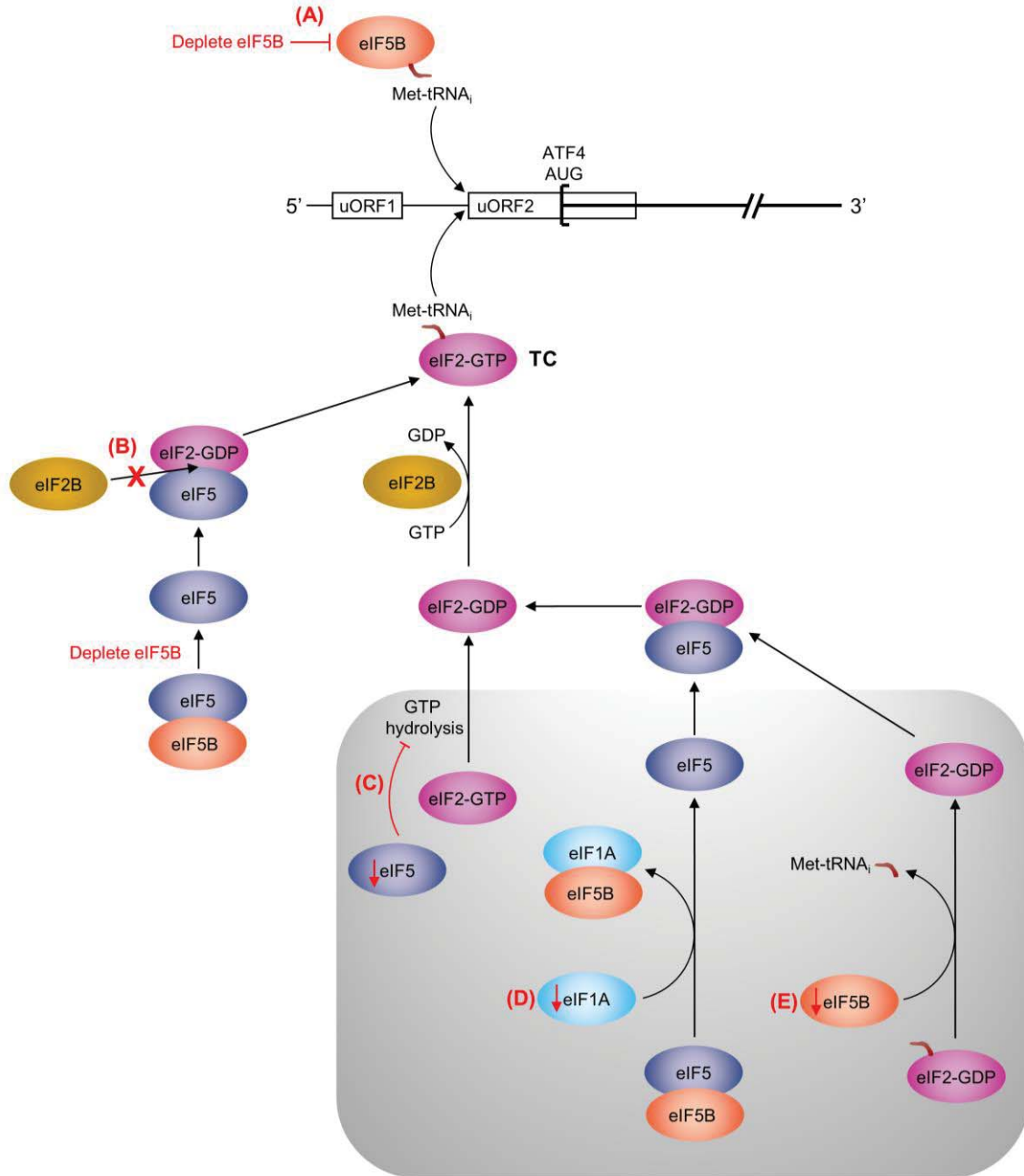
Figure 2.7 Possible mechanisms for uORF2-mediated repression of *ATF4* translation by eIF5B, eIF1A, and eIF5. The *ATF4* mRNA is represented as a horizontal black line, with uORF1 and uORF2 represented as rectangles and the *ATF4* start codon represented as a square bracket. In the established mechanism of ATF4 repression, translation re-initiation will tend to occur at the uORF2 start codon when ternary complex (TC) is abundant; however, when TC abundance is decreased (e.g. by phosphorylation of eIF2α), re-initiation will be delayed, allowing the ribosome to bypass uORF2 and initiate translation of *ATF4* [24]. Here, we propose several potential mechanisms (A-E, highlighted in red), for uORF2-mediated repression of *ATF4* by eIF5B (light orange), eIF5 (dark blue), and

48

eIF1A (light blue). The pre-initiation complex (PIC) is represented by the grey box. Note that this is not meant to be an exhaustive list and that anyone (or any combination) of these mechanisms might be at play. (A) eIF5B might deliver initiator-tRNA to uORF2, providing an alternative to eIF2-GTP (pink). Depletion of eIF5B would consequently decrease translation initiation at the uORF2 start codon, increasing the translation of *ATF4*. (B) As eIF5B interacts with eIF5 [26], depletion of eIF5B could lead to an increase in free eIF5. Available eIF5 can form a complex with eIF2-GDP that can prevent the interaction of eIF2 with eIF2B (yellow), slowing TC re-formation [37,45]. (C) Depletion of eIF5 would inhibit GTP hydrolysis by eIF2 [37-40], preventing its release from the PIC and, subsequently, TC re-formation. (D) Depletion of eIF1A would prevent the displacement of eIF5B from eIF5 [26], inhibiting the release of eIF5 and eIF2 from the PIC and, thus, inhibiting TC re-formation. (E) Depletion of eIF5B would inhibit the displacement of eIF2-GDP from initiator-tRNA [37-40], thus inhibiting TC re-formation.

References

1   Lacerda, R., Menezes, J. & Romao, L. More than just scanning: the importance of cap-independent mRNA translation initiation for cellular stress response and cancer. *Cell Mol Life Sci* **74**, 1659-1680, doi:10.1007/s00018-016-2428-2 (2017).

2   Silvera, D., Formenti, S. C. & Schneider, R. J. Translational control in cancer. *Nat Rev Cancer* **10**, 254-266, doi:10.1038/nrc2824 (2010).

3   Sharma, D. K., Bressler, K., Patel, H., Balasingam, N. & Thakor, N. Role of Eukaryotic Initiation Factors during Cellular Stress and Cancer Progression. *Journal of nucleic acids* **2016**, 8235121-8235119, doi:10.1155/2016/8235121 (2016).

4   Mitchell, S. F. *et al.* The 5'-7-methylguanosine cap on eukaryotic mRNAs serves both to stimulate canonical translation initiation and to block an alternative pathway. *Mol Cell* **39**, 950-962, doi:10.1016/j.molcel.2010.08.021 (2010).

5   Lee, S. *et al.* Upregulation of eIF5B controls cell-cycle arrest and specific developmental stages. *Proceedings of the National Academy of Sciences* **111**, E4315-E4322, doi:10.1073/pnas.1320477111 (2014).

6   Morris, D. R. & Geballe, A. P. Upstream open reading frames as regulators of mRNA translation. *Mol Cell Biol* **20**, 8635-8642 (2000).

7   Young, S. K. & Wek, R. C. Upstream Open Reading Frames Differentially Regulate Gene-specific Translation in the Integrated Stress Response. *JOURNAL OF BIOLOGICAL CHEMISTRY* **291**, 16927-16935, doi:10.1074/jbc.R116.733899 (2016).

8   Starck, S. R. *et al.* Translation from the 5' untranslated region shapes the integrated stress response. *Science* **351**, aad3867, doi:10.1126/science.aad3867 (2016).

9   B'Chir, W. *et al.* The eIF2alpha/ATF4 pathway is essential for stress-induced autophagy gene expression. *Nucleic Acids Res* **41**, 7683-7699, doi:10.1093/nar/gkt563 (2013).

10   Pakos-Zebrucka, K. *et al.* The integrated stress response. *EMBO Rep* **17**, 1374-1395, doi:10.15252/embr.201642195 (2016).

11   Carroll, M., Dyer, J. & Sossin, W. S. Serotonin increases phosphorylation of synaptic 4EBP through TOR, but eukaryotic initiation factor 4E levels do not limit somatic cap-dependent translation in aplysia neurons. *Mol Cell Biol* **26**, 8586-8598, doi:10.1128/MCB.00955-06 (2006).

12   Thakor, N. & Holcik, M. IRES-mediated translation of cellular messenger RNA operates in eIF2α- independent manner during stress. *Nucleic Acids Research* **40**, 541-552, doi:10.1093/nar/gkr701 (2012).

13   Lee, J. H., Choi, S. K., Roll-Mecak, A., Burley, S. K. & Dever, T. E. Universal conservation in translation initiation revealed by human and archaeal homologs of bacterial translation initiation factor IF2. *Proc Natl Acad Sci U S A* **96**, 4342-4347 (1999).

14   Laursen, B. S., Sorensen, H. P., Mortensen, K. K. & Sperling-Petersen, H. U. Initiation of protein synthesis in bacteria. *Microbiol Mol Biol Rev* **69**, 101-123, doi:10.1128/MMBR.69.1.101-123.2005 (2005).

15   Shin, B. S. *et al.* Uncoupling of initiation factor eIF5B/IF2 GTPase and translational activities by mutations that lower ribosome affinity. *Cell* **111**, 1015-1025 (2002).

16   Pestova, T. V., de Breyne, S., Pisarev, A. V., Abaeva, I. S. & Hellen, C. U. eIF2-dependent and eIF2-independent modes of initiation on the CSFV IRES: a common role of domain II. *EMBO J* **27**, 1060-1072, doi:10.1038/emboj.2008.49 (2008).

17   Yamamoto, H. *et al.* Structure of the mammalian 80S initiation complex with initiation factor 5B on HCV-IRES RNA. *Nat Struct Mol Biol* **21**, 721-727, doi:10.1038/nsmb.2859 (2014).

18   Terenin, I. M., Dmitriev, S. E., Andreev, D. E. & Shatsky, I. N. Eukaryotic translation initiation machinery can operate in a bacterial-like mode without eIF2. *Nat Struct Mol Biol* **15**, 836-841, doi:10.1038/nsmb.1445 (2008).

19   Ho, J. J. D. *et al.* Oxygen-Sensitive Remodeling of Central Carbon Metabolism by Archaic eIF5B. *Cell Reports* **22**, 17-26, doi:10.1016/j.celrep.2017.12.031 (2018).

20   Ross, J. A. *et al.* Eukaryotic initiation factor 5B (eIF5B) provides a critical cell survival switch to glioblastoma cells via regulation of apoptosis. *Cell Death Dis* **10**, 57, doi:10.1038/s41419-018-1283-5 (2019).

21   Choi, S. K., Lee, J. H., Zoll, W. L., Merrick, W. C. & Dever, T. E. Promotion of met-tRNAiMet binding to ribosomes by yIF2, a bacterial IF2 homolog in yeast. *Science* **280**, 1757-1760 (1998).

22   Lee, S. *et al.* Upregulation of eIF5B controls cell-cycle arrest and specific developmental stages. *Proc Natl Acad Sci U S A* **111**, E4315-4322, doi:10.1073/pnas.1320477111 (2014).

23   Faye, M. D., Graber, T. E. & Holcik, M. Assessment of selective mRNA translation in mammalian cells by polysome profiling. *J Vis Exp*, e52295, doi:10.3791/52295 (2014).

24   Vattem, K. M. & Wek, R. C. Reinitiation involving upstream ORFs regulates ATF4 mRNA translation in mammalian cells. *Proceedings of the National Academy of Sciences of the United States of America* **101**, 11269-11274, doi:10.1073/pnas.0400541101 (2004).

25   Heifetz, A., Keenan, R. W. & Elbein, A. D. Mechanism of action of tunicamycin on the UDP-GlcNAc:dolichyl-phosphate Glc-NAc-1-phosphate transferase. *Biochemistry* **18**, 2186-2192 (1979).

26   Lin, K. Y., Nag, N., Pestova, T. V. & Marintchev, A. Human eIF5 and eIF1A Compete for Binding to eIF5B. *Biochemistry* **57**, 5910-5920, doi:10.1021/acs.biochem.8b00839 (2018).

27   Kim, E. *et al.* eIF2A, an initiator tRNA carrier refractory to eIF2alpha kinases, functions synergistically with eIF5B. *Cell Mol Life Sci* **75**, 4287-4300, doi:10.1007/s00018-018-2870-4 (2018).

28   Dey, S. *et al.* Both transcriptional regulation and translational control of ATF4 are central to the integrated stress response. *J Biol Chem* **285**, 33165-33174, doi:10.1074/jbc.M110.167213 (2010).

29   Barbosa, C., Peixeiro, I. & Romao, L. Gene Expression Regulation by Upstream Open Reading Frames and Human Disease. *PLOS GENETICS* **9**, e1003529, doi:10.1371/journal.pgen.1003529 (2013).

30   Calvo, S. E., Pagliarini, D. J. & Mootha, V. K. Upstream open reading frames cause widespread reduction of protein expression and are polymorphic among humans. *Proceedings of the National Academy of Sciences* **106**, 7507-7512, doi:10.1073/pnas.0810916106 (2009).

31   Bach, J. *et al.* Coagulation factor XII (FXII) activity, activated FXII, distribution of FXII C46T gene polymorphism and coronary risk. *J Thromb Haemost* **6**, 291-296, doi:10.1111/j.1538-7836.2007.02839.x (2008).

32   Liu, L. *et al.* Mutation of the CDKN2A 5' UTR creates an aberrant initiation codon and predisposes to melanoma. *Nat Genet* **21**, 128-132, doi:10.1038/5082 (1999).

33   Hellen, C. U. T., Pestova, T. V., de Breyne, S., Abaeva, I. S. & Pisarev, A. V. eIF2-dependent and eIF2-independent modes of initiation on the CSFV IRES: a common role of domain II. *The EMBO Journal* **27**, 1060-1072, doi:10.1038/emboj.2008.49 (2008).

34   Chan, C. P., Kok, K. H., Tang, H. M., Wong, C. M. & Jin, D. Y. Internal ribosome entry site-mediated translational regulation of ATF4 splice variant in mammalian unfolded protein response. *Biochim Biophys Acta* **1833**, 2165-2175, doi:10.1016/j.bbamcr.2013.05.002 (2013).

35   Choi, S. K. *et al.* Physical and functional interaction between the eukaryotic orthologs of prokaryotic translation initiation factors IF1 and IF2. *Mol Cell Biol* **20**, 7183-7191 (2000).

36   Fringer, J. M., Acker, M. G., Fekete, C. A., Lorsch, J. R. & Dever, T. E. Coupled release of eukaryotic translation initiation factors 5B and 1A from 80S ribosomes following subunit joining. *Mol Cell Biol* **27**, 2384-2397, doi:10.1128/MCB.02254-06 (2007).

37   Singh, C. R. *et al.* An eIF5/eIF2 complex antagonizes guanine nucleotide exchange by eIF2B during translation initiation. *EMBO J* **25**, 4537-4546, doi:10.1038/sj.emboj.7601339 (2006).

38   Cheung, Y. N. *et al.* Dissociation of eIF1 from the 40S ribosomal subunit is a key step in start codon selection in vivo. *Genes Dev* **21**, 1217-1230, doi:10.1101/gad.1528307 (2007).

39   Unbehaun, A., Borukhov, S. I., Hellen, C. U. & Pestova, T. V. Release of initiation factors from 48S complexes during ribosomal subunit joining and the link between establishment of codon-anticodon base-pairing and hydrolysis of eIF2-bound GTP. *Genes Dev* **18**, 3078-3093, doi:10.1101/gad.1255704 (2004).

40   Kapp, L. D. & Lorsch, J. R. GTP-dependent recognition of the methionine moiety on initiator tRNA by translation factor eIF2. *J Mol Biol* **335**, 923-936 (2004).

41   Acker, M. G. *et al.* Kinetic analysis of late steps of eukaryotic translation initiation. *J Mol Biol* **385**, 491-506, doi:10.1016/j.jmb.2008.10.029 (2009).

42   Acker, M. G., Shin, B. S., Dever, T. E. & Lorsch, J. R. Interaction between eukaryotic initiation factors 1A and 5B is required for efficient ribosomal subunit joining. *J Biol Chem* **281**, 8469-8475, doi:10.1074/jbc.M600210200 (2006).

43   Olsen, D. S. *et al.* Domains of eIF1A that mediate binding to eIF2, eIF3 and eIF5B and promote ternary complex recruitment in vivo. *EMBO J* **22**, 193-204, doi:10.1093/emboj/cdg030 (2003).

44   Marintchev, A., Kolupaeva, V. G., Pestova, T. V. & Wagner, G. Mapping the binding interface between human eukaryotic initiation factors 1A and 5B: a new interaction between old partners. *Proc Natl Acad Sci U S A* **100**, 1535-1540, doi:10.1073/pnas.0437845100 (2003).

45   Kozel, C. *et al.* Overexpression of eIF5 or its protein mimic 5MP perturbs eIF2 function and induces ATF4 translation through delayed re-initiation. *Nucleic Acids Res* **44**, 8704-8713, doi:10.1093/nar/gkw559 (2016).

CHAPTER 3

Depletion of eukaryotic initiation factor 5B (eIF5B) reprograms the transcriptome profile of the cell

A modified version of Figure 3.6 in this section has been published in *Cell Death & Disease* (2019), 10(57)

Eukaryotic initiation factor 5B (eIF5B) provides a critical cell survival switch in glioblastoma cells via regulation of apoptosis.

Joseph Ross, Keiran Vanden Dungen, **Kamiko Bressler**, Mikayla Fredriksen, Divya Khandige Sharma, Nirujah Balasingham, and Nehal Thakor

3.1 Abstract

During the ISR, global translation initiation is attenuated, and rather, non-canonical mechanisms allow specific transcripts to be translated. eIF5B has known roles in canonical translation and has been implicated in several non-canonical mechanisms involving IRES and uORF elements. Our recent study confirmed that eIF5B represses the non-canonical translation of master transcription factor *ATF4*. As such, I hypothesized that eIF5B could be regulating other master transcription factors, and subsequently be largely influencing the transcriptome profile. To this end, I completed the transcriptome analysis. We confirmed the activation of the JNK-arm of the MAPK pathway, as well as enhanced expression of dyskerin in the ribosome biogenesis pathway upon eIF5B depletion. As dyskerin is known to regulate p27, I determined that eIF5B depletion results in upregulation of p27 at the protein level. Through luciferase reporter assays, I determined this regulation to likely be IRES-dependent. Interestingly, flow cytometry confirmed that eIF5B does not have a role in the regulation of the cell cycle, but rather p27 is observed to have a potential cytoprotective role.

Keywords: Eukaryotic initiation factor 5B (eIF5B), internal ribosomal entry sites (IRESs), non-canonical translation initiation, p27, cyclin-dependent kinase inhibitor 1B (CDKN1B), dyskerin, cell cycle regulation

3.2 Introduction

The translation is a complex process involving over twelve initiation factors and is tightly regulated, specifically at initiation, which is the rate-limiting step.[1] When translation is dysregulated, it can result in diseases including cancer. In response to stress conditions such as hypoxia, nutrient or amino acid starvation, or ER stress, one of four kinases become

56

activated: PERK, PKR, HRI, and GCN2, which phosphorylate the alpha (α) subunit of eIF2.[2] Phosphorylation of eIF2α blocks the eIF2B-mediated exchange of GDP for GTP, which consequently prevents the formation of ternary complex.[3] The ternary complex is required to deliver initiator-tRNA to the ribosomal complex, to form the 43S pre-initiation complex. Thus, global translation initiation is attenuated, but specific transcripts involved in adaptation to stress such as *ATF4* are translated through non-canonical mechanisms.[4]

We recently determined that eIF5B represses ATF4, which is a master transcription factor controlling the ISR pathway.[5] As such, I hypothesized that eIF5B may serve to regulate other transcription factors, and largely influence signaling pathways in the cellular transcriptome. We observe in this study through transcriptome analysis that eIF5B is indeed regulating multiple important cellular pathways, and we verify specifically two targets: phosphorylated JNK of the MAPK pathway, and dyskerin of the ribosome biogenesis pathway.

I show through transcriptome analysis that the JNK-MAPK axis is activated upon depletion of eIF5B. MAPK is a complex signaling pathway that regulates extracellular signals to intracellular responses, impacting cellular processes of growth, proliferation, differentiation, and apoptosis.[6] MAPK kinase 4 (MKK4) and MAPK kinase 7 (MKK7) are known to activate JNK through dual phosphorylation on threonine and tyrosine residues (within Thr-Pro-Tyr motif) in response to various cell stresses including heat shock, oxidative stress, cytokines, and growth factor deprivation.[6] The JNK-arm of MAPK signaling is heavily implicated in differentiation and cell death. c-Jun is a direct target of JNK, which dimerizes with c-Fos to form the AP-1 transcription factor, promoting cell death.[7] As JNK is one of the three major groups of MAPK kinases (classical extracellular

signal-regulated kinase (ERK), and p38), we suggest that eIF5B depletion upregulates the JNK arm of the complex MAPK signaling pathway.

Transcriptome analysis showed upregulation of *dyskerin* upon eIF5B depletion, and we thus hypothesized that eIF5B may play a role in ribosome biogenesis. Dyskerin is a pseudouridine synthase encoded by the dyskerin pseudouridine synthase (*DKC1*) gene, and is known to have additional roles in telomere maintenance and splicing of mRNAs.[8] Dyskerin functions in ribonucleoprotein complexes with H/ACA small nucleolar RNAs to catalyze the isomerization between uridines into pseudouridines on rRNA.[8] Interestingly, Bellodi *et al*. (2010) determined that removal of *DKC1* results in a translational defect in the synthesis of proteins including p27, which have IRES-elements in their transcripts.[9] In hypomorphic DKC1[m] mice, IRES-dependent translation initiation of *p27* was severely impaired in the pituitary, due to a defect in the 48S preinitiation complex.[9] This confirms the importance of dyskerin in rRNA modification, which is necessary for proper formation of the ribosomal machinery utilized in IRES-dependent translation. Here, I verified that depletion of eIF5B resulted in upregulation of dyskerin at the protein level. Interestingly, dyskerin has been shown to regulate several IRES-containing transcripts, including *p27*.[9]

p27 is a protein known to be regulated at many levels and has been well studied specifically at the transcriptional and post-translational level. p27 is a CKI which is responsible for cell cycle arrest at the G1 phase.[10] p27 is able to induce cell cycle arrest through binding cyclin-CDK complexes, and through preventing activation of CDK activating kinase (CAK)-mediated phosphorylation of the complex.[10] The transition from resting state (G0) to proliferation is largely dependent on the degradation of p27.[11] Several independent mechanisms were recently uncovered that regulate *p27* translation. During the

cell cycle progression of HeLa cells, *p27* mRNA levels do not change significantly, despite the observed induction or reduction of p27 protein levels, confirming the importance of post-transcriptional regulation.[12] Sustained translation of *p27* under poor growth conditions relies on an IRES element in the 5′-UTR.[13,14] Though the *p27* uORF is known to strongly repress translation, it has been shown that *in vivo* initiation can occur through a 356 nucleotide IRES element positioned downstream of the uORF in the 5' UTR of *p27*.[12]

In addition to its known roles in non-canonical translation, eIF5B has been implicated in cell cycle regulation in multiple studies.[15,16] eIF5B depletion has been associated with increased phosphorylated cell division control 2 (Cdc2), which is a marker for immaturity, suggesting a critical role for eIF5B in cell cycle transitions.[15] eIF5B has been shown to be upregulated in developmental cell states known to have reduced general translation, specifically the transition state of proliferating mammalian cells to G0.[16] When eIF5B was depleted from serum-starved THP cells, G0 arrest was hastened, while eIF5B overexpression promoted maturation and cell death (as opposed to G0).[16] These findings suggest a key role for eIF5B in cell cycle regulation, which I hypothesized could be occurring through non-canonical translational regulation of *p27*.

I show here that eIF5B depletion results in upregulation of dyskerin, and its known regulation target of p27 at the protein level. I confirmed *via* RT-qPCR that p27 upregulation is not occurring at the steady-state mRNA transcript level, and I further suggest *via* luciferase assays that the upregulation is occurring translationally through an IRES-element. Further, I showed that eIF5B depletion is not affecting the regulation of the cell cycle through propidium iodide staining and flow cytometry, but rather the upregulation of p27 supports a cytoprotective role. These results together suggest that eIF5B translationally

represses p27, potentially through its effect on dyskerin and subsequent ribosomal modification.

3.3 Materials and Methods

3.3.1 Cell Culture and Reagents

U343 and HEK 293T were propagated in Dulbecco's high modified Eagle's medium (DMEM; HyClone) with 4 mM L-glutamine, 4500 mg/L glucose, and 1 mM sodium pyruvate, supplemented with 10% fetal bovine serum (FBS; Gibco) and 1% penicillin-streptomycin (Gibco). Cells were incubated at 37 ºC in a humidified 5% CO_2 incubator. Cell lines were routinely tested for mycoplasma contamination with a PCR mycoplasma detection kit (ABM). The identity of U343 was verified by STR analysis. Reverse transfections were carried out using Lipofectamine RNAiMAX (Invitrogen) according to the manufacturer's instructions. Non-specific control siRNA (siC) was obtained from Qiagen. Stealth RNAi™ siRNA targeting eIF5B (HSS114469/70/71) was obtained from Invitrogen, and siRNA targeting p27 (12324S) was obtained by Cell Signaling Tech.

3.3.2 RNA Isolation

U343 cells were seeded at 300,000 cells/well (HEK 293T cells seeded at 200,000 cells/well) and reverse-transfected in 6-well plates. After 96 hours, RNA was isolated essentially as described [17] except that proteinase K treatment was replaced by incubation with 1% SDS at 65ºC for 1 min, and hot acid phenol:chloroform (5:1; Ambion) was used to extract the RNA.

3.3.3 RNA-seq Data Analysis

Data analysis and sequencing was performed using the Illumina NextSeq500 platform, with 75 bp single-end configuration. Illumina TruSeq directional (polyA selection) was used for library construction. The reference genome (Human GRCh37 Ensembl) was downloaded from Illumina iGENOME, and basecalling and demultiplexing were done using the Illumina CASAVA 1.9 pipeline.

Upon initial sequencing, the library quality control was measured *via* FastQC 0.11.5. Reads were then mapped to the human genome (Ensembl, GRCh37) using hisat2 version 2.0.5.[18] SAM files generated by hisat2 were converted to BAM, sorted and indexed using samtools 1.7. Reads mapping to genes were counted using featureCounts version 1.6.1.[19] Differentially expressed genes were detected using DESeq2 1.18.1 Bioconductor package.[20] Genes with adjusted p-values (Bonferroni-Hochberg adjustment for multiple comparisons) less than 0.1 and over the 2-fold change were selected as differentially expressed. Over-represented gene ontology (GO) terms were detected with topGO 2.30.1 bioconductor package.[21] TopGO analysis was conducted separately on up-, down- and all differentially expressed genes. Over-representation analysis of biochemical pathways was performed using GOstats 2.44.2 bioconductor package [22] with pathway data obtained from the Kyoto Encyclopedia of Genes and Genomes (KEGG) *via* KEGG.db 3.2.3 bioconductor package. Similarly to topGO analysis, over-represented pathways were detected separately for up-, down- and all differentially expressed genes. In addition, up- and down-regulated pathways were detected using Generally Applicable Gene set enrichment (GAGE)

61

implemented in a bioconductor package gage 2.28.2.[23] The analysis is performed on log2 fold changes on pathways level and is unidirectional.

3.3.4 Western Blotting

Cells were seeded at 300,000 cells/well for U343, and 200,000 cells/well for HEK 293T, and reverse-transfected in 6-well plates. After 96 hours, cells were harvested in RIPA lysis buffer supplemented with protease inhibitors. Equal amounts of soluble protein (typically 25 µg per well) were resolved by SDS-PAGE and transferred onto nitrocellulose membranes (GE healthcare). Primary antibodies were detected with anti-rabbit-HRP conjugate (Abcam) in an AI600 imager (GE) and densitometry performed using the AI600 analysis software.

3.3.5 Luciferase Reporter Assays

U343 cells were seeded at 10,000 cells per well in a 96-well plate and reverse transfected with control or eIF5B-specific siRNAs. After 48 hours, the cells were forward transfected with plasmids encoding the following p27-luc reporters: ctrl (plasmid control), 5' UTR, Δd, and Δ2. The p27-luciferase reporters were a kind gift from Dr. Ludger Hengst.[12] After a further 48 hours, the cells were lysed and luciferase activity measured using a firefly luciferase assay kit (E1500; Promega) and a Cytation 5 plate reader (BioTek). Immediately following the readings, RNA (for RT-qPCR analysis) was extracted from the lysates as described above.

3.3.6 Flow Cytometry

U343 cells were seeded at 300,000 cells/well and reverse transfected in 6-well dishes with control or eIF5B-specific siRNAs. After 96 hours, the cells were harvested by trypsinization, rinsed with PBS and fixed with 70% ice-cold ethanol. Fixed cells were treated with RNase A (0.625 mg/mL) before staining with 50 µg/mL Propidium Iodide at 37°C for 30 min and determining cellular DNA content on a FACS Canto II flow cytometer (Becton-Dickinson).

3.3.7 RT-qPCR

RNA was isolated using a New England Biolabs Monarch Total RNA Miniprep kit, and cDNA was generated from equal volumes of RNA using the qScript cDNA synthesis kit (Quanta Biosciences). Quantitative PCR was performed in a CFX-96 real-time thermocycler (Bio-Rad) with PerfeCTa SYBR Green SuperMix (Quanta Biosciences) according to the manufacturer's instructions. Negative controls without template DNA were run in duplicate. Each reaction was run in duplicate with the following cycle conditions: 1 cycle at 95°C for 3 min followed by 45 cycles of 95°C for 15 s, the annealing temperature of 55°C for 35 s, and 72°C for 1 min. A melting curve step was added to check the purity of the PCR product. This step consisted of a ramp of the temperature from 65 to 95°C at an increment of 0.5°C and a hold for 5 seconds at each step. Expression levels of p27 mRNAs (relative to β-actin mRNA) were determined using the ΔCt method.

3.3.8 Statistical Analyses

Unless otherwise specified, all quantitative data represent the mean ± standard error on the mean (SEM) for at least 3 independent biological replicates. Statistical significance was determined by an unpaired, two-tailed t-test without assuming equal variance. The significance level was set at a p-value of 0.05. Data were analyzed using GraphPad Prism, version 7.

3.4 Results

3.4.1 eIF5B depletion results in transcriptome-wide changes in signaling pathways

Upon transcriptome analysis, eIF5B depletion was confirmed to result in significant transcriptome-wide changes as observed in biological triplicate (Figure 3.1). The heatmap shows the top 500 differentially expressed genes, with evident differences between eIF5B depleted and control HEK 293T samples (Figure 3.1, red upregulated, green downregulated). Through KEGG analysis, significantly upregulated and downregulated genes were sorted into biologically relevant signaling pathways (Table 3.1, 3.2). Pathways that were significantly upregulated included neuroactive ligand-receptor interaction, Notch signalling, and extracellular matrix (ECM)-receptor interactions (Table 3.1). Pathways that were significantly downregulated included retinol metabolism, osteoclast differentiation, and phenylalanine metabolism (Table 3.2). Transcriptome data confirms that the depletion of eIF5B results in significant transcriptome-wide changes in signaling pathways.
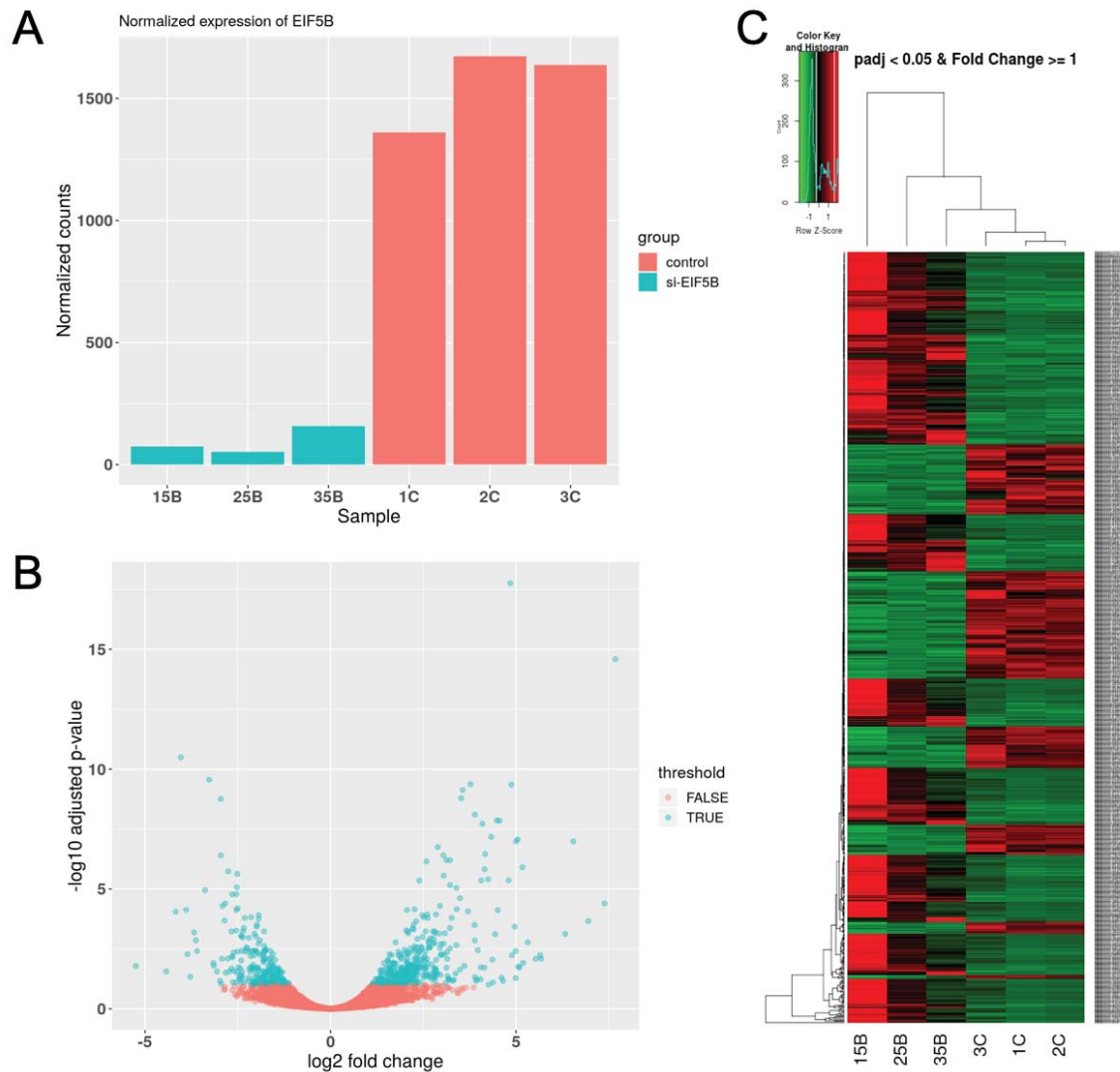
Figure 3.1: Normalized expression of eIF5B in HEK 293T samples, confirmed eIF5B to be depleted in three biological replicates (A). Volcano plot confirming significant (blue) upregulated and downregulated transcripts (B), and heatmap showing top 500 differential variable genes upon eIF5B depletion confirm that eIF5B depletion results in transcriptome-wide changes (C). The experiment was performed in collaboration with Dr. Igor Kovalchuk, and assistance was received from Dr. Slava Ilnystkyy.

Table 3.1 Significantly upregulated genes in three biological replicates of eIF5B depleted HEK 293T samples as determined by transcriptome analysis, and sorted *via* KEGG pathway analysis.

	KEGGID	Count	Size	Term	Genes
	4080	11	98	Neuroactive ligand-receptor interaction	1141;5023;9568;1813
Gene ID		Gene Symbol		Name	Species
	1137	CHRNA4		cholinergic receptor nicotinic alpha 4 subunit(CHRNA4)	Homo sapiens
	1141	CHRNB2		cholinergic receptor nicotinic beta 2 subunit(CHRNB2)	Homo sapiens
	1813	DRD2		dopamine receptor D2(DRD2)	Homo sapiens
	2151	F2RL2		coagulation factor II thrombin receptor like 2(F2RL2)	Homo sapiens
	2899	GRIK3		glutamate ionotropic receptor kainate type subunit 3(GRIK3)	Homo sapiens
	2901	GRIK5		glutamate ionotropic receptor kainate type subunit 5(GRIK5)	Homo sapiens
	2914	GRM4		glutamate metabotropic receptor 4(GRM4)	Homo sapiens
	5023	P2RX1		purinergic receptor P2X 1(P2RX1)	Homo sapiens
	9568	GABBR2		gamma-aminobutyric acid type B receptor subunit 2(GABBR2)	Homo sapiens
	11255	HRH3		histamine receptor H3(HRH3)	Homo sapiens
	55584	CHRNA9		cholinergic receptor nicotinic alpha 9 subunit(CHRNA9)	Homo sapiens
	4950	3	13	Maturity onset diabetes of the young	168620;3171;3172
Gene ID		Gene Symbol		Name	Species
	3171	FOXA3		forkhead box A3(FOXA3)	Homo sapiens
	3172	HNF4A		hepatocyte nuclear factor 4 alpha(HNF4A)	Homo sapiens
	168620	BHLHA15		basic helix-loop-helix family member a15(BHLHA15)	Homo sapiens
	4330	5	45	Notch signaling pathway	388585;5986;1840;28
Gene ID		Gene Symbol		Name	Species
	1840	DTX1		deltex E3 ubiquitin ligase 1(DTX1)	Homo sapiens
	5986	RFNG		RFNG O-fucosylpeptide 3-beta-N-acetylglucosaminyltransferase(RFN	Homo sapiens
	9612	NCOR2		nuclear receptor corepressor 2(NCOR2)	Homo sapiens
	28514	DLL1		delta like canonical Notch ligand 1(DLL1)	Homo sapiens
	388585	HES5		hes family bHLH transcription factor 5(HES5)	Homo sapiens
	4512	6	64	ECM-receptor interaction	3371;7058;3680;3913
Gene ID		Gene Symbol		Name	Species
	3371	TNC		tenascin C(TNC)	Homo sapiens
	3674	ITGA2B		integrin subunit alpha 2b(ITGA2B)	Homo sapiens
	3680	ITGA9		integrin subunit alpha 9(ITGA9)	Homo sapiens
	3913	LAMB2		laminin subunit beta 2(LAMB2)	Homo sapiens
	7058	THBS2		thrombospondin 2(THBS2)	Homo sapiens
	7060	THBS4		thrombospondin 4(THBS4)	Homo sapiens
	670	3	17	One carbon pool by folate	25902;471;160428
Gene ID		Gene Symbol		Name	Species
	471	ATIC		5-aminoimidazole-4-carboxamide ribonucleotide formyltransferase	Homo sapiens
	25902	MTHFD1L		methylenetetrahydrofolate dehydrogenase (NADP+ dependent) 1-lik	Homo sapiens
	160428	ALDH1L2		aldehyde dehydrogenase 1 family member L2(ALDH1L2)	Homo sapiens
	4510	11	170	Focal adhesion	3371;7058;5154;2575
Gene ID		Gene Symbol		Name	Species
	595	CCND1		cyclin D1(CCND1)	Homo sapiens
	894	CCND2		cyclin D2(CCND2)	Homo sapiens
	3371	TNC		tenascin C(TNC)	Homo sapiens
	3674	ITGA2B		integrin subunit alpha 2b(ITGA2B)	Homo sapiens
	3680	ITGA9		integrin subunit alpha 9(ITGA9)	Homo sapiens
	3913	LAMB2		laminin subunit beta 2(LAMB2)	Homo sapiens
	4636	MYL5		myosin light chain 5(MYL5)	Homo sapiens
	5154	PDGFA		platelet derived growth factor subunit A(PDGFA)	Homo sapiens
	7058	THBS2		thrombospondin 2(THBS2)	Homo sapiens
	7060	THBS4		thrombospondin 4(THBS4)	Homo sapiens
	25759	SHC2		SHC adaptor protein 2(SHC2)	Homo sapiens
	603	2	9	Glycosphingolipid biosynthesis - globo series	2523;6482
Gene ID		Gene Symbol		Name	Species
	2523	FUT1		fucosyltransferase 1 (H blood group)(FUT1)	Homo sapiens
	6482	ST3GAL1		ST3 beta-galactoside alpha-2,3-sialyltransferase 1(ST3GAL1)	Homo sapiens
	5144	3	23	Malaria	7058;3039;7060
Gene ID		Gene Symbol		Name	Species
	3039	HBA1		hemoglobin subunit alpha 1(HBA1)	Homo sapiens
	7058	THBS2		thrombospondin 2(THBS2)	Homo sapiens
	7060	THBS4		thrombospondin 4(THBS4)	Homo sapiens

5410	5	61	Hypertrophic cardiomyopathy (HCM)	7171;3680;6262;775;
Gene ID		**Gene Symbol**	**Name**	**Species**
	775	CACNA1C	calcium voltage-gated channel subunit alpha1 C(CACNA1C)	Homo sapiens
	3674	ITGA2B	integrin subunit alpha 2b(ITGA2B)	Homo sapiens
	3680	ITGA9	integrin subunit alpha 9(ITGA9)	Homo sapiens
	6262	RYR2	ryanodine receptor 2(RYR2)	Homo sapiens
	7171	TPM4	tropomyosin 4(TPM4)	Homo sapiens

250	3	25	Alanine, aspartate and glutamate metabolism	445;2673;790
Gene ID		**Gene Symbol**	**Name**	**Species**
	445	ASS1	argininosuccinate synthase 1(ASS1)	Homo sapiens
	790	CAD	carbamoyl-phosphate synthetase 2, aspartate transcarbamylase, and	Homo sapiens
	2673	GFPT1	glutamine--fructose-6-phosphate transaminase 1(GFPT1)	Homo sapiens

260	3	25	Glycine, serine and threonine metabolism	51268;29958;875
Gene ID		**Gene Symbol**	**Name**	**Species**
	875	CBS	cystathionine-beta-synthase(CBS)	Homo sapiens
	29958	DMGDH	dimethylglycine dehydrogenase(DMGDH)	Homo sapiens
	51268	PIPOX	pipecolic acid and sarcosine oxidase(PIPOX)	Homo sapiens

5414	5	65	Dilated cardiomyopathy	7171;3680;6262;775;
Gene ID		**Gene Symbol**	**Name**	**Species**
	775	CACNA1C	calcium voltage-gated channel subunit alpha1 C(CACNA1C)	Homo sapiens
	3674	ITGA2B	integrin subunit alpha 2b(ITGA2B)	Homo sapiens
	3680	ITGA9	integrin subunit alpha 9(ITGA9)	Homo sapiens
	6262	RYR2	ryanodine receptor 2(RYR2)	Homo sapiens
	7171	TPM4	tropomyosin 4(TPM4)	Homo sapiens

4010	11	221	MAPK signaling pathway	1649;26291;5154;226
Gene ID		**Gene Symbol**	**Name**	**Species**
	775	CACNA1C	calcium voltage-gated channel subunit alpha1 C(CACNA1C)	Homo sapiens
	1649	DDIT3	DNA damage inducible transcript 3(DDIT3)	Homo sapiens
	1843	DUSP1	dual specificity phosphatase 1(DUSP1)	Homo sapiens
	1850	DUSP8	dual specificity phosphatase 8(DUSP8)	Homo sapiens
	2264	FGFR4	fibroblast growth factor receptor 4(FGFR4)	Homo sapiens
	5154	PDGFA	platelet derived growth factor subunit A(PDGFA)	Homo sapiens
	5600	MAPK11	mitogen-activated protein kinase 11(MAPK11)	Homo sapiens
	5924	RASGRF2	Ras protein specific guanine nucleotide releasing factor 2(RASGRF2)	Homo sapiens
	8912	CACNA1H	calcium voltage-gated channel subunit alpha1 H(CACNA1H)	Homo sapiens
	22808	MRAS	muscle RAS oncogene homolog(MRAS)	Homo sapiens
	26291	FGF21	fibroblast growth factor 21(FGF21)	Homo sapiens

524	1	3	Butirosin and neomycin biosynthesis	80201
Gene ID		**Gene Symbol**	**Name**	**Species**
	80201	HKDC1	hexokinase domain containing 1(HKDC1)	Homo sapiens

4964	2	17	Proximal tubule bicarbonate reclamation	5106;478
Gene ID		**Gene Symbol**	**Name**	**Species**
	478	ATP1A3	ATPase Na+/K+ transporting subunit alpha 3(ATP1A3)	Homo sapiens
	5106	PCK2	phosphoenolpyruvate carboxykinase 2, mitochondrial(PCK2)	Homo sapiens

Table 3.2: Significantly downregulated genes in three biological replicates of eIF5B depleted HEK 293T samples as determined by transcriptome analysis, and sorted *via* KEGG pathway analysis.

	KEGGID	Count	Size	Term	Genes
	5323	5	54	**Rheumatoid arthritis**	**3109;534;8792**
Gene ID		**Gene Symbol**		**Name**	**Species**
	534	ATP6V1G2		ATPase H+ transporting V1 subunit G2(ATP6V1G2)	Homo sapiens
	1513	CTSK		cathepsin K(CTSK)	Homo sapiens
	3109	HLA-DMB		major histocompatibility complex, class II, DM beta(HLA-DMB)	Homo sapiens
	3115	HLA-DPB1		major histocompatibility complex, class II, DP beta 1(HLA-DPB1)	Homo sapiens
	8792	TNFRSF11A		TNF receptor superfamily member 11a(TNFRSF11A)	Homo sapiens
	830	3	20	**Retinol metabolism**	**9227;56603;86**
Gene ID		**Gene Symbol**		**Name**	**Species**
	8608	RDH16		retinol dehydrogenase 16 (all-trans)(RDH16)	Homo sapiens
	9227	LRAT		lecithin retinol acyltransferase (phosphatidylcholine--retinol O-acylt	Homo sapiens
	56603	CYP26B1		cytochrome P450 family 26 subfamily B member 1(CYP26B1)	Homo sapiens
	4514	5	83	**Cell adhesion molecules (CAMs)**	**999;3109;9369**
Gene ID		**Gene Symbol**		**Name**	**Species**
	999	CDH1		cadherin 1(CDH1)	Homo sapiens
	3109	HLA-DMB		major histocompatibility complex, class II, DM beta(HLA-DMB)	Homo sapiens
	3115	HLA-DPB1		major histocompatibility complex, class II, DP beta 1(HLA-DPB1)	Homo sapiens
	9076	CLDN1		claudin 1(CLDN1)	Homo sapiens
	9369	NRXN3		neurexin 3(NRXN3)	Homo sapiens
	4380	5	86	**Osteoclast differentiation**	**5608;3554;879**
Gene ID		**Gene Symbol**		**Name**	**Species**
	1513	CTSK		cathepsin K(CTSK)	Homo sapiens
	3455	IFNAR2		interferon alpha and beta receptor subunit 2(IFNAR2)	Homo sapiens
	3554	IL1R1		interleukin 1 receptor type 1(IL1R1)	Homo sapiens
	5608	MAP2K6		mitogen-activated protein kinase kinase 6(MAP2K6)	Homo sapiens
	8792	TNFRSF11A		TNF receptor superfamily member 11a(TNFRSF11A)	Homo sapiens
	360	2	13	**Phenylalanine metabolism**	**314;8639**
Gene ID		**Gene Symbol**		**Name**	**Species**
	314	AOC2		amine oxidase, copper containing 2(AOC2)	Homo sapiens
	8639	AOC3		amine oxidase, copper containing 3(AOC3)	Homo sapiens
	5310	2	13	**Asthma**	**3109;3115**
Gene ID		**Gene Symbol**		**Name**	**Species**
	3109	HLA-DMB		major histocompatibility complex, class II, DM beta(HLA-DMB)	Homo sapiens
	3115	HLA-DPB1		major histocompatibility complex, class II, DP beta 1(HLA-DPB1)	Homo sapiens
	5332	2	17	**Graft-versus-host disease**	**3109;3115**
Gene ID		**Gene Symbol**		**Name**	**Species**
	3109	HLA-DMB		major histocompatibility complex, class II, DM beta(HLA-DMB)	Homo sapiens
	3115	HLA-DPB1		major histocompatibility complex, class II, DP beta 1(HLA-DPB1)	Homo sapiens
	410	2	18	**beta-Alanine metabolism**	**314;8639**
Gene ID		**Gene Symbol**		**Name**	**Species**
	314	AOC2		amine oxidase, copper containing 2(AOC2)	Homo sapiens
	8639	AOC3		amine oxidase, copper containing 3(AOC3)	Homo sapiens
	350	2	25	**Tyrosine metabolism**	**314;8639**
Gene ID		**Gene Symbol**		**Name**	**Species**
	314	AOC2		amine oxidase, copper containing 2(AOC2)	Homo sapiens
	8639	AOC3		amine oxidase, copper containing 3(AOC3)	Homo sapiens
	260	2	25	**Glycine, serine and threonine metabolism**	**314;8639**
Gene ID		**Gene Symbol**		**Name**	**Species**
	314	AOC2		amine oxidase, copper containing 2(AOC2)	Homo sapiens
	8639	AOC3		amine oxidase, copper containing 3(AOC3)	Homo sapiens
	100	2	18	**Steroid biosynthesis**	**6307;6713**
Gene ID		**Gene Symbol**		**Name**	**Species**
	6713	SQLE		squalene epoxidase(SQLE)	Homo sapiens
	6307	MSMO1		methylsterol monooxygenase 1(MSMO1)	Homo sapiens
	5320	2	19	**Autoimmune thyroid disease**	**3109;3115**
Gene ID		**Gene Symbol**		**Name**	**Species**
	3109	HLA-DMB		major histocompatibility complex, class II, DM beta(HLA-DMB)	Homo sapiens
	3115	HLA-DPB1		major histocompatibility complex, class II, DP beta 1(HLA-DPB1)	Homo sapiens

5330	2	19 Allograft rejection		3109;3115
Gene ID	**Gene Symbol**	**Name**		**Species**
3109	HLA-DMB	major histocompatibility complex, class II, DM beta(HLA-DMB)		Homo sapiens
3115	HLA-DPB1	major histocompatibility complex, class II, DP beta 1(HLA-DPB1)		Homo sapiens
4940	**2**	**23 Type I diabetes mellitus**		**3109;3115**
Gene ID	**Gene Symbol**	**Name**		**Species**
3109	HLA-DMB	major histocompatibility complex, class II, DM beta(HLA-DMB)		Homo sapiens
3115	HLA-DPB1	major histocompatibility complex, class II, DP beta 1(HLA-DPB1)		Homo sapiens
4672	**2**	**23 Intestinal immune network for IgA production**		**3109;3115**
Gene ID	**Gene Symbol**	**Name**		**Species**
3109	HLA-DMB	major histocompatibility complex, class II, DM beta(HLA-DMB)		Homo sapiens
3115	HLA-DPB1	major histocompatibility complex, class II, DP beta 1(HLA-DPB1)		Homo sapiens
5150	**2**	**27 Staphylococcus aureus infection**		**3109;3115**
Gene ID	**Gene Symbol**	**Name**		**Species**
3109	HLA-DMB	major histocompatibility complex, class II, DM beta(HLA-DMB)		Homo sapiens
3115	HLA-DPB1	major histocompatibility complex, class II, DP beta 1(HLA-DPB1)		Homo sapiens
5130	**3**	**47 Pathogenic Escherichia coli infection**		**999;10552;907**
Gene ID	**Gene Symbol**	**Name**		**Species**
999	CDH1	cadherin 1(CDH1)		Homo sapiens
9076	CLDN1	claudin 1(CLDN1)		Homo sapiens
10552	ARPC1A	actin related protein 2/3 complex subunit 1A(ARPC1A)		Homo sapiens
4971	**3**	**52 Gastric acid secretion**		**3766;482;3759**
Gene ID	**Gene Symbol**	**Name**		**Species**
482	ATP1B2	ATPase Na+/K+ transporting subunit beta 2(ATP1B2)		Homo sapiens
3759	KCNJ2	potassium voltage-gated channel subfamily J member 2(KCNJ2)		Homo sapiens
3766	KCNJ10	potassium voltage-gated channel subfamily J member 10(KCNJ10)		Homo sapiens
4080	**4**	**98 Neuroactive ligand-receptor interaction**		**1903;1910;214**
Gene ID	**Gene Symbol**	**Name**		**Species**
1136	CHRNA3	cholinergic receptor nicotinic alpha 3 subunit(CHRNA3)		Homo sapiens
1903	S1PR3	sphingosine-1-phosphate receptor 3(S1PR3)		Homo sapiens
1910	EDNRB	endothelin receptor type B(EDNRB)		Homo sapiens
2149	F2R	coagulation factor II thrombin receptor(F2R)		Homo sapiens
4620	**3**	**61 Toll-like receptor signaling pathway**		**5608;1513;345**
Gene ID	**Gene Symbol**	**Name**		**Species**
1513	CTSK	cathepsin K(CTSK)		Homo sapiens
3455	IFNAR2	interferon alpha and beta receptor subunit 2(IFNAR2)		Homo sapiens
5608	MAP2K6	mitogen-activated protein kinase kinase 6(MAP2K6)		Homo sapiens
4142	**4**	**110 Lysosome**		**6272;9741;151**
Gene ID	**Gene Symbol**	**Name**		**Species**
1513	CTSK	cathepsin K(CTSK)		Homo sapiens
2517	FUCA1	fucosidase, alpha-L- 1, tissue(FUCA1)		Homo sapiens
6272	SORT1	sortilin 1(SORT1)		Homo sapiens
9741	LAPTM4A	lysosomal protein transmembrane 4 alpha(LAPTM4A)		Homo sapiens
4130	**2**	**34 SNARE interactions in vesicular transport**		**6843;8676**
Gene ID	**Gene Symbol**	**Name**		**Species**
6843		vesicle associated membrane protein 1(VAMP1)		Homo sapiens
8676		syntaxin 11(STX11)		Homo sapiens

Table 3.3 Select genes involved in MAPK signaling. All examined genes were found to be non-significantly upregulated or downregulated in eIF5B depleted samples.

	Significance	log2 Fold Change	15B	25B	35B	1C	2C	3C
MAP4K4	FALSE	0.810047218	1639.715356	1844.90782	2336.13945	1194.30854	1000.69317	1124.39575
MAP3K1	FALSE	-0.12961699	69.48896246	209.703714	399.934554	323.790316	236.370629	183.091262
MAP3K7	FALSE	0.225221722	351.9279711	610.322658	1637.99283	943.946084	797.103872	483.576334
MAP2K1	FALSE	-0.497484515	580.5690734	1219.43316	1160.67963	1393.35997	1487.23709	1301.02497
MAP2K3	FALSE	-0.169513625	2156.399416	1072.15569	507.742999	954.56216	1233.61313	2012.92688
MAPK1	FALSE	-0.258156529	1519.790856	2576.44649	3170.78548	3074.23865	2770.88489	2846.53062
MAPK3	FALSE	0.572063694	9889.848463	4158.92163	1704.06897	2576.16776	3077.99417	4941.31007
MAPK12	FALSE	1.235648283	5847.159954	2244.92068	867.684098	991.718426	1254.31713	1558.42974
MAPK14	FALSE	-0.363588128	687.0440965	1044.27601	1067.65138	1144.76685	1235.33847	1222.40343
MAPKAPK2	FALSE	-1.135759636	1415.557413	936.39375	590.338179	1683.53271	1863.3597	2916.53611
RPS6KA3	FALSE	0.70631018	305.9755927	743.660279	1921.42471	804.167751	619.394567	397.41574
MAPK8	FALSE	-0.874605518	124.4076586	267.281323	546.867032	676.77484	631.471898	413.570851

3.4.2 eIF5B depletion leads to upregulation of MAPK signaling

Transcriptome analysis confirmed the upregulation of the MAPK signaling pathway upon eIF5B depletion (Table 3.1). However, analysis of additional previously studied genes involved in MAPK signaling showed no significant difference in eIF5B depleted cells for any examined transcripts (Table 3.3).[24] Interestingly, Jiang *et al*. (2016) found all gene targets, except for MAPK8 (JNK) in Table 3.3 to be downregulated in eIF5B depleted HEK 293T and HepG2 cells. We thus chose to validate the transcriptome effect on MAPK signaling, by performing Western blotting on JNK and phosphorylated JNK. Upon eIF5B depletion in HEK 293T cells, protein levels of phosphorylated JNK significantly increased approximately 2-fold, despite a decrease in overall JNK levels (Figure 3.2). This confirms that, although less JNK is present in cells depleted of eIF5B, the JNK is being activated at higher levels, as JNK must be dual phosphorylated in order to become active.[6] In the MAPK signaling cascade, JNK is phosphorylated upon activation by MKK4 and MKK7, ultimately resulting in activation/phosphorylation of transcription factors for target genes.[25] As such, our observation that depletion of eIF5B results in upregulation of phosphorylated JNK, confirms that the JNK axis of MAPK signaling is activated in response to eIF5B depletion.
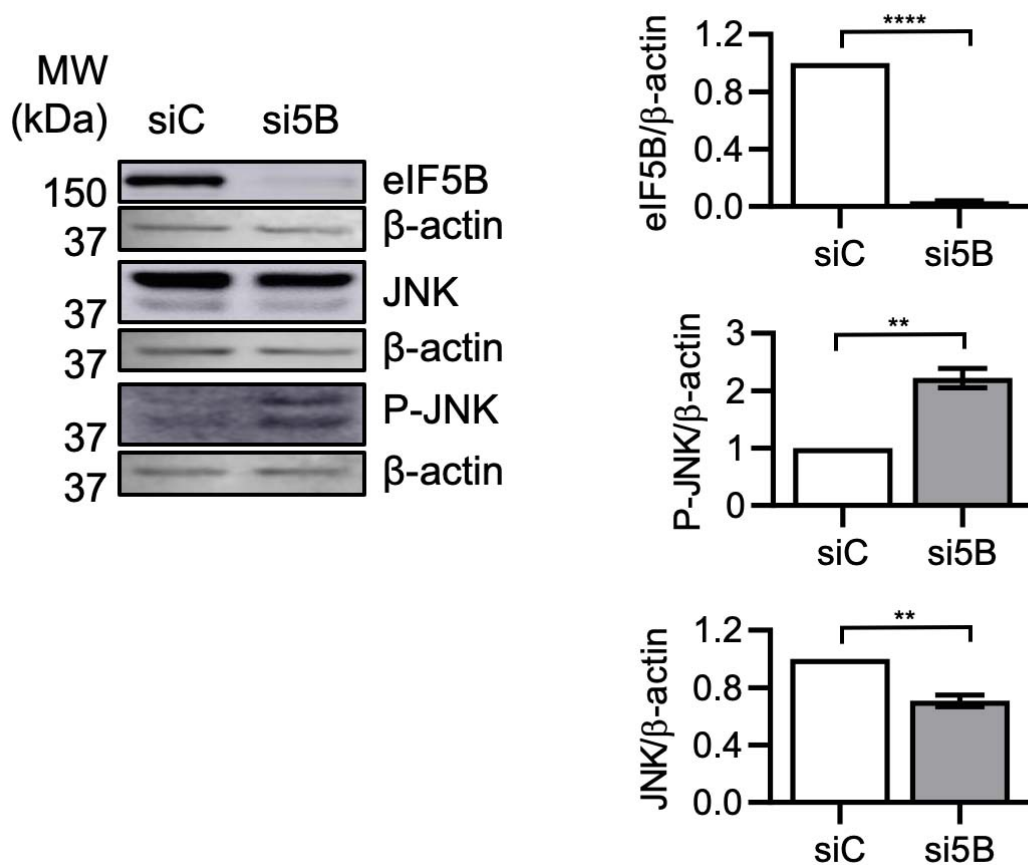
Figure 3.2: Depletion of eIF5B leads to increased levels of the phosphorylated JNK protein (p-46 and p-54 JNK isoforms) in HEK 293T cells. HEK 293T were reverse-transfected with a non-specific control siRNA (siC) or an eIF5B-specific siRNA pool (si5B), incubated 96 hours, harvested in RIPA lysis buffer, and 20 µg of total protein resolved by SDS-PAGE before performing immunoblotting. Quantifications of levels of normalized eIF5B and phosphorylated JNK protein, confirm the upregulated of phosphorylated JNK upon depletion of eIF5B. Data are expressed as mean ± SEM for 3 independent biological replicates. *, $p < 0.05$; **, $p < 0.01$; ***, $p < 0.001$; ****, $p < 0.0001$. Assistance was received in this experiment by Dr. Joe Ross.

3.4.3 eIF5B depletion results in upregulation of dyskerin

Transcriptome analysis confirmed the upregulation of the *DKC1* gene (dyskerin) of the ribosome biogenesis pathway. KEGG pathway analysis showed variable effects on many proteins involved in ribosome biogenesis, however, the significant upregulation of *dyskerin* was observed in all three biological replicates of eIF5B depletion (Figure 3.3).

Dyskerin upregulation was then validated *via* Western blotting and was shown to be upregulated significantly approximately 3.5-fold in HEK 293T cells and 2-fold in U343 cells upon depletion of eIF5B (Figure 3.4). Western blotting confirmed that the effect observed at the transcriptome-level by eIF5B was being observed at the functional protein level. As the regulation of p27 by eIF5B has been previously confirmed in U343 cells, and p27 is not present at detectable levels in HEK293T, the Western blotting was performed in biological triplicate in U343 cells, as was the rest of the study.[9] These experiments confirmed that eIF5B depletion results in the upregulation of dyskerin protein in both HEK 293T and U343 cells, suggesting a potential role for indirect regulation of p27.
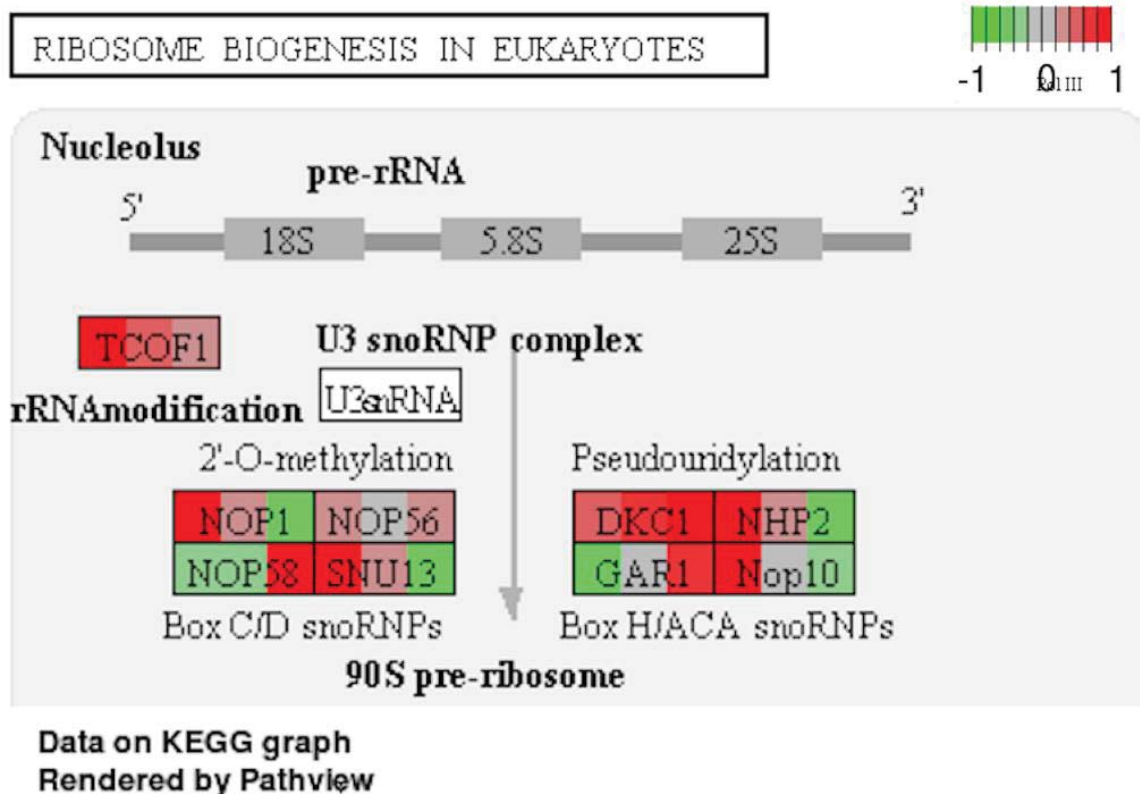

Figure 3.3: Transcriptome analysis showing the affected pathway of ribosome biogenesis upon eIF5B depletion. *DKC1* (dyskerin) is upregulated at the transcriptome-level upon three biological replicates of eIF5B depleted HEK 293T samples.
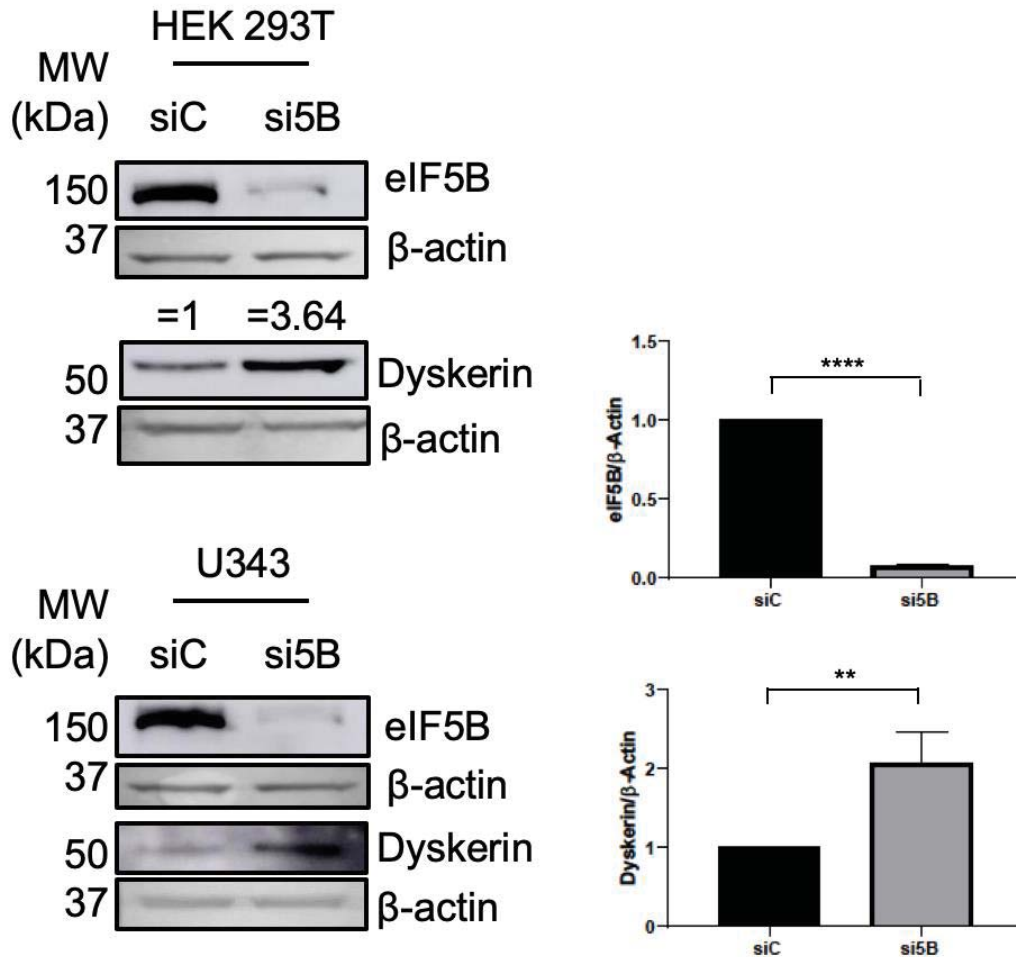
Figure 3.4 Depletion of eIF5B leads to increased levels of the dyskerin in both HEK 293T cells and U343 cells. Cells were reverse-transfected with a non-specific control siRNA (siC) or an eIF5B-specific siRNA pool (si5B), incubated 96 hours, harvested in RIPA lysis buffer, and 20 µg of total protein resolved by SDS-PAGE before performing immunoblotting. Quantitations for HEK 293T shown relative to actin above bands. U343 quantitations shown on right with data expressed as mean ± SEM for at 3 independent biological replicates. *, $p < 0.05$; **, $p < 0.01$; ***, $p < 0.001$; ****, $p < 0.0001$.

3.4.4 eIF5B depletion results in IRES-dependent upregulation of p27

As depletion of eIF5B in HEK 293T resulted in significantly increased protein levels of dyskerin, which is known to regulate p27, we next investigated whether eIF5B depletion affected the levels of p27. Depletion of eIF5B in U343 cells resulted in a significant approximately 2-fold increase in p27 protein levels (Figure 3.5). When tested

in non-cancerous HEK 293T cells, p27 protein levels were undetected in all conditions, consistent with literature findings (Figure 3.5).[26,27] RT-qPCR was performed to determine whether the effect was occurring transcriptionally, and no significant change was observed in the steady-state mRNA levels of p27 when normalized to actin in eIF5B depleted U343 cells (Figure 3.5 C). This suggests that a translational effect may be occuring. To further verify the effect as translational, as well as investigate whether eIF5B was utilizing the IRES-element in the transcript of *p27*, the activity of *p27*-luciferase reporters was measured in control and eIF5B depleted cells. Note that these *p27*-luc monocistronic constructs are transcribed from a heterologous promoter [12] and that I normalized the luciferase activity to steady-state levels of *p27*-luc mRNA in order to ensure that the results reflected the translation of the construct rather than effects on transcription or mRNA turnover. As the 5' UTR of *p27* contains both an IRES and a uORF element, constructs containing truncated 5' UTRs with only the uORF (Δ2), only the IRES (Δd), and both elements (5'UTR) were tested in presence and absence of eIF5B (Figure 3.5 D). In the presence of the uORF alone or in combination with the IRES (Δ2, 5' UTR), luciferase expression was significantly repressed independently of eIF5B depletion, confirming that the uORF is repressive and that eIF5B does not act on the uORF to regulate the translation of *p27* mRNA (Figure 3.5 E). However, in the presence of the IRES alone (Δd), depletion of eIF5B results in a significant increase in luciferase activity (Figure 3.5 E), suggesting that the regulation of *p27* is likely dependent on its IRES- element. These experiments together suggest that eIF5B represses expression of *p27* translationally, which is likely dependent on an IRES element. However, the mRNAs originating from the monocistronic *p27*-luc reporters would contain the 5' m^7G cap, so the possibility of cap-dependent translation cannot be

eliminated. To fully conclude that eIF5B is regulating *p27* translation through an IRES-element, bicistronic reporter assays should be performed. As dyskerin is known to regulate *p27* through its IRES element, this suggests that eIF5B may be regulating p27 through its effect on dyskerin.
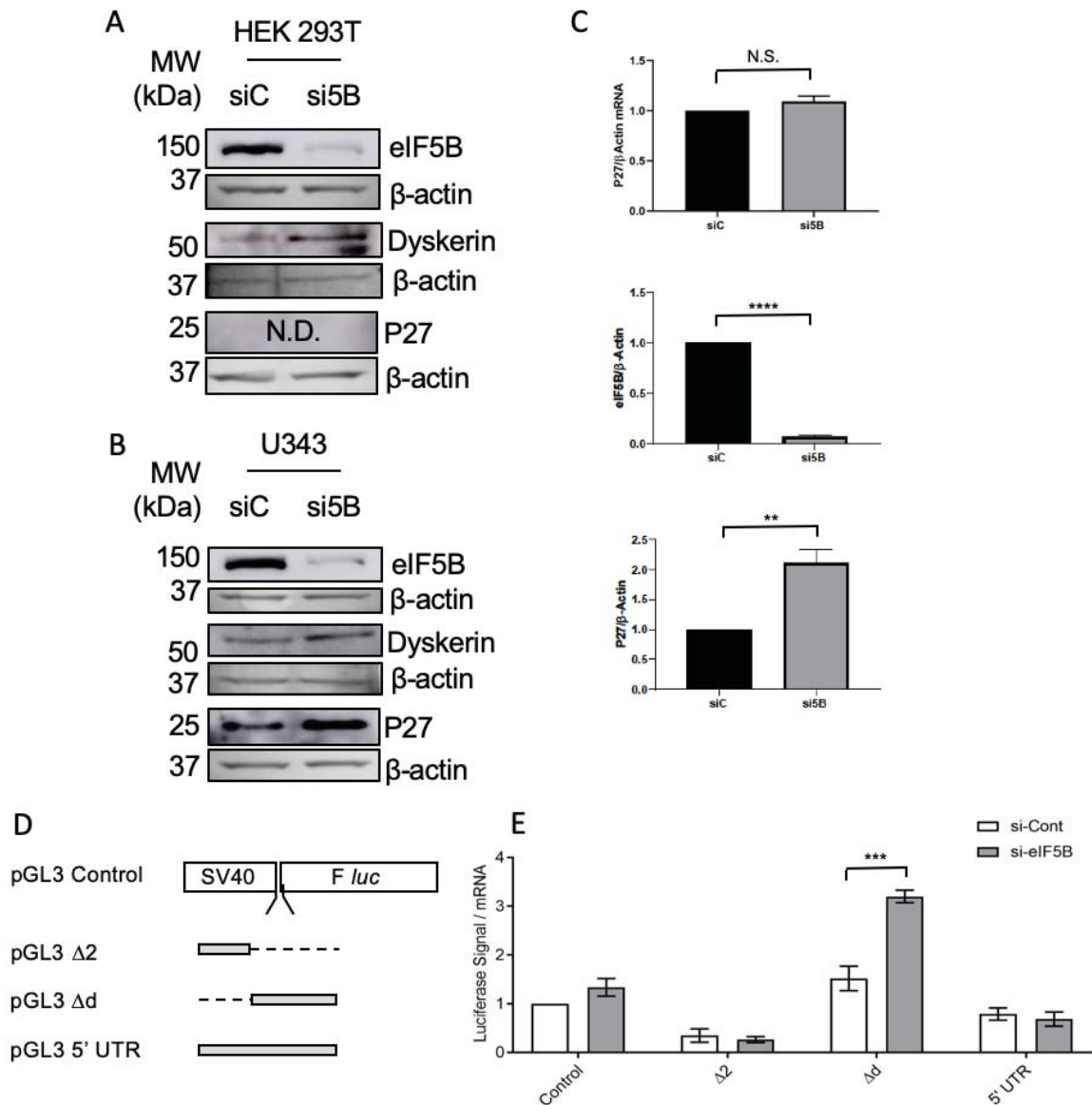
Figure 3.5 Depletion of eIF5B results in upregulation of p27 at the protein level in U343 (B) cells, however, p27 protein levels are undetectable in HEK 293T cells (A). Dyskerin is upregulated in both cell lines upon depletion of eIF5B, note that images shown for dyskerin were used for the quantification in Figure 3.4. RT-qPCR of p27 steady-state mRNA levels relative to actin, confirm that depletion of eIF5B does not result in regulation of p27 at the

transcriptional/transcript-stability level (C). Data are expressed as mean ± SEM for 3 independent biological replicates. *, $p < 0.05$; **, $p < 0.01$; ***, $p < 0.001$; ****, $p < 0.0001$. Luciferase activity is depleted in the presence of a uORF, and the entire p27 5'UTR, confirming the uORF presence as repressive (D,E). Rather in the presence of the IRES alone, eIF5B depletion results in increased luciferase activity, confirming that eIF5B upregulates p27 translationally likely through an IRES-element.

3.4.5 eIF5B-mediated repression of p27 does not affect cell cycle regulation

As p27 was shown to be upregulated by the depletion of eIF5B, I next wanted to determine whether this was causing a phenotype in the cell cycle. I hypothesized that eIF5B depletion would lead to cell cycle arrest at the G1 phase, as increased p27 would inhibit the G1 to S phase transition.[13] However, PI staining and flow cytometry demonstrated that, relative to control cells, eIF5B depletion had no significant effect on the percentage of U343 cells in G_0/G_1, S, or G_2/M phases of the cell cycle (Figure 3.6), ruling out an effect of eIF5B on cell cycle regulation. When further examined by Western blotting, it was determined that though eIF5B depletion resulted in an increase in p27 protein levels, it also resulted in a subsequent decrease in p21 levels (Figure 3.7). p21 is another member of the KIP CKI family, which is also responsible for preventing the transition from G1 to S phase in the cell cycle.[18] I hypothesize that the opposing effects on p27 and p21 observed in the absence of eIF5B likely cancel out an effect on the cell cycle, which further explain the flow cytometry results observed in Figure 3.6. However, when p27 was depleted, increased levels of cleaved cysteine-aspartic protease (caspase)-9 were observed in both normal and TRAIL-treated U343 cells (Figure 3.7). TRAIL is a ligand that binds cellular death receptors to activate the extrinsic apoptosis pathway.[28] A key element of apoptosis is activation of caspase cascades, including the cleaving of caspase 9. As caspase 9 is cleaved when activated and plays a critical role

in deciding cell fate and activation of apoptosis and autophagy, this suggests rather that

p27 is playing a cytoprotective role, as opposed to a role in cell cycle regulation.[29,30]
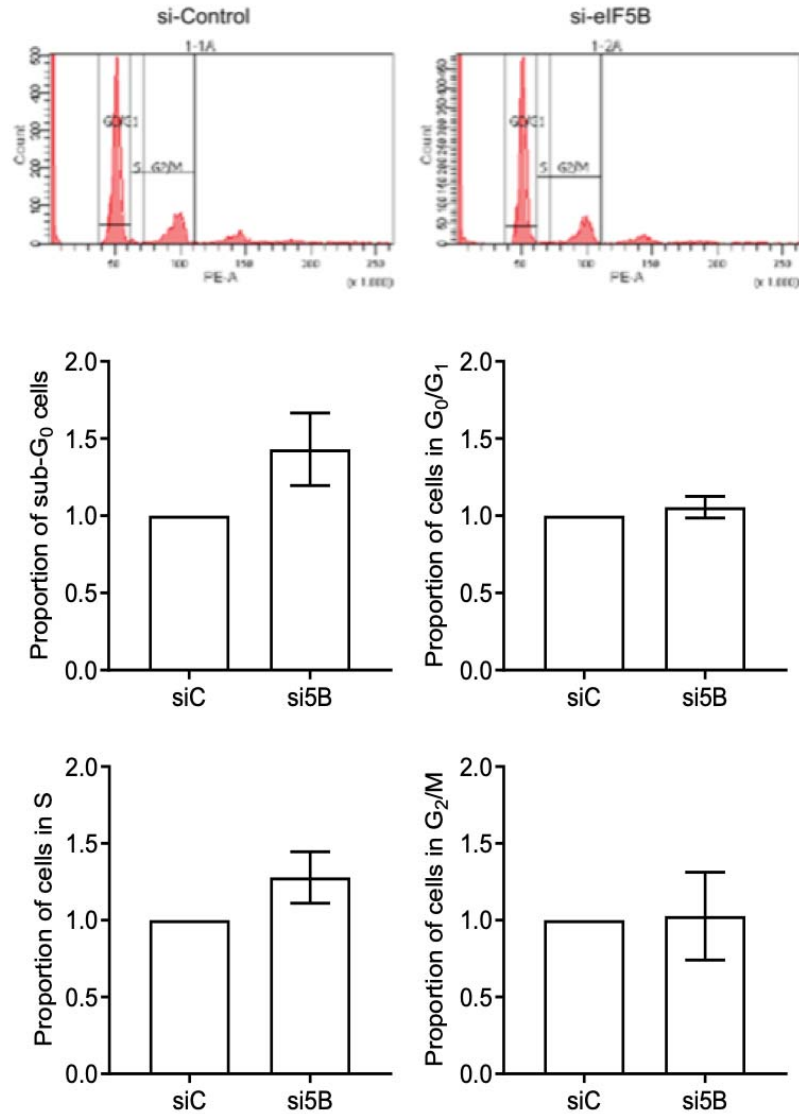
Figure 3.6 Depletion of eIF5B does not significantly affect cell cycle progression. U343 cells were depleted of eIF5B, and cellular DNA content was analyzed by propidium iodide staining and flow cytometry. Representative images showing the number of cells in G_0/G_1, S, or G_2/M phases, as well as sub-G_0 cells, are shown. Percentage of sub-G_0 cells (top left), cells in G_0/G_1 (top right), S-phase (bottom left), and G_2/M (bottom right). siC, non-specific siRNA; si5B, eIF5B-specific siRNA. Data are expressed as mean ± SEM for four independent biological replicates.

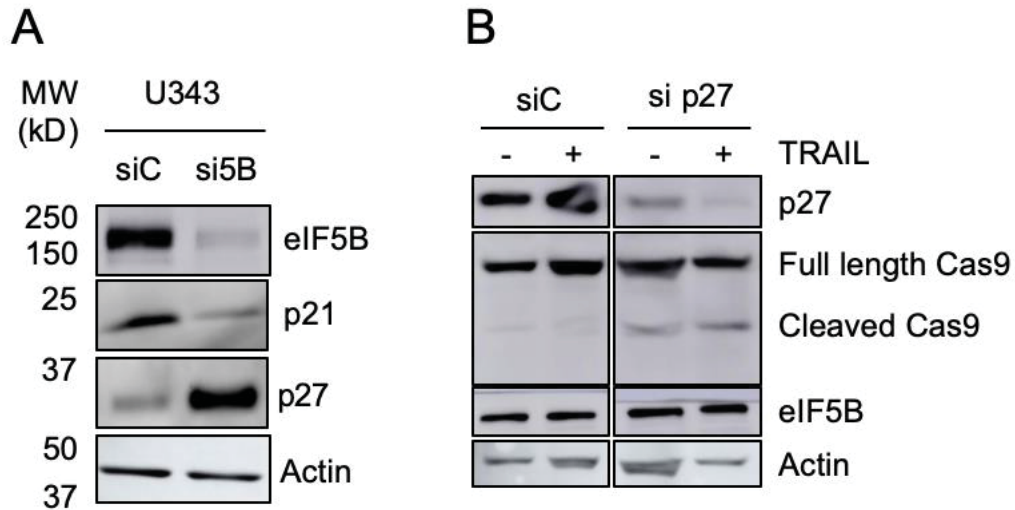Figure 3.7 Depletion of eIF5B results in the upregulation of p27, and the downregulation of p21 at the protein level, as compared to actin (A). Depletion of p27 in combination with TRAIL treatment results in increased cleaved caspase 9, suggesting an effect on apoptosis as opposed to the cell cycle (B).

3.5 Discussion

In this work, we confirm that eIF5B largely affects the cellular transcriptome, resulting in significant changes in signaling pathways. Specifically, we verified that the MAPK pathway is upregulated upon depletion of eIF5B through transcriptome analysis, followed by determination of upregulated phosphorylated JNK protein levels. I additionally verified the upregulation of dyskerin, a component of the ribosome biogenesis pathway, at the protein level. As dyskerin is known to influence rRNA modification and regulate levels of IRES-containing proteins including p27, I investigated the regulation of eIF5B on p27. I found that upon eIF5B depletion, p27 protein levels are significantly increased. eIF5B depletion does not cause increased *p27* at the steady-state mRNA levels, however using luciferase reporter assays, I confirmed that eIF5B likely represses *p27* translationally through its IRES-element. However, eIF5B depletion does not result in regulation of the cell cycle through p27. As such, I suggest that through enhanced dyskerin

expression, depletion of eIF5B upregulates the IRES-dependent translation initiation of *p27*. This work offers new insight into the potential roles of eIF5B in non-canonical translation mechanisms.

The confirmation that upon eIF5B depletion, phosphorylation of JNK increases validates the upregulation of the JNK-arm of the MAPK pathway. This is supported by literature, in which we recently showed that eIF5B depletion results in increased reactive oxygen species (ROS).[27] ROS are known to have roles in promoting the activation of JNK.[31] Jiang *et al.* (2016) determined select genes involved in MAPK signaling (Table 3.3), other than JNK (*MAPK8*), to be downregulated significantly upon eIF5B depletion.[24] We did not observe significant up- or down-regulation for any of these genes (Table 3.3), and rather we observed upregulation of other genes involved in MAPK signaling (Table 3.1). Important to note, in contrast to our transcriptome analysis, Jiang *et al.* (2016) performed RT-qPCR analysis with no minimum thresholds for determination of gene up- or down-regulation.[24] Based on these observations, we conclude that eIF5B depletion results in activation of the JNK-arm of the MAPK pathway.

MAPK cascades are known to have a key role in relaying and amplifying extracellular signals to biological responses involving proliferation, differentiation, and apoptosis. The three MAPK families of the classical MAPK (ERK), JNK/ SAPK and p38 kinase are activated in series following activation of a MAPK kinase kinase (MKKK), and MKK.[25] JNK specifically is activated by a wide range of cellular stresses such as UV and ionizing radiation, metabolic inhibitors, inflammatory cytokines, and chemotherapeutic drugs, and subsequently phosphorylates and activates targets including c-Jun, ATF2, ETS-1 like protein (Elk1), p53, deleted in pancreatic cancer 4 (DPC4), and nuclear factor of

activated T cells (NFAT4).[32] The c-Jun proto-oncoprotein is an important effector of the JNK pathway. In particular, regulation of c-Jun by JNK modulates stress-induced apoptosis in multiple cancerous and non-cancerous cell types.[7,32] Interestingly, ERK and JNK cross-activation results in vascular endothelial growth factor (VEGF)-induced G1/S progression and cell proliferation.[33] These results suggest that crosstalk between MAPK family members of JNK and ERK influence the cell division and differentiation. Our findings that eIF5B depletion results in upregulated MAPK signaling, specifically through JNK, suggest that eIF5B may influence many cellular pathways including proliferation, apoptosis, and the cell cycle, offering regulation and further knowledge into cellular biology and health and disease.

In addition, I confirmed that depletion of eIF5B results in the upregulation of dyskerin observed through transcriptome analysis and verified at the protein level. Dyskerin is known to associate with small RNAs containing the H/ACA motif, including telomerase RNA, Cajal body RNAs, and snoRNAs.[34] Dyskerin has highly defined roles in telomerase maintenance, and as a pseudouridine synthase modifying rRNA. Mutated *DKC1* leads to X-linked dyskeratosis congenita (X-DC) which is a rare disease that leads to bone marrow failure and increased susceptibility to cancer.[34] Interestingly, Dkc1[m] mice showed decreased rRNA pseudouridylation, but not an impairment in global cap-dependent translation.[35] However, it has been determined that Dkc1-induced reduction of modified uridine in ribosomes resulted in greater than a 25% decrease in polysome association for three particular IRES-containing mRNAs: p27, XIAP, and Bcl-xL.[35] Protein levels of these targets were significantly decreased in Dkc1[m] lymphocytes, despite no difference in transcript or protein stability levels.[35] These findings highly suggest that

dyskerin is required for the modification of rRNA in ribosomes in order to carry out IRES-mediated translation. As such, I suggest that the upregulation of dyskerin from eIF5B depletion may result in consequent upregulation of p27 likely through its IRES-element.

I indeed confirmed that, upon depletion of eIF5B, p27 protein levels were increased. p27 expression is known to be upregulated transcriptionally by the transcription factor MENIN and inhibited by oncogenic transcription factors MYC and PIM.[36] However, I did not observe transcriptional regulation of *p27* upon eIF5B depletion when I examined the steady-state mRNA levels. At the post-transcriptional level, p27 has multiple sites at which amino acids are phosphorylated, resulting in its localization into the cytoplasm, as well as its degradation.[36] Further, more studies have been investigating the translational regulation of p27, as it contains both a uORF and an IRES element in its 5' UTR.

More than five studies have analyzed *p27* 5′-UTR sequences using bicistronic vectors and all have concluded that an IRES is present within the 5' UTR of *p27*.[13,14,37,38] Multiple studies have demonstrated *p27* IRES-dependent expression in a cell-free *in vitro* translation system, further confirming its functionality and ability to initiate translation.[37,38] Kullmann *et al*. (2002) found that the presence of the *p27* 5′-UTR makes an expression of the downstream cistron resistant to the effects of a phosphatidylinositol-3 kinase inhibitor that represses global cap-dependent translation, confirming that some form of non-canonical translation is functioning.[39]

I performed monocistronic luciferase reporter assays using truncated forms of the 5' UTR of *p27*, and observed repression of luciferase activity in the presence of *p27s* known uORF. This is in agreement with Gopfert *et al*.'s (2003) determination of *p27s* uORF to be repressive to its coding sequence *in vitro*.[12] This uORF is highly conserved in

most vertebrates, coding 29 amino acids in length for humans.[12] eIF5B depletion had no effect on luciferase activity in presence of the uORF, confirming that the regulation of *p27* by eIF5B was independent of the uORF. However, I observed that upon depletion of eIF5B, luciferase activity increased significantly for the construct containing the IRES element of *p27*. This construct being monocistronic, does not rule out the cap-dependent initiation, and thus it can be suggested but not fully confirmed that eIF5B facilitates IRES-dependent repression of *p27*. Current literature has determined that IRES-mediated translation defects in Dkc1^m cells are due to intrinsic ribosomal defects.[9] Yoon *et al.* (2006) used the CrPV IRES (which relies solely on ribosomal subunits to initiate translation) to show that in X-DC patient cells, there was an overall decrease in CrPV IRES activity.[35] This study suggested that the depletion or removal of dyskerin results in a change of RNA modification (specifically, pseudouridylation) to the ribosome, which in turn attenuates IRES-dependent translation.[35] I propose here that the depletion of eIF5B, which results in upregulation of dyskerin, is likely resulting in the upregulation of the IRES-dependent translation of *p27*.

Importantly, the most well-characterized cellular role of p27 is as a cyclin-dependent kinase inhibitor, which regulates the passage between phases of the cell cycle.[40] Progression through the cell cycle is mediated by the interactions between serine-threonine CDKs, cyclins, and CKIs. p27 is known to have negative effects on the activities of CDK2 with cyclin E or A, yet p27 can also act in opposition to activate cyclin D/CDK4.[40] p27 is able to cause cell cycle arrest at the G1 phase, which has many applications in health and disease. Mice with p27 knockout develop multiorgan hyperplasia and pituitary tumors, supporting the role of p27 in proliferation and differentiation.[40] Additionally,

haploinsufficient mice are more sensitive to malignant tumor induction by radiation and chemical carcinogens.[40,41] Some cancer types have p27 gene biallelic losses or mutations, resulting in lower levels of p27. Interestingly a study of 246 breast cancer patients showed that low p27 and elevated cyclin E proteins had the highest mortality.[40] These findings suggest a critical role for p27 in the regulation of cell cycle progression, as low or absent p27 levels contribute to various cancer progression and development.

Though I found eIF5B depletion to result in upregulation of p27, interestingly, I did not observe any effect on the cell cycle when eIF5B was depleted. Upon Western blotting, I determined that though p27 was upregulated in response to depletion of eIF5B, p21 was downregulated. Interestingly, p21 is known to be a direct regulatory target of p53 (which is activated by phosphorylation of JNK).[42] p27 and p21 are both members of the G1-checkpoint CDK inhibitor family, and many reporters have found them to have similar roles in the cell cycle and even paradoxical roles in facilitating both association of cyclin D to CDK4/6 into the nucleus and sequestering cyclin D to CDK4/6 complexes.[18] Further, p21 and p27 were found to be partially functionally redundant in the cell cycle progression in response to DNA damage in glioma stem cells.[43] Accordingly, I suggest that depletion of eIF5B results in opposing levels of p27 and p21, which both act on the transition between G1/S phase, subsequently producing no net effect.

I determined that rather than an effect on the cell cycle, p27 upregulation upon depletion of eIF5B may have a cytoprotective role. This was supported by the observation of depletion of p27 resulting in increased cleaved caspase-9 *via* Western blotting. Although p27 is most classified by its role in cell cycle regulation and arrest, p27 has been reported to participate in cell cycle-independent functions including apoptosis/ cell death-processes,

83

cell migration, and DNA repair.[44] Hiromura *et al.* (1999) showed that p27 knockout mesangial cells and fibroblasts had significantly increased levels of apoptosis when deprived of growth factors, which was rescued by expression of p27.[44] In agreement, our findings suggest that p27 may have a cytoprotective role, rather than affecting the cell cycle are consistent with the literature.[44]

Overall, we define the role of eIF5B in non-canonical translation initiation and show that eIF5B depletion results in significant changes to the cells transcriptome profile. We verify the upregulation of the MAPK pathway, and of dyskerin upon eIF5B depletion. Further, we suggest that eIF5B depletion results in upregulation of *p27* likely in an IRES-dependent manner, through upregulation of dyskerin and stabilization of RNA modifications on the ribosome.

References

1   Graber, T. E. & Holcik, M. Cap-independent regulation of gene expression in apoptosis. *Mol Biosyst* **3**, 825-834, doi:10.1039/b708867a (2007).

2   Pakos-Zebrucka, K. *et al.* The integrated stress response. *EMBO Rep* **17**, 1374-1395, doi:10.15252/embr.201642195 (2016).

3   Starck, S. R. *et al.* Translation from the 5' untranslated region shapes the integrated stress response. *Science* **351**, aad3867, doi:10.1126/science.aad3867 (2016).

4   Dey, S. *et al.* Both transcriptional regulation and translational control of ATF4 are central to the integrated stress response. *J Biol Chem* **285**, 33165-33174, doi:10.1074/jbc.M110.167213 (2010).

5   Ross, J. A., Bressler, K. R. & Thakor, N. Eukaryotic Initiation Factor 5B (eIF5B) Cooperates with eIF1A and eIF5 to Facilitate uORF2-Mediated Repression of ATF4 Translation. *Int J Mol Sci* **19**, doi:10.3390/ijms19124032 (2018).

6   Cargnello, M. & Roux, P. P. Activation and function of the MAPKs and their substrates, the MAPK-activated protein kinases. *Microbiol Mol Biol Rev* **75**, 50-83, doi:10.1128/MMBR.00031-10 (2011).

7   Xia, Z., Dickens, M., Raingeaud, J., Davis, R. J. & Greenberg, M. E. Opposing effects of ERK and JNK-p38 MAP kinases on apoptosis. *Science* **270**, 1326-1331 (1995).

8   Heiss, N. S. *et al.* Gene structure and expression of the mouse dyskeratosis congenita gene, dkc1. *Genomics* **67**, 153-163, doi:10.1006/geno.2000.6227 (2000).

9   Bellodi, C. *et al.* Loss of function of the tumor suppressor DKC1 perturbs p27 translation control and contributes to pituitary tumorigenesis. *Cancer Res* **70**, 6026-6035, doi:10.1158/0008-5472.CAN-09-4730 (2010).

10   Moller, M. B. P27 in cell cycle control and cancer. *Leuk Lymphoma* **39**, 19-27, doi:10.3109/10428190009053535 (2000).

11   Hara, T. *et al.* Degradation of p27(Kip1) at the G(0)-G(1) transition mediated by a Skp2-independent ubiquitination pathway. *J Biol Chem* **276**, 48937-48943, doi:10.1074/jbc.M107274200 (2001).

12   Gopfert, U., Kullmann, M. & Hengst, L. Cell cycle-dependent translation of p27 involves a responsive element in its 5 '-UTR that overlaps with a uORF. *HUMAN MOLECULAR GENETICS* **12**, 1767-1779, doi:10.1093/hmg/ddg177 (2003).

13   Miskimins, W. K., Wang, G., Hawkinson, M. & Miskimins, R. Control of cyclin-dependent kinase inhibitor p27 expression by cap-independent translation. *Mol Cell Biol* **21**, 4960-4967, doi:10.1128/MCB.21.15.4960-4967.2001 (2001).

14   Kullmann, M., Gopfert, U., Siewe, B. & Hengst, L. ELAV/Hu proteins inhibit p27 translation via an IRES element in the p27 5'UTR. *Genes Dev* **16**, 3087-3099, doi:10.1101/gad.248902 (2002).

15   Choi, S. K., Lee, J. H., Zoll, W. L., Merrick, W. C. & Dever, T. E. Promotion of met-tRNAiMet binding to ribosomes by yIF2, a bacterial IF2 homolog in yeast. *Science* **280**, 1757-1760 (1998).

16   Lee, S. *et al.* Upregulation of eIF5B controls cell-cycle arrest and specific developmental stages. *Proc Natl Acad Sci U S A* **111**, E4315-4322, doi:10.1073/pnas.1320477111 (2014).

17   Faye, M. D., Graber, T. E. & Holcik, M. Assessment of selective mRNA translation in mammalian cells by polysome profiling. *J Vis Exp*, e52295, doi:10.3791/52295 (2014).

18   Abukhdeir, A. M. & Park, B. H. P21 and p27: roles in carcinogenesis and drug resistance. *Expert Rev Mol Med* **10**, e19, doi:10.1017/S1462399408000744 (2008).

19   Liao, Y., Smyth, G. K. & Shi, W. featureCounts: an efficient general purpose program for assigning sequence reads to genomic features. *Bioinformatics* **30**, 923-930, doi:10.1093/bioinformatics/btt656 (2014).

20   Love, M. I., Huber, W. & Anders, S. Moderated estimation of fold change and dispersion for RNA-seq data with DESeq2. *Genome Biol* **15**, 550, doi:10.1186/s13059-014-0550-8 (2014).

21   Alexa, A., Rahnenfuhrer, J. & Lengauer, T. Improved scoring of functional groups from gene expression data by decorrelating GO graph structure. *Bioinformatics* **22**, 1600-1607, doi:10.1093/bioinformatics/btl140 (2006).

22 Falcon, S. & Gentleman, R. Using GOstats to test gene lists for GO term association. *Bioinformatics* **23**, 257-258, doi:10.1093/bioinformatics/btl567 (2007).

23 Luo, W., Friedman, M. S., Shedden, K., Hankenson, K. D. & Woolf, P. J. GAGE: generally applicable gene set enrichment for pathway analysis. *BMC Bioinformatics* **10**, 161, doi:10.1186/1471-2105-10-161 (2009).

24 Jiang, X. *et al.* Proteomic Analysis of eIF5B Silencing-Modulated Proteostasis. *PLoS One* **11**, e0168387, doi:10.1371/journal.pone.0168387 (2016).

25 Zhang, W. & Liu, H. T. MAPK signal pathways in the regulation of cell proliferation in mammalian cells. *Cell Res* **12**, 9-18, doi:10.1038/sj.cr.7290105 (2002).

26 Korbonits, M. *et al.* Expression of phosphorylated p27(Kip1) protein and Jun activation domain-binding protein 1 in human pituitary tumors. *J Clin Endocrinol Metab* **87**, 2635-2643, doi:10.1210/jcem.87.6.8517 (2002).

27 Ross, J. A. *et al.* Eukaryotic initiation factor 5B (eIF5B) provides a critical cell survival switch to glioblastoma cells via regulation of apoptosis. *Cell Death Dis* **10**, 57, doi:10.1038/s41419-018-1283-5 (2019).

28 Nagane, M., Huang, H. J. & Cavenee, W. K. The potential of TRAIL for cancer chemotherapy. *Apoptosis* **6**, 191-197 (2001).

29 Li, P. *et al.* Caspase-9: structure, mechanisms and clinical application. *Oncotarget* **8**, 23996-24008, doi:10.18632/oncotarget.15098 (2017).

30 Han, J. *et al.* A Complex between Atg7 and Caspase-9: A NOVEL MECHANISM OF CROSS-REGULATION BETWEEN AUTOPHAGY AND APOPTOSIS. *J Biol Chem* **289**, 6485-6497, doi:10.1074/jbc.M113.536854 (2014).

31 Shi, Y. *et al.* ROS-dependent activation of JNK converts p53 into an efficient inhibitor of oncogenes leading to robust apoptosis. *Cell Death Differ* **21**, 612-623, doi:10.1038/cdd.2013.186 (2014).

32 May, G. H., Allen, K. E., Clark, W., Funk, M. & Gillespie, D. A. Analysis of the interaction between c-Jun and c-Jun N-terminal kinase in vivo. *J Biol Chem* **273**, 33429-33435 (1998).

33   Pedram, A., Razandi, M. & Levin, E. R. Extracellular signal-regulated protein kinase/Jun kinase cross-talk underlies vascular endothelial cell growth factor-induced endothelial cell proliferation. *J Biol Chem* **273**, 26722-26728 (1998).

34   Rocchi, L., Barbosa, A. J., Onofrillo, C., Del Rio, A. & Montanaro, L. Inhibition of human dyskerin as a new approach to target ribosome biogenesis. *PLoS One* **9**, e101971, doi:10.1371/journal.pone.0101971 (2014).

35   Yoon, A. *et al.* Impaired control of IRES-mediated translation in X-linked dyskeratosis congenita. *Science* **312**, 902-906, doi:10.1126/science.1123835 (2006).

36   Hnit, S. S. *et al.* p27(Kip1) signaling: Transcriptional and post-translational regulation. *Int J Biochem Cell Biol* **68**, 9-14, doi:10.1016/j.biocel.2015.08.005 (2015).

37   Cho, S., Kim, J. H., Back, S. H. & Jang, S. K. Polypyrimidine tract-binding protein enhances the internal ribosomal entry site-dependent translation of p27Kip1 mRNA and modulates transition from G1 to S phase. *Mol Cell Biol* **25**, 1283-1297, doi:10.1128/MCB.25.4.1283-1297.2005 (2005).

38   Shi, Y., Sharma, A., Wu, H., Lichtenstein, A. & Gera, J. Cyclin D1 and c-myc internal ribosome entry site (IRES)-dependent translation is regulated by AKT activity and enhanced by rapamycin through a p38 MAPK- and ERK-dependent pathway. *J Biol Chem* **280**, 10964-10973, doi:10.1074/jbc.M407874200 (2005).

39   Jiang, H., Coleman, J., Miskimins, R., Srinivasan, R. & Miskimins, W. K. Cap-independent translation through the p27 5'-UTR. *Nucleic Acids Res* **35**, 4767-4778, doi:10.1093/nar/gkm512 (2007).

40   Chiarle, R., Pagano, M. & Inghirami, G. The cyclin dependent kinase inhibitor p27 and its prognostic role in breast cancer. *Breast Cancer Res* **3**, 91-94 (2001).

41   Fero, M. L., Randel, E., Gurley, K. E., Roberts, J. M. & Kemp, C. J. The murine gene p27Kip1 is haplo-insufficient for tumour suppression. *Nature* **396**, 177-180, doi:10.1038/24179 (1998).

42   Kim, E. M. *et al.* The p53/p21 Complex Regulates Cancer Cell Invasion and Apoptosis by Targeting Bcl-2 Family Proteins. *Cancer Res* **77**, 3092-3100, doi:10.1158/0008-5472.CAN-16-2098 (2017).

43   Morris-Hanon, O. *et al.* The Cell Cycle Inhibitors p21(Cip1) and p27(Kip1) Control Proliferation but Enhance DNA Damage Resistance of Glioma Stem Cells. *Neoplasia* **19**, 519-529, doi:10.1016/j.neo.2017.04.001 (2017).

44   Lim, S. & Kaldis, P. Cdks, cyclins and CKIs: roles beyond cell cycle regulation. *Development* **140**, 3079-3093, doi:10.1242/dev.091744 (2013).

CHAPTER 4

General Conclusion

General Conclusion:

In this thesis, I investigate and further define the role of eIF5B in non-canonical translation. We confirm that eIF5B represses the translation of ATF4, in a uORF-dependent mechanism. eIF5B-mediated repression occurs in cooperation with eIF1A and eIF5 and utilizes the downstream overlapping uORF (uORF2) of *ATF4*. We additionally examine transcriptome changes in eIF5B depleted cells and verify that the JNK-arm of the MAPK pathway is upregulated in response to eIF5B depletion. Transcriptome data confirm the upregulation of dyskerin in eIF5B depleted cells, and I show that p27 (a protein known to be regulated by dyskerin) is likely regulated translationally through eIF5B, potentially dependent on its IRES-element. Overall, this work furthers the understanding of non-canonical translation initiation and the role of eIF5B.

4.1 Future experiments

To fully elucidate the regulation of p27 by eIF5B, it must be confirmed that the mechanism is IRES-dependent and that the regulation is occurring by affecting the levels of dyskerin and subsequently the levels of rRNA modifications in the ribosome. First, polysome profiling should be performed in eIF5B depleted cells, to measure the translational efficiency of *p27*. Based on the significant increase of luciferase activity that I observed in the luciferase assays with the Δd construct (IRES- element only), I expect that the polysome profiling will show a shift from monosomes to polysomes, confirming that eIF5B regulates *p27* at the translational level. To fully confirm that the regulation of *p27* is IRES-dependent, luciferase reporter assays should be performed using bicistronic constructs in addition to the monocistronic constructs which I have completed. Bicistronic

constructs would allow both cap-dependent, and IRES-dependent translation to be measured simultaneously, and normalized to each other, to decisively conclude that the IRES-element is responsible for the change in translational efficiency of *p27*. These experiments would confirm that eIF5B regulates p27 translationally in an IRES-dependent mechanism.

To confirm that the regulation of p27 *via* eIF5B is occurring through dyskerin, the luciferase assay with the Δd construct should be repeated, in the presence of both eIF5B and dyskerin depletion. As I hypothesize that eIF5B depletion is upregulating dyskerin, which is, in turn, upregulating p27, the depletion of dyskerin would prevent *p27* upregulation in all cases. The luciferase assay would show no significant difference between eIF5B depleted and control cells, upon dyskerin depletion, showing a rescued phenotype. If the effect appears to be dependent on dyskerin, levels of NHP2, GAR1, and NOP10 should be measured *via* Western blot, upon depletion of eIF5B. NHP2, GAR1, and NOP10 are highly conserved proteins that form a complex with dyskerin in the formation of H/ACA mature ribonucleoproteins (RNPs).[1] I would expect the protein levels of dyskerin's interaction partners in pseudouridylation to be upregulated as well if increased rRNA modification is occurring. To additionally verify rRNA modification levels, H/ACA snoRNA levels (ex: snR82, snR83, snR84) should be measured *via* RT-qPCR. H/ACA snoRNAs, when associated with dyskerin, are responsible for modifying nucleotides in the ribosome, and their association is necessary for the stability of pseudouridylation.[2] Increased H/ACA snoRNA levels upon eIF5B depletion, would confirm that the upregulation of dyskerin is resulting in increased pseudouridylation of rRNA in the ribosome. Lastly, the levels of c-myc should be examined *via* Western blot, upon eIF5B

depletion. c-myc is an IRES-containing transcription factor implicated in the pathogenesis of multiple cancers and is known to regulate dyskerin.[1] I hypothesize that eIF5B may be regulating the transcription factor of c-myc, which is resulting in downstream regulation of dyskerin and ultimately p27.

4.2 Concluding remarks

Though cap-dependent canonical translation and the eukaryotic initiation factors involved in the process are well-defined, much is unknown about the factors involved in non-canonical translation mechanisms. Non-canonical translation initiation involving uORFs is becoming a large focus of research. This can be attributed to the prevalence of uORFs, with approximately 49% of human transcripts containing start codons in their 5' UTRs.[3] uORFs are particularly common to classes of mRNA involved in the cell cycle, cell differentiation, and cell death.[3] Additionally, though uORFs have previously been thought of as repressors or inhibitors of downstream translation initiation, more examples are now being discovered of uORFs promoting downstream translation initiation, specifically under stress.[4]

ATF4 is one of the most studied transcripts, in regards to its upregulated translation under stress conditions through its uORFs. However, until this study, uORF-dependent translation initiation of *ATF4* has only been reported upon phosphorylation of eIF2α (activation of the ISR). Krishna *et al*. (2004) determined that upon eIF2α phosphorylation a higher proportion of ribosomes pass over ATF4s second uORF, allowing for increased translation of ATF4s coding sequence.[5] Using the same luciferase reporter constructs, we showed that depletion of eIF5B was able to produce a parallel effect to phosphorylation of

eIF2α. This is novel information, as eIF2α is the only initiation factor that has been shown to regulate transcripts containing uORFs. We suggest that eIF5B depletion regulates ATF4, potentially by converging on a shared regulatory point.

This observation could suggest that eIF5B directly delivers initiator-tRNA to ATF4s transcript, and as such, depletion of eIF5B would lower the concentration of ternary complex. This has been previously shown, in the IRES-dependent translation of HCV, CSFV, and XIAP mRNAs, as well as under hypoxic conditions.[6-9] As such, our findings are consistent with the literature in that eIF5B has been shown to deliver initiator-tRNA, however we expand the knowledge in the field by suggesting that this mechanism exists in a uORF-dependent context. Another possibility which we suggest is that eIF5B works with eIF5 and/or eIF1A, and the stoichiometry between these proteins affects the concentration of ternary complex, which in turn results in uORF-mediated regulation of ATF4. It has been confirmed in the literature that eIF5B interacts with both eIF5 and eIF1A [10,11], however, the potential for these proteins to cooperate in uORF-mediated translation initiation is novel, and offers new regulatory targets in gene expression regulation. Overall, Chapter 2 provides insight into the role of eIF5B in uORF-mediated translation initiation.

We chose to analyze the transcriptome changes in eIF5B depleted cells, based on our findings that eIF5B regulated the master transcription factor ATF4. We hypothesized that eIF5B may regulate other master transcription factors, and subsequently regulate cellular signalling pathways. We found that upon depletion of eIF5B, the JNK-arm of the MAPK pathway was significantly upregulated. As many cancers including melanomas have mutations in proteins of the MAPK pathway, knowledge of the regulation of MAPK is valuable.[12] We confirmed that phosphorylation of JNK significantly increases upon

eIF5B depletion, despite lowered levels of JNK total protein. As dual phosphorylation of JNK is required for its activation in the MAPK pathway, we validated that the JNK arm of the MAPK pathway is upregulated in eIF5B depleted cells.[12] However, different stress stimuli are known to activate different MAPK family members including JNK, ERK, and P38 with different responses produced. It is known that most but not all stimuli that activate P38 MAPKs also stimulate JNK MAPKs, suggesting that our validation of JNK does not fully define or predict the cellular outcome.[13] As such, we conclude that eIF5B regulates phosphorylation and activation of JNK, which suggests a role in MAPK signaling.

Our transcriptome analysis also showed upregulation of dyskerin, upon eIF5B depletion. We confirmed the upregulation of dyskerin at the protein level upon eIF5B depletion *via* Western blotting. As dyskerin is a pseudouridine synthase, important to RNA modification [14], this suggests a novel role for eIF5B in ribosome biogenesis. Bellodi *et al*. (2010) determined that IRES-mediated translation defects in Dkc1[m] cells were due to intrinsic ribosomal defects [15], showing that dyskerin is critical to IRES-dependent translation, specifically of *p27*. In our study, we observed p27 levels to increase upon eIF5B depletion, which was specific to *p27s* IRES-element. Though it is possible that eIF5B's ability to interact with and deliver initiator-tRNA is mediating *p27*s regulation, we suggest that eIF5Bs regulation of dyskerin is in turn regulating p27. This would suggest that eIF5B depletion upregulates dyskerin, which produces a functional phenotype, in that ribosomes have fewer defects due to problems in RNA modification. This is in agreement with the literature confirming that removal of dyskerin results in defective ribosomes and thus impaired IRES-mediated translation of *p27*.[15] This mechanism requires further confirmation as discussed previously in this thesis. However, our study furthers the

mechanisms of regulation through eIF5B, including transcriptome data that implicates eIF5B in MAPK signaling, and ribosome biogenesis.

Overall, this thesis examines and defines novel roles for eIF5B in gene expression regulation, specifically targeting non-canonical translation initiation mechanisms. We suggest that eIF5B participates in both uORF-mediated and IRES-mediated translation initiation of particular transcripts, both leading to altered cellular phenotypes. This information is critical to furthering the understanding of the cellular biology of protein synthesis.

References

1   Alawi, F. & Lin, P. Dyskerin is required for tumor cell growth through mechanisms that are independent of its role in telomerase and only partially related to its function in precursor rRNA processing. *Mol Carcinog* **50**, 334-345, doi:10.1002/mc.20715 (2011).

2   Bellodi, C. *et al.* H/ACA small RNA dysfunctions in disease reveal key roles for noncoding RNA modifications in hematopoietic stem cell differentiation. *Cell Rep* **3**, 1493-1502, doi:10.1016/j.celrep.2013.04.030 (2013).

3   Barbosa, C., Peixeiro, I. & Romao, L. Gene Expression Regulation by Upstream Open Reading Frames and Human Disease. *PLOS GENETICS* **9**, e1003529, doi:10.1371/journal.pgen.1003529 (2013).

4   Young, S. K. & Wek, R. C. Upstream Open Reading Frames Differentially Regulate Gene-specific Translation in the Integrated Stress Response. *JOURNAL OF BIOLOGICAL CHEMISTRY* **291**, 16927-16935, doi:10.1074/jbc.R116.733899 (2016).

5   Vattem, K. M. & Wek, R. C. Reinitiation involving upstream ORFs regulates ATF4 mRNA translation in mammalian cells. *Proceedings of the National Academy of Sciences of the United States of America* **101**, 11269-11274, doi:10.1073/pnas.0400541101 (2004).

6   Pestova, T. V., de Breyne, S., Pisarev, A. V., Abaeva, I. S. & Hellen, C. U. eIF2-dependent and eIF2-independent modes of initiation on the CSFV IRES: a common role of domain II. *EMBO J* **27**, 1060-1072, doi:10.1038/emboj.2008.49 (2008).

7   Terenin, I. M., Dmitriev, S. E., Andreev, D. E. & Shatsky, I. N. Eukaryotic translation initiation machinery can operate in a bacterial-like mode without eIF2. *Nat Struct Mol Biol* **15**, 836-841, doi:10.1038/nsmb.1445 (2008).

8   Thakor, N. & Holcik, M. IRES-mediated translation of cellular messenger RNA operates in eIF2α- independent manner during stress. *Nucleic Acids Research* **40**, 541-552, doi:10.1093/nar/gkr701 (2012).

9   Ho, J. J. D. *et al.* Oxygen-Sensitive Remodeling of Central Carbon Metabolism by Archaic eIF5B. *Cell Reports* **22**, 17-26, doi:10.1016/j.celrep.2017.12.031 (2018).

10   Lin, K. Y., Nag, N., Pestova, T. V. & Marintchev, A. Human eIF5 and eIF1A Compete for Binding to eIF5B. *Biochemistry* **57**, 5910-5920, doi:10.1021/acs.biochem.8b00839 (2018).

11   Nag, N. *et al.* eIF1A/eIF5B interaction network and its functions in translation initiation complex assembly and remodeling. *Nucleic Acids Res* **44**, 7441-7456, doi:10.1093/nar/gkw552 (2016).

12   Cargnello, M. & Roux, P. P. Activation and function of the MAPKs and their substrates, the MAPK-activated protein kinases. *Microbiol Mol Biol Rev* **75**, 50-83, doi:10.1128/MMBR.00031-10 (2011).

13   Zhang, W. & Liu, H. T. MAPK signal pathways in the regulation of cell proliferation in mammalian cells. *Cell Res* **12**, 9-18, doi:10.1038/sj.cr.7290105 (2002).

14   Zhao, Y., Dunker, W., Yu, Y. T. & Karijolich, J. The Role of Noncoding RNA Pseudouridylation in Nuclear Gene Expression Events. *Front Bioeng Biotechnol* **6**, 8, doi:10.3389/fbioe.2018.00008 (2018).

15   Bellodi, C. *et al.* Loss of function of the tumor suppressor DKC1 perturbs p27 translation control and contributes to pituitary tumorigenesis. *Cancer Res* **70**, 6026-6035, doi:10.1158/0008-5472.CAN-09-4730 (2010).